Comparison between theoretical and practical compression capacities of deep / long piles

مقارنة مابين قدرة تحمل الخوازيق العميقة للضغط في الحالتين النظرية والعملية

by

MOHAMED NABIL OMAR

A dissertation submitted in fulfilment

of the requirements for the degree of

MSc. Structural Engineering

at

The British University in Dubai

Prof. Abid Abu Tair

November 2017

DECLARATION

I warrant that the content of this research is the direct result of my own work and that any use made in it of published or unpublished copyright material falls within the limits permitted by international copyright conventions.

I understand that a copy of my research will be deposited in the University Library for permanent retention.

I hereby agree that the material mentioned above for which I am author and copyright holder may be copied and distributed by The British University in Dubai for the purposes of research, private study or education and that The British University in Dubai may recover from purchasers the costs incurred in such copying and distribution, where appropriate.

I understand that The British University in Dubai may make a digital copy available in the institutional repository.

I understand that I may apply to the University to retain the right to withhold or to restrict access to my thesis for a period which shall not normally exceed four calendar years from the congregation at which the degree is conferred, the length of the period to be specified in the application, together with the precise reasons for making that application.

Mohamed Nabil

Mohamed Nabil Omar

COPYRIGHT AND INFORMATION TO USERS

ABSTRACT

The rate of build of high-rise buildings has accelerated rapidly, especially in the Arabian Gulf, over the last few decades, due to rapid urbanization and significant improvements in the field of the high-rise construction and technology. Many challenges were faced by the engineers in the design and construction of such buildings. One of the major challenges was the foundation systems, which are required to ensure the stability of the buildings. The common type of foundation system which is used in case of high- rise buildings is piles foundation system.

In the most standards and codes of practice such as British Standard and ASTM, the piles specifications and recommendations are stated for short piles which has a maximum depth range between 18.0 to 20.0 m. Theoretical equations for pile design, charts and different soil factors and parameters are based on old studies of short piles behavior. In this research, a comparison was conducted between the theoretical pile compression capacity which is calculated from the theoretical equations and the practical pile compression capacity which is derived from the results of pile's static load test.

The study covered three different cases of bored piles constructed in U.A.E especially in Dubai. The piles used in this research have a depth ranging from 30.0 to 65.0 m. This type of piles is classified in this research as **long or deep piles**. A finite element model of each pile was modeled by using PLAXIS 2D software, to compare the practical and theoretical piles capacities. It was found that the theoretical compression pile capacity is 60 to 70% of the practical pile capacity with the same specifications (pile diameter and pile depth). As a conclusion of the results, the theoretical equations which are used to calculate the pile compression capacity can be improved to give results very near from the practical condition.

Keywords: high-raise buildings, piles, long piles, PLAXIS 2D, piling equipment.

الملخص

معدل بناء المباني العالية قد ازداد بمعدل سريع وخاصة في الخليج العربي في العقود الاخيرة وذلك نتيجة النمو الحضاري و التطور الملحوظ في مجال انشاء المباني والابراج العالية. كثير من التحديات قد واجهت المصممين لتلك النوعية من المباني. واحد من التحديات الرئيسة هو الاساسات المستخدمة لتحقيق الاتزان للمباني الشاهقة الارتفاع. وتعتبر الاساسات العميقة (الخوازيق) من اكثر انواع الاساسات المستخدمة في حالة المباني شاهقة الارتفاع.

في معظم المراجع والاكواد علي سبيل المثال الكود البريطاني والكود الامريكي, يتم تحديد مواصفات وتوصيات الخوازيق علي اساس الخوازيق القصيرة والتي لا يتعدي عمقها عن 18 الي 20 متر. كما ان معظم المعادلات النظرية والرسومات البيانية ومعاملات التربة المختلفة تعتمد علي دراسات قديمة قد اجريت علي سلوك الخوازيق العادية (القصيرة). في هذا البحث سنقوم بمقارنة قدرة تحمل الخوازيق لاحمال الضغط المحسوبة من المعادلات النظرية وتلك المحسوبة من نتيجة اختبارات تحميل فعلية للخوازيق العميقة.

الدراسة تغطي ثلاث حالات مختلفة لخوازيق قد تم تنفيذها فعليا في الامارات وخاصة ان دبي. تتراوح اعماق الخوازيق المستخدمة في هذا البحث ما بين 30 الي 65 متر. سيتم تصنيف تلك الخوازيق في هذا البحث الي نوعية الخوازيق العميقة او الطويلة. سيتم نمذجة الخوازيق باستخدام برنامج PLAXIS 2D للمقارنة مابين قدرة تحمل الخوازيق لاحمال الضغط في كلا من الحالة النظرية والحالة العملية. وكنتيجة لذلك تم وجد ان قدرة تحمل الخوازيق المحسوبة با ستخدام المعادلات النظرية القديمة تساوي تقريبا 60 الي 70% من قدرة تحمل الخوازيق المحسوبة من نتائج اختبارات التحميل. كنتيجة للدراسة يمكن تعديل المعادلات النظرية المستخدمة في حساب قدرة تحمل الخوازيق لاحمال الضغط لتحقيق نتائج اقرب ما يكون من النتائج العملية.

ACKNOWLEDGEMENTS

I would like to express my gratitude to my supervisor Prof. Abid Abu Tair for the useful comments, remarks and engagement through the learning process of this master thesis. Furthermore, I would like to thank Prof. Abid Abu Tair for introducing me to the topic as well for the support on the way.

Table of Contents

List of Figures

List of Tables

List of Abbreviations

P_{SU} =	ultimate pile skin friction resistance
P_{BU} =	ultimate pile end bearing resistance
W_P =	pile weight
Ab =	Cross sectional area
C =	Cohesion of the soil
σvb =	Vertical stress of the soil at the level of the pile's base
γ =	Soil unit weight
d =	Pile diameter
$Nc, Nq, N\gamma$ =	Soil bearing capacity factors
$\sigma' v$ =	effective vertical stress along pile shaft
$\sigma' vb$ =	effective vertical stress at the pile base level
$F\omega$ =	correction factor for tapered pile (=1.0 for uniform diameter pile)
σ'_{v0} =	the effective soil overburden pressure at the pile base level
N_q =	pile bearing capacity factor
A_b =	the area of the pile base "cross sectional area"
K_s =	coefficient of the soil horizontal stress
δ =	friction angle between the pile & soil
A_s =	the area of the pile shaft
α =	reduction factor related to q_{uc}
β =	correction factor related to the discontinuity spacing in the rock mass
δ =	elastic deformation of the pile
P =	applied load
L =	pile length
E =	elastic modulus of the pile's material
A =	cross sectional area of the pile
Q_u =	ultimate pile capacity
δ_u =	pile displacement at failure
Q_u =	ultimate pile capacity
Δ =	pile displacement

INTRODUCTION

In the last two decades the high rise buildings construction has been significantly improved. In addition, the construction tools and equipment have been developed to be more effective and to provide the ability to construct such high rise buildings. The common foundation system which is used in case of high rise buildings is the piling foundation system. Recently the construction of piling foundation system has been improved to achieve depths which were impossible to reached before, by using the advanced piling machines.

Practically and based on actual case of studies, it has been found that there is a big difference between the calculated pile capacity based on the results of static load tests and the estimated pile capacities obtained using classical theoretical equations. These differences are increased in case of the increased of pile depths. This research will compare between the theoretical pile capacity and the practical pile capacity. Also numerical model will be developed to identify a more accurate numerical pile capacity.

Three case studies will be discussed in this research, these cases are from real projects that have been constructed in Dubai. The projects data such as soil investigation reports, piling drawings and the results of piles' static load test have been collected from the projects' consultant for further development and research.

AIMS AND OBJECTIVES

The aim of this research is to conduct a comparison between theoretical pile capacity derived using classical soil mechanics equations with real static test results of piles constructed in Dubai and to propose more optimum design models.

The objectives of this research are as follow;

1. Calculate the practical pile capacity from the results of static load test in each case of study.
2. Model the selected pile of each case of study by using a finite element software, and estimate the numerical pile capacity by using a prescribed settlement on the pile head.
3. Comparison between the practical, theoretical and numerical compression pile capacity will be done to identify the differences.
4. further research to specify the differences between the theoretical pile capacity and numerical pile capacity, the compassion will be done for pile skin friction resistance and end bearing resistance separately. This further research will be done based on the developed pile model.

CHAPTER 1 - LITERATURE REVIEW

A pile is a structural element whose function is to transfer the superstructure loads through weak soil layers to the hard soil strata or the rock layers. Another use of the pile which is the resistance to the uplift force, in case of high rise building subjected to overturning force or to support a structure has a low weight compared to the uplift force which is generated from high water table. This type of piles is called **tension piles**. Piles are mainly used to resist a compression forces from the superstructure and in this case the piles are classified as a **comparison piles**.

PILES HISTORY

Driven piles as type of structures foundation is one of the oldest types which used to ensure the stability of different types of structures like buildings and bridges. In U.K there are so many examples of timber piles used to support different bridges constructed by the Romans. In the old ages, piles of timber has been used in the construction of great monasteries's foundations which has been constructed in Europe. In China, the wooden piles were used by the builders especially the bridges' builders of the Han Dynasty (200 BC to AD 200). Based on that, the rules have been established in the beginning of using the piles foundation by which the pile capacity was determined from its resistance to the driving force by a hammer of known weight and with a known height of drop.

Timber, as a result of its quality joined with delicacy, strength and simplicity of cutting and taking care of, remained the main material utilized for heaping until nearly late circumstances. It was supplanted by concrete and steel simply because these more up to date materials could be manufactured into units that were equipped for managing compressive, twisting and ductile powers a long ways past the limit of a timber heap of like measurements. Concrete piles has been devolved to provide the ability to construct the piles in a drilled holes (bored piles) in situations where noise, vibration and ground heave had to be avoided.

Reinforced concrete piles, which were developed as structural elements in the previous two centuries, and it has been widely used instead of timber piles. The concrete piles can be formed in different shapes to suit the structure requirement and the imposed load. The durability and the reaction with the different types of soil layers gives the concrete another advantage. Steel piles are a common type of piles especially in marine structure due to the ease of the installation. Nowadays there are different types of paints and chemicals used to improve the steel resistance to corrosion and can increase the steel piles' durability.

TYPES OF PILE

Most of standard codes classified the types of piles to three main categories, the first category is the **large displacement piles** which include solid or hollow sections closed at their end, driven or caste in place into the ground. The second category is **small displacement piles** which have the same function of the first category but with small sections. This types includes steel rolled H or I section. The third type is **replacement piles**, these types constructed by replacing the soil by boring using different types of the drilling techniques. Then filling the bore by the used pile material such as concrete, timber or steel.

LARGE DISPLACEMENT PILES – DRIVEN TYPES

1. Timber with different section shapes.
2. Precast concrete soiled or tubular sections.
3. Restressed concrete piles.
4. Steel tubes or boxes with closed end.

LARGE DISPLACEMENT PILES – DRIVEN AND CAST IN PLACE TYPES

1. Steel tubes driven after placing concrete.
2. Precast concrete sections filled by concrete.
3. Steel shell driven and then filled with concrete.

SMALL DISPLACEMENT PILES

1. Precast concrete tubular section driven with open end.
2. Pre-stressed concrete tubular section driven with open end.
3. Steel H sections.
4. Steel tube or box section driven with open end and soil removed as required.

REPLACEMENT PILES

1. Concrete bored piles.
2. Cement mortar casted in the drilled hole.
3. Steel sections placed into drilled hole.

The selection criteria of the used pile type depend on different factors, the major factor is the type of the soil layers, where driven piles can be easily used in weak soil layers compared to replacement piles used with hard soil layers. In the second place, there are important factors such as the superstructure's material, the availability of the used pile materials, the used pile machines and techniques and the requirements for pile durability.

SELECTION OF PILE TYPE

The selection of the pile type depends on three major factors; the first factor is the **LOCATION AND THE TYPE OF THE STRUCTURE**. The second factor is the **GROUND CONDITIONS** such as cohesive and loose soil. This factor effect on the choosing of the pile material and the installation technique. For example, the drilling of piles in cohesive soil layers can be performed without using a bentonite slurry to protect the borehole side from failure unlike the drilling in the loose soil or clay layers.

The third factor is the **DURABILITY** of the piles, this factor effect on the selecting of the pile material. For example, in some countries the using of wood as a pile foundation can be cheap compared to any other material like steel and reinforced concrete. But in terms of durability the using of reinforced concrete or steel instead of wood as a pile foundation can be considered as a durable option.

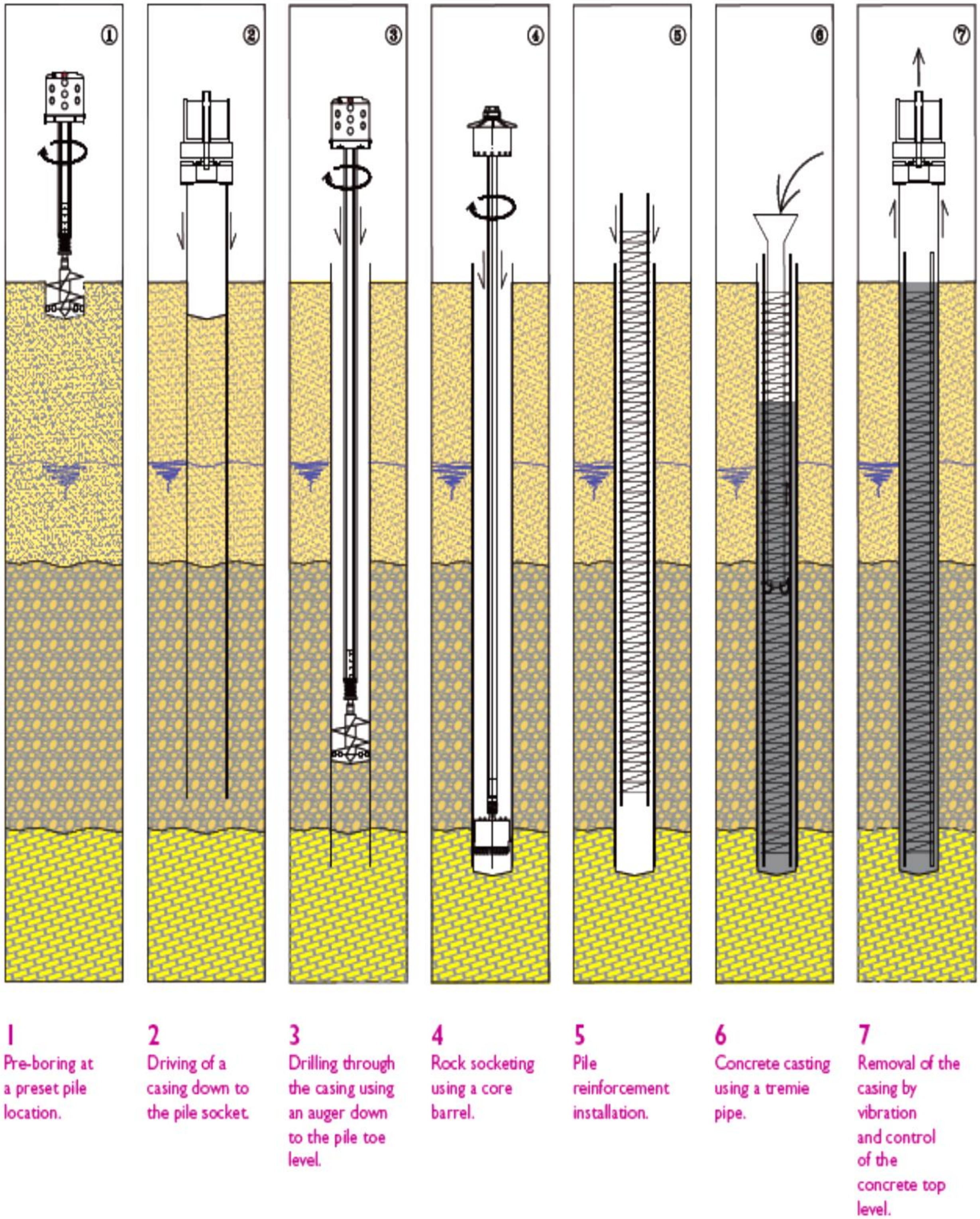

Figure 1. Bored Cast in Situ - Casing Method

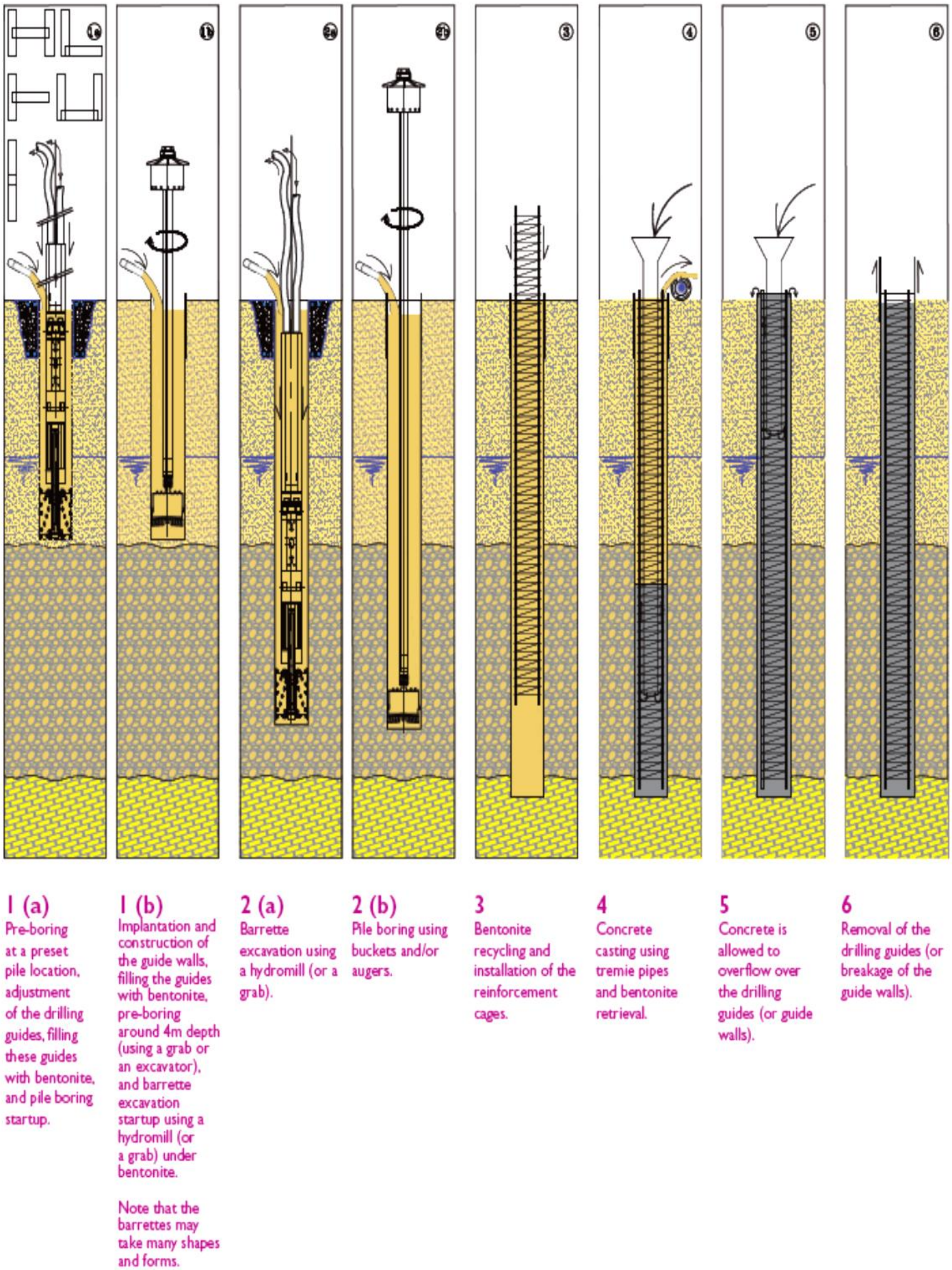

Figure 2. Bored Piles - By using Bentonite Slurry

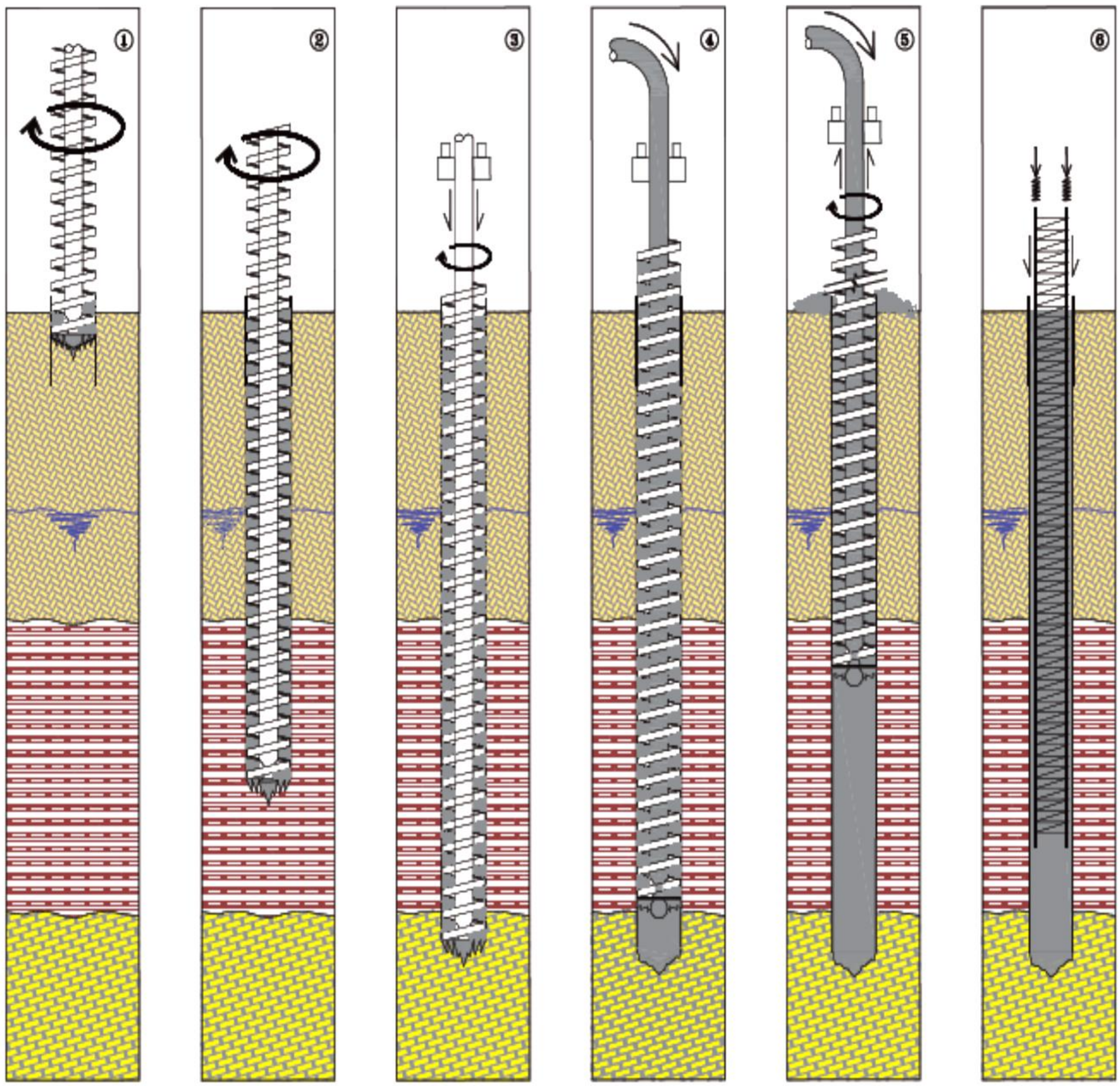

1
Pre-boring at a preset pile location and adjustment of the drilling guides.

2
Drilling down to the pile toe level using a continuous hollow auger.

3
Rock socketing by rotating the auger and pushing it downwards.

4
Concrete casting through the hollow auger.

5
Auger removal by rotation and auger cleaning while casting the concrete.

6
After concrete casting, pile reinforcement installation by vibration.

Figure 3. Flight Auger Piles - CFA

ULTIMATE LOAD CAPACITY OF SINGLE PILES

GENERAL CONSIDERATION

This section will cover the geotechnical method to estimate the compression pile capacity. In the past time, much research work was done to express a method based on the practical soil mechanics theory. For example, the calculation of skin friction on a pile shaft was based on a simple relationship between the effective overburden pressure, the drained angle of shearing resistance of the soil and the coefficient of earth pressure at rest, but they realized through the results of the practical tests and researches that the pile's skin friction resistance should modified by a factor takes into consideration the installation technique of the pile.

In the same way, the calculation of the pile end bearing resistance was based on the soil shearing resistance at the pile toe level, but the researcher recognized the importance of the pile settlement at the pile's working load. A methods have developed to estimate the pile's settlement, based on elastic theory and considering the skin friction transfer between the pile surface and surrounded soil.

THE PILE BEHAVIOR UNDER LOAD

A pile is subjected to a compression load at a steady rate of application, the resulting load - settlement relationship plotted in the following figure. The curve starting with linear relationship from the origin point to point A, this is mean if the load released at any stage up to point 'A' the deformation or settlement of the pile head will return to its original condition. when the loading increased beyond point 'A' the relationship will have changed from linear to nonlinear relationship, and there will be yielding at the pile - soil interface till reaching the maximum shaft friction 'point 'B'. In case, the pile load released during this stage the pile head will have reached to point 'C'. and the distance 'OC' will be the displacement which is required to achieve the full pile shaft resistance, usually this distance is equal to 0.3% to 1% of the pile width or diameter. The pile end bearing resistance requires more settlement to achieve the full mobilization, point 'D', this is movement is based on the pile diameter in the range of 10% to 20% of the pile width or diameter. after point 'D' the pile will move downward without any increase in the load "failure point".

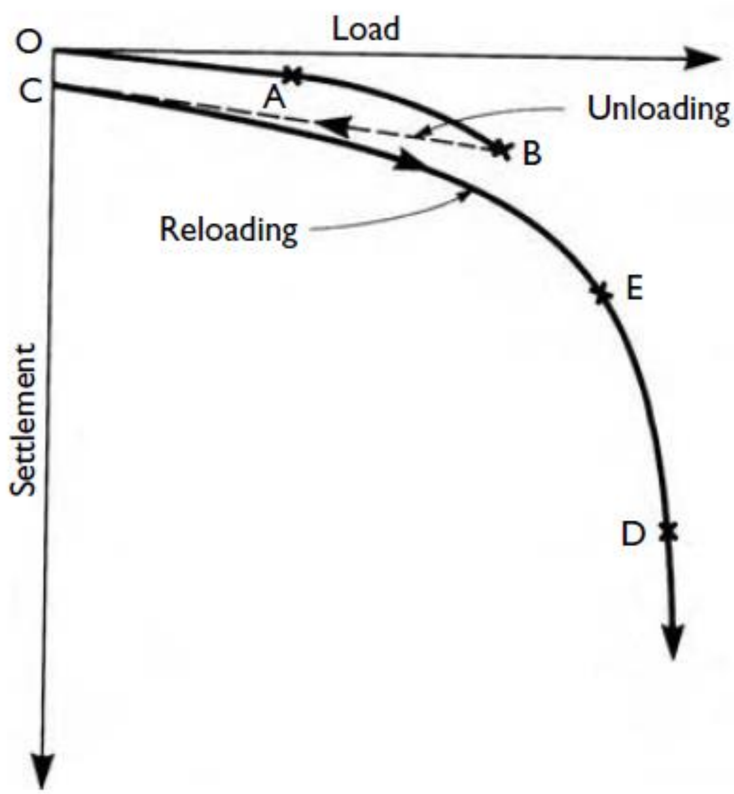

Figure 4. Load - settlement curve of pile subjected to compression load

1. PILES IN SAND SOIL

The ultimate pile capacity, Pu, of a single pile is equal to the summation of the ultimate skin friction and end bearing resistances, less the pile weight;

$$P_U = P_{SU} + P_{BU} - W_P \qquad \ldots.. \quad \textit{Eq. (1)}$$

Where,

P_{SU} = ultimate pile skin friction resistance

P_{BU} = ultimate pile end bearing resistance

W_P = pile weight

For sand soil, there was an empirical method developed and reviewed by Vesic (1967),

$$P_U = \int_0^L C(ca + \sigma v\, Ks\, \tan \emptyset a)\, dz + Ab\,(cNc + \sigma vbNq + 0.5\, \gamma dN\gamma)w \quad \ldots.. \quad \textit{Eq. (2)}$$

Where,

Ab = Cross sectional area

C = Cohesion of the soil

σvb = Vertical stress of the soil at the level of the pile's base

γ = Soil unit weight

d = Pile diameter

$Nc, Nq, N\gamma$ = Soil bearing capacity factors

Another method to calculate the ultimate pile capacity in sand soil (Broms, 1966; Nordlund, 1963) assume that the vertical soil stresses σv and σvb in Eq. 2 are the effective vertical stresses caused by the soil overburden. However, a research by Vesic (1967) and Kerisel (1961) indicated that the pile shaft and base resistances are not increasing linearly with the depth, but reached a constant value at a certain depth. Vesic also found that the ratio between the pile base resistance and its skin frictions resistance fb/fs, in homogenous soil is independent of pile size and the installation method of the pile. Certain design approaches have incorporated Vesic's research results by specifying an upper limit of the shaft and base resistances. For example, McClelland et al. (1969) have suggested, for dense sand, the following design parameters: angle of internal friction Ø = 30; Ks = 0.7 (compression load) or 0.5 (tension load), with maximum value of shaft resistance equal to 96 KN/m2; and Nq = 41, with maximum base resistance equal to 9.6 MN/m2.

However, such method takes little consideration of natural sand and may not reflect the value of the pile capacity with respect to pile penetration. Moreover, the limiting of the pile shaft and base resistances will only become operative at relatively large penetrations.

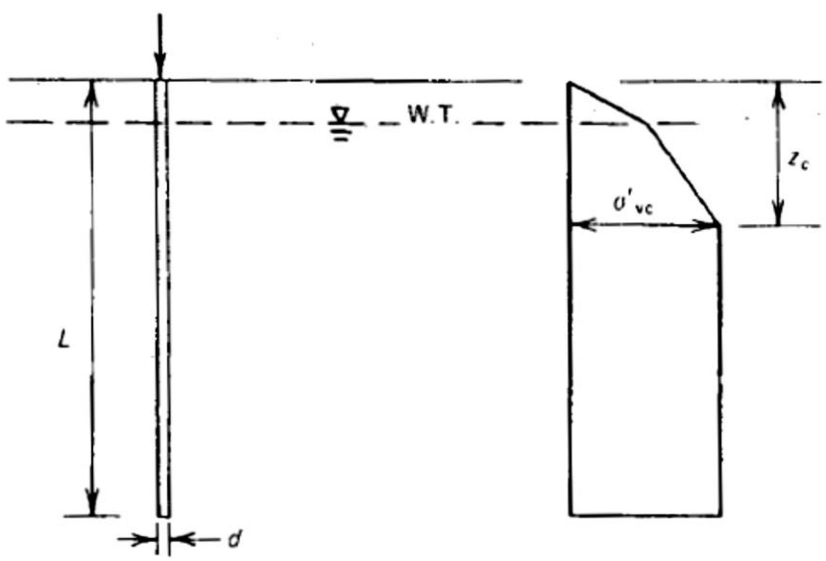

Figure 5. Simplified of vertical stress adjacent pile in sand soil

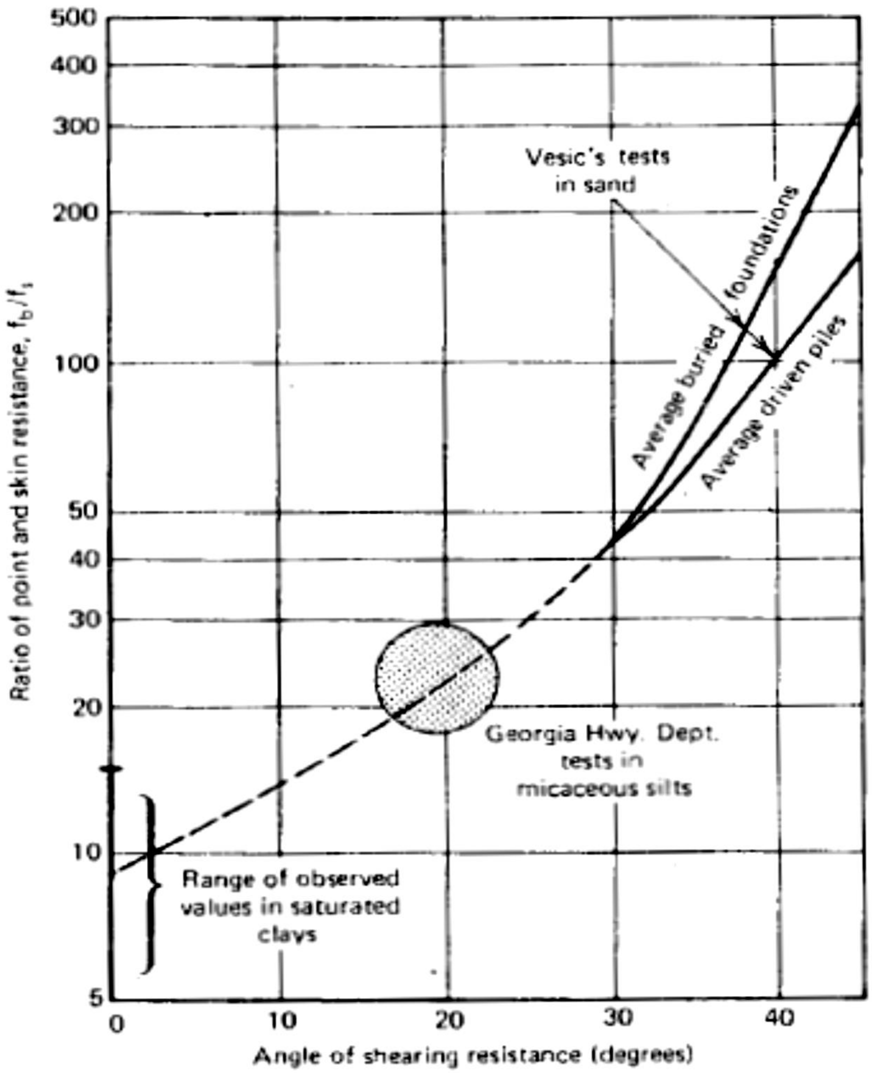

Figure 6. Variation of fb/fs with Ø (Vesic, 1967)

In Eq. 2, if the pile and soil adhesion ca and the term cNc are taken equal to zero, and the term 0.5 is neglected because of the small value compared to Nq term, the ultimate pile capacity load of single pile in sand can be expressed as per the following equation:

$$P_U = \int_0^L F\omega\ C\ \sigma'v\ Ks\ \tan \emptyset' a\,.\,dz + \ Ab\ \sigma' vbNq\ .w \qquad \ldots\ldots \quad \textit{Eq. (3)}$$

Where,

$\sigma' v$ = effective vertical stress along pile shaft

$\sigma' vb$ = effective vertical stress at the pile base level

$F\omega$ = correction factor for tapered pile (=1.0 for uniform diameter pile)

From the test results, which had been done by Vesic (1967), the values of Ks, $\tan \emptyset' a$, and Zc/d have been calculated in terms of the sand soil relative density Dr, also expressed in terms of the angle of internal friction $\emptyset'$, by using the suggested relationship by Meyerhof (1956):

$\emptyset' = 28 + 15Dr$ ….. *Eq. (4)*

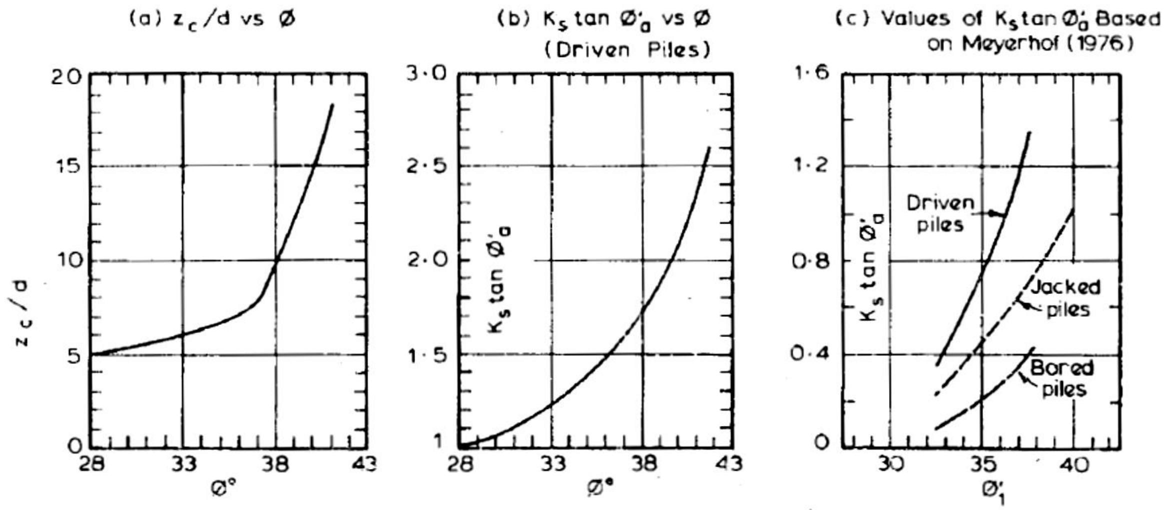

Figure 7. Values of Ks, $tan\, \emptyset' a$, and Zc/d for piles in sand

Fig. 8 is showing the relationship between the bearing capacity factor Nq and the angle of internal friction, these values have been developed by Berezantzev et al. (1961). Vesic (1967) has stated that there is a significant variation in the theoretical values of Nq which are derived from different investigations, also he stated that the values of Berezantzev et al. appear to fit the obtained values from the different investigations. The values of taper correction factor $F\omega$ are plotted against the angle of internal friction in Fig. 9 and have been expressed from the test results which is developed by Nordund (1963).

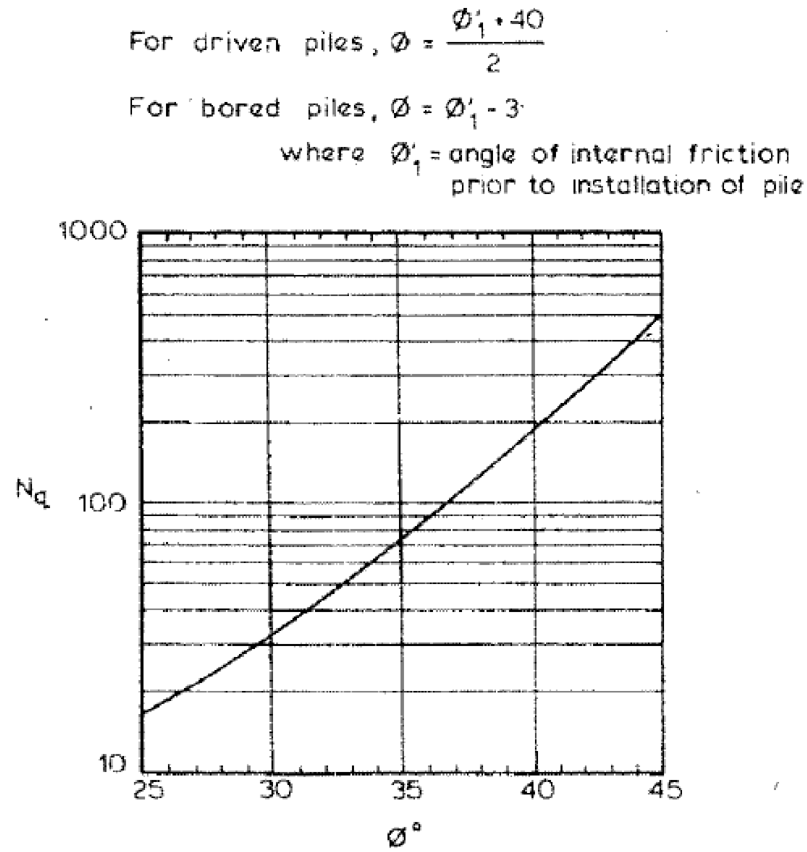

Figure 8. Relationship between Nq and Ø (after Berezantzev et al., 1961).

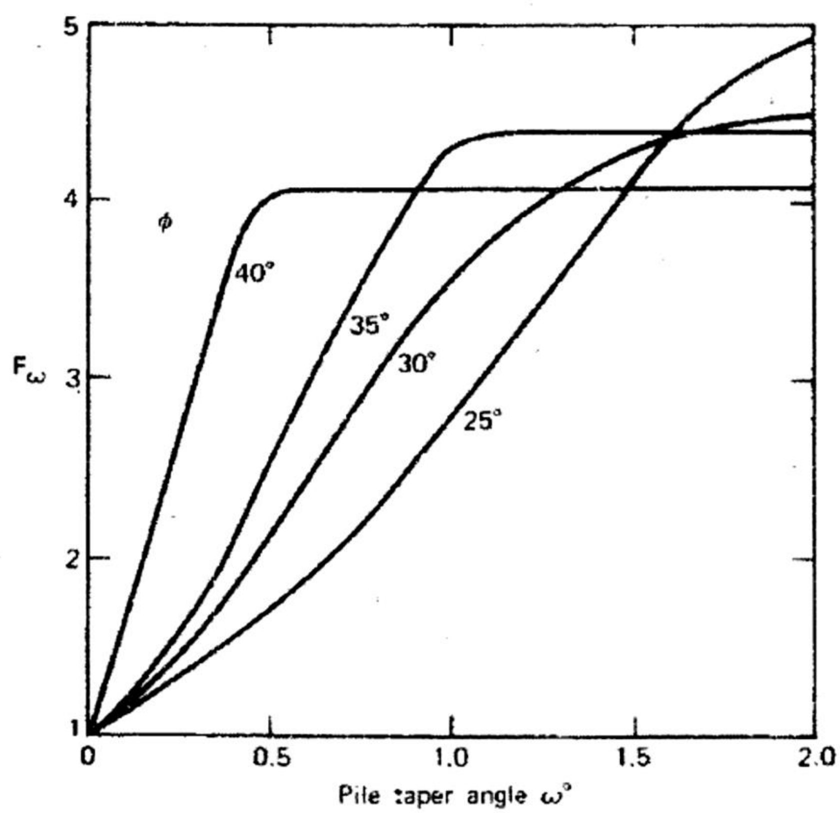

Figure 9. Pile taper factor $F\omega$ (after Nordlund, 1963).

According to Michael Tomlinson and John Woodward (1977), the classical equation to calculate the compression pile capacity in the sand soil is;

`

$$Q_P = N_q \, \sigma'_{v0} \, A_b + \frac{1}{2} K_s \, \sigma'_{v0} \, \tan\delta \; A_s \qquad \ldots\ldots \quad Eq.\ (5)$$

Where,

σ'_{v0} = the effective soil overburden pressure at the pile base level

N_q = pile bearing capacity factor

A_b = the area of the pile base “cross sectional area”

K_s = coefficient of the soil horizontal stress

δ = the angle of friction between pile and soil

A_s = the area of the pile shaft

The factors N_q, K_s are empirical factors obtained from the results of piles static load tests, δ is obtained from the field test and laboratory tests on the friction angle between the different soil types and different pile materials. The value of the empirical coefficient of the pile bearing N_q is developed as stated in the previous paragraphs by Berezantzev et al. (1961) and it has been found that this coefficient is based on the angle of shear resistance ($\emptyset'$) and the ratio between the pile penetration depth over the pile width (diameter), this relationship is shown in the figure 10. Vesic (1967) previously confirmed that these N_q values give results which is almost near to the practical conditions. Another criterion developed by Brinch Hansen to evaluate the factor of the pile bearing N_q, but the values should be multiplied by a shape factor 1.3 for the square and circular pile’s base cross section.

The second term in the equation 5 is used to calculate the pile skin friction resistance to the compression loading. The value of the factor K_s is very critical and difficult to evaluate, because it is depending on the soil’s stress and the installation method of the piles. For example, the using of driven pile technique is increasing the horizontal soil stress from its original K_0 value and the using of bored pile technique can loosen the soil, and reduce the horizontal soil stress. These factors are as follows;

1. The soil stress and its history.
2. The ratio between the pile penetration depth and the pile width or diameter.
3. The shape and the stiffness of the pile.
4. The pile material.

Table 1. The coefficient of the soil horizontal stress, K_S

Installation method	K_S / K_0
Large displacement of driven piles	1.0 *to* 2.0
Small displacement of driven piles	0.75 *to*1.25
Bored and cast-in-place piles	0.7 *to* 1.0
Jetted piles	0.5 *to* 0.7

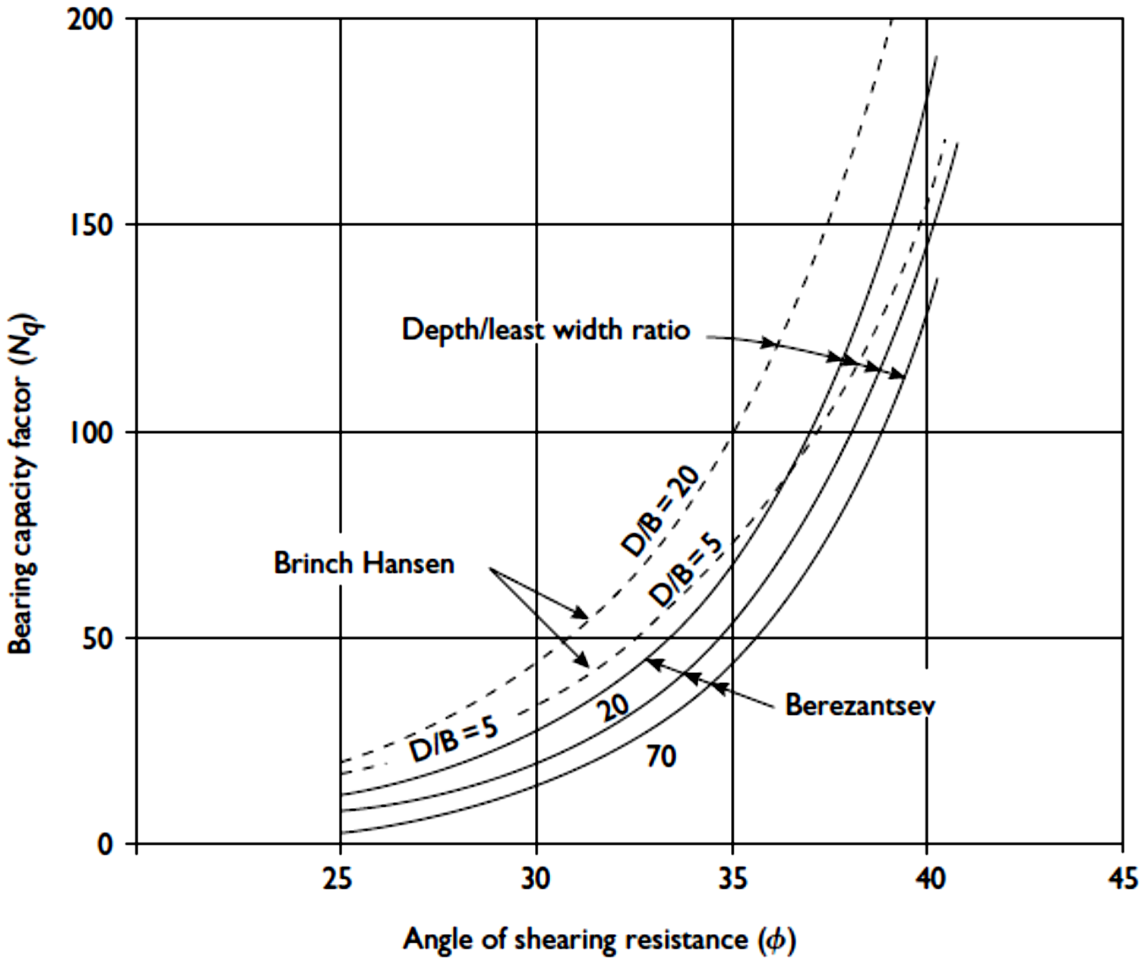

Figure 10. Pile bearing capacity factor N_q

The friction angle between the pile and the soil δ can be assumed based on practical studies as percent from the angle of shearing resistance ($\emptyset'$) of the soil. The angle of shearing resistance can be assumed based on the relationship with standard penetration test (SPT) values as shown in figure11. This factor is depending on the pile surface material. Kulhawy (1984) established some values for this factor based on the pile / soil interface condition and it can be applying for the driven and bored piles.

Table 2. The friction angle between the soil and pile with various interface conditions per Kulhawy (1984).

Interface condition between the pile & soil	**The friction angle between the pile & soil [δ]**
Smooth (coated) steel/sand	$0.5\ \emptyset'$ - $0.7\ \emptyset'$
Rough (corrugated) steel/sand	$0.7\ \emptyset'$ - $0.9\ \emptyset'$
Precast concrete/sand	$0.8\ \emptyset'$ - $1.0\ \emptyset'$
Cast-in-place concrete/sand	$1.0\ \emptyset'$
Timber/sand	$0.8\ \emptyset'$ - $0.9\ \emptyset'$

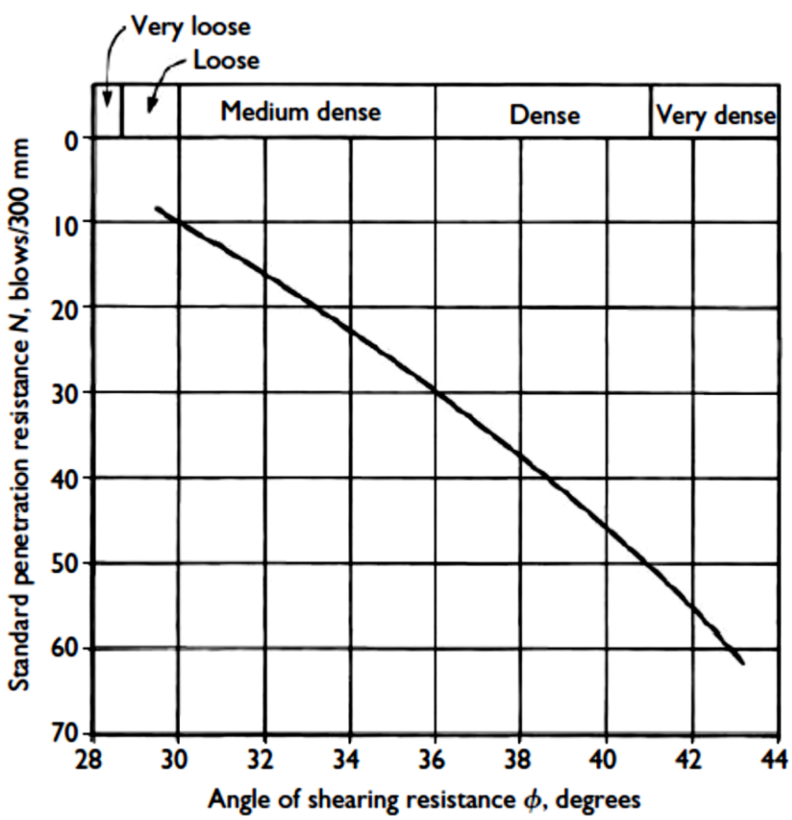

Figure 11. SPT N-values and angle of shearing resistance relationship

2. PILES IN ROCK SOIL

Bored piles which are drilled into rock soil layer act as friction and end bearing piles. Wyllie (1991) estimated the factors and coefficients which are used to estimate the skin friction resistance through the rock socket. For the end bearing and pile settlement factors are summarized in the following items;

1. The socket length to the diameter ration.
2. The rock soil properties like modulus of elasticity and rock strength.
3. The base condition of the drilled pile shaft with respect to the removal of the drilled shaft material.
4. The creep of the pile material.
5. Settlement of the pile head.

Figure 12 showing the effect of the ratio between the rock socket depth and pile diameter, for example if it is required to utilize base and skin friction resistance of the pile depth in the rock layer should be less than 4 times the pile width or diameters.

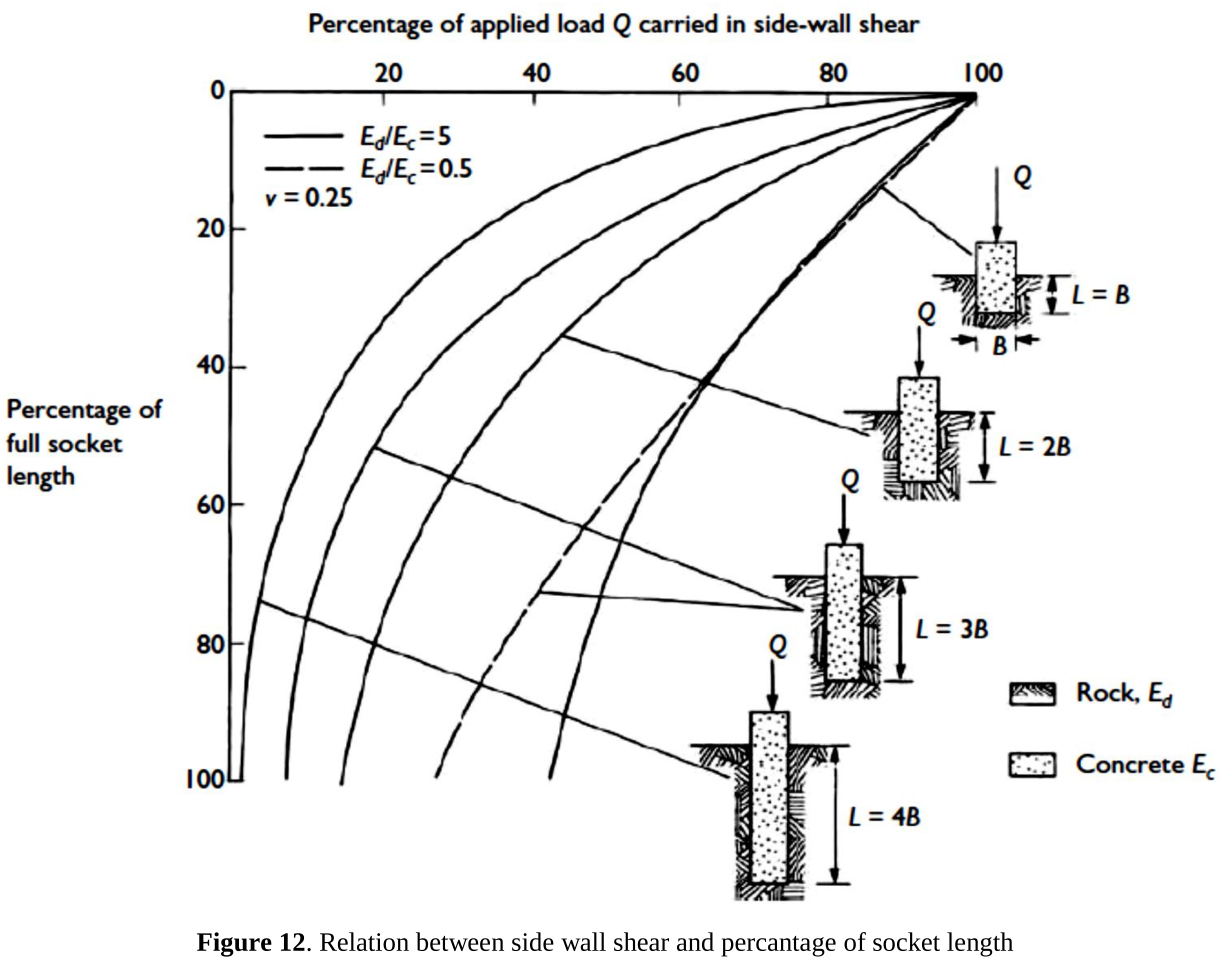

Figure 12. Relation between side wall shear and percantage of socket length

The condition of the pile's surrounding soil layers is very important factor, and it has a significant impact on the pile skin friction. For example, the drilling in clayey shale, or clayey weathered marl cause a softening in borehole wall, as well as, the using of the bentonite slurry in the drilling process has the same impact on the pile skin friction. This impact can be avoided by using a temporary casing technique in the installation of the pile, the casing should be extending to the head of rock soil layer. Wyllie (1991) stated that if the bentonite slurry used in the drilling process of the pile, the rock friction resistance should be reduced by 25% compared to clean rock socket, unless pile load test done to verify the actual value of the friction resistance.

The **shaft resistance** of the pile in the rock soil, depends on the bond between the pile material which is concrete and the rock soil. The bond between the concrete and the rock soil is based on the unconfined compression strength of the rock soil, the rock socket bond stress has been developed by Horvarth (1978), Rosenberg and Journeaux (1976), and Williams and Pells (1981). The ultimate skin friction resistance f_s , in the rock soil can be calculated by the following equation;

$$f_s = \alpha \, \beta \, q_{uc} \qquad \text{….. } \quad Eq. (6)$$

Where,

α = reduction factor related to q_{uc} as shown in figure 13.

β = correction factor related to the discontinuity spacing in the rock mass as shown in figure 14.

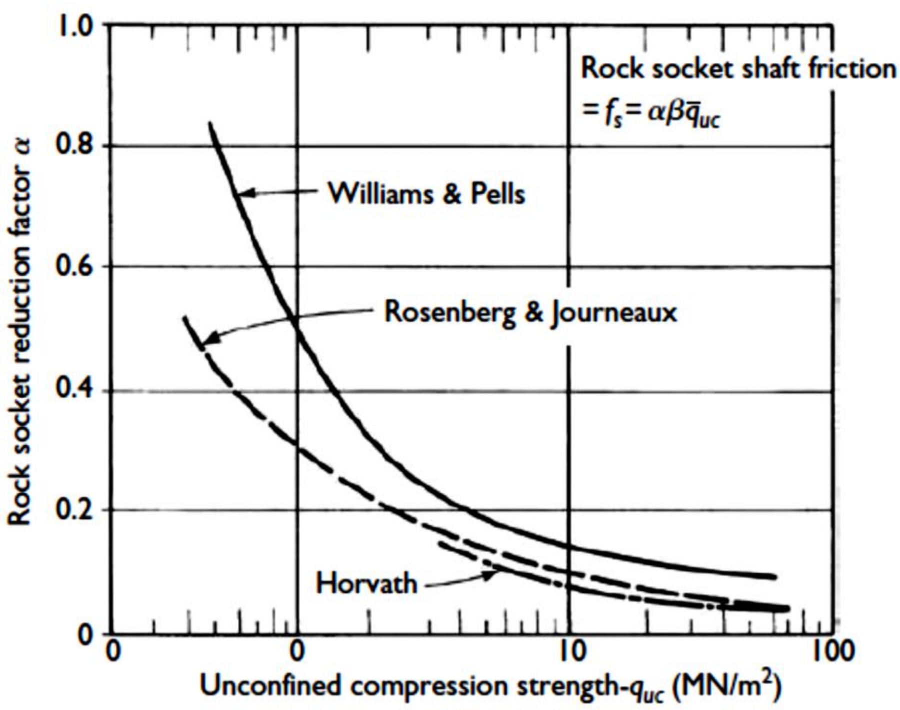

Figure 13. Reduction factors for rock socket shaft friction

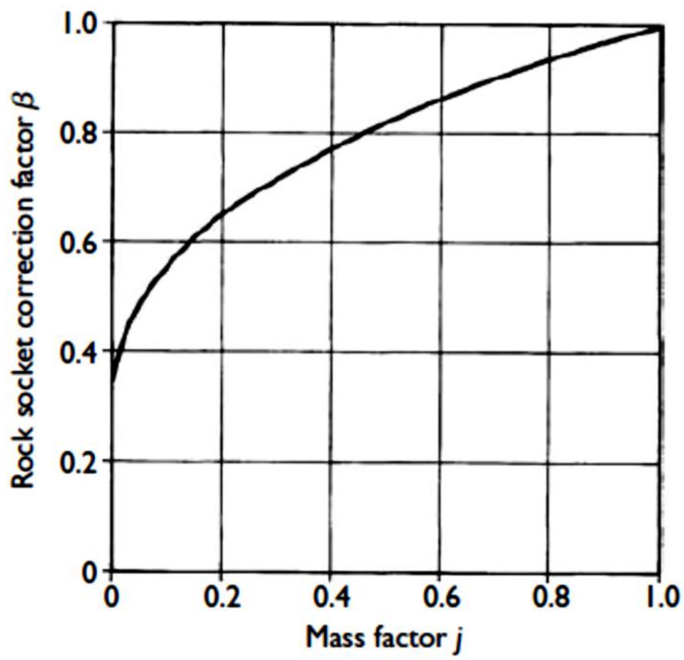

Figure 14. Reduction factors for discontinuities in rock mass (after Williams and Pells)

The Williams and Pells (1981) curve in figure 13 is greater than other curves, but the β factor is having the same value in all curves and it is dependent on the mass factor, j, which is the ratio between the rock's elastic modulus and the intact rock as shown in figure 15. In case if the mass factor j is not identified from the load test, it can be estimated with respect to the rock quality designation (RQD) or the discontinuity spacing quoted by Hobbs (1975) as follows;

Table 3. Mass factor j value with respect to RQD and the discontinuity spacing.

RQD (%)	Fracture frequency per meter	Mass factor *j*
0 – 25	15	0.2
25 – 50	15 - 18	0.2
50 – 75	8 - 5	0.2 – 0.5
75 – 90	5 - 1	0.5 – 0.8
90 – 100	1	0.8 - 1

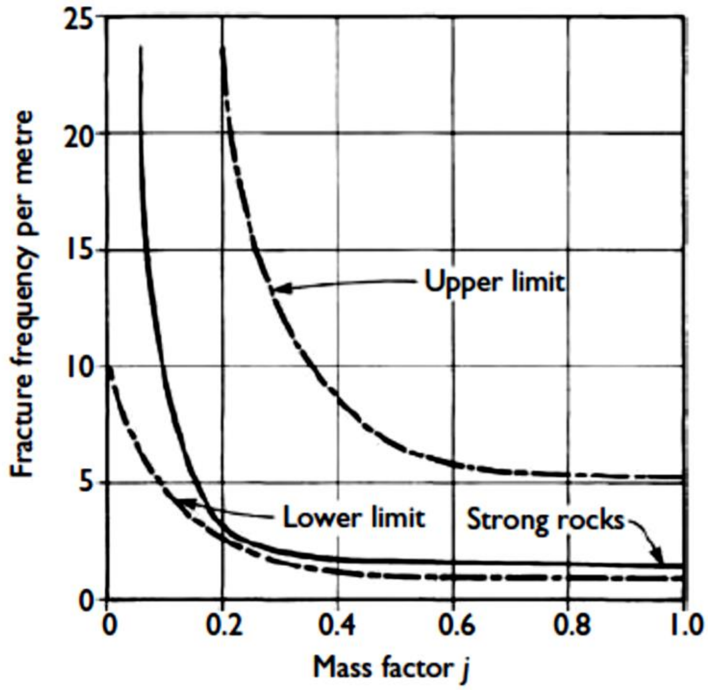

Figure 15. Mass factor value (after Hobbs)

The method used to calculate the pile ultimate **bearing resistance** assume that the pile capacity is a combination between skin friction and end bearing resistances. Both resistances are based on correlations between the pile static load test and the result of filed test in rock formations or laboratory tests. the following is the equation which is used to calculate the pile base resistance for the driven and bored piles;

$$q_b = 2\, N_{\emptyset}\, q_{uc} \qquad \text{….. } \mathit{Eq.\ (7)}$$

Where the bearing capacity factor $N_{\emptyset}$ is equal to;

$$N_{\emptyset} = tan^2(\,45 + \frac{\emptyset}{2}) \qquad \text{….. } \mathit{Eq.\ (8)}$$

The following table shows the variations in the value of bearing resistance factor $N_\emptyset$ for driven and bored piles in different types of rock soil;

Table 4. Ultimate end bearing resistance of piles in weak mudstones, siltstones and sandstones

Description of rock	**Pile type**	**Plate or pile diameter [mm]**	**Observed bearing pressure at failure [MN/m^2]**	**Calculated $N_\emptyset$**
Mudstone / siltstone moderately weak	Bored pile	900	5.6	0.25
Mudstone, highly to moderately weathered weal	Plate test	457	9.2	1.25
Cretaceous mudstone weak, weathered, clayey	Bored pile	670	6.8	3.0
Weak carbonate siltstone/sandstone	Driven	762	5.11	1.5
Calcareous sandstone weak	Driven tube	200	3.0	1.2
Sandstone, weak to moderately weak	Driven	275	19 (from dynamic pile test)	1.75

The pile bearing resistance in weak rock soil depends on the drilling techniques. The use of percussive drilling equipment causes a formation of a soft sludge material at the bottom level of the drilled pile shaft. This is not only causing a reduction in the pile's base resistance, it makes it difficult to identify the accurate classification of the rock soil and difficult to estimate the soil parameters at the base level. In case of weathered mudstones, siltstones and shales undisturbed samples should be collected during the soil investigation stage and shear strength tests should be made and the results will be used to calculate the base resistance. To identify the weathered mudstones, siltstones and shales properties, an uniaxial compression tests should be made on the rock samples to obtain the compression strength. The base resistance can be calculated based on the uniaxial compression test results by using the relationship between q_{uc} and RQD as shown in table 5;

Table 5. Ultimate base resistance of piles in rock soil in terms of RQD

RQD (%)	$\boldsymbol{q_{ub}}$	$\boldsymbol{c}$	$\emptyset$ º
0 – 70	$0.33\ q_{uc}$	$0.1\ q_{uc}$	30
70 - 100	$0.33 - 0.8\ q_{uc}$	$0.1\ q_{uc}$	30 - 60

It is recommended that the pile base resistance which is calculated based on the above description, should be adopted with caution due to the risk of high base settlement. usually a reduction factor equal to 20% is used to control the high values of pile base resistance. In case of using low values of safety factors in the calculation of pile load capacity, this may lead to that the pile settlement due to friction could break the bond between the surrounded soil and the pile material and this will affect directly the calculated pile load capacity especially when the pile capacity is shared between the base and shaft resistance. Therefore, it is recommended to use a reduction factor equal to 30% to 40% to the high value of pile skin friction resistance.

1. PREDICTION OF PILE CAPACITY FROM NON-DESTRUCTIVE STATIC LOAD TEST

Static load testing is still the most reliable method to determine the actual pile ultimate capacity. This method involves physical loading of the pile by using for example massive concrete cubes as shown in Figure 16, with specific dimensions and weight at specific time interval and monitoring the pile settlement of the pile head until failure. The applied load should be increased gradually up to the maximum value of the applied load or up to the maximum allowable pile settlement (pile failure point) then the load should decrease gradually as well. The results of the static load test are plotted as load - settlement curve. And the failure load is calculated, the failure load is the load where the pile is subjected to excessive settlement under small or no load increase.

The pile static load test can be categorized into two categories; the first category is the **failure load test** where the pile is loaded until the failure. The failure load test is necessary to determine the pile's ultimate capacity. The second category is the **proof test** which is used to check the ability of the pile to support a specific service load, usually the loading is up to 1.5 to 2.0 times the design load. Most of time the proof test does not provide the pile's ultimate capacity, therefore this test is not providing a clear information about the pile capacity and it is not support the geotechnical engineers to do a cost saving in the foundation cost.

Figure 16. Pile Static Load Test

Vesic (1977) stated that the scale of the load - settlement curve is based on the elastic deformation of the pile and is expressed as;

$$\delta = PL/EA \qquad \ldots\ldots \quad Eq.\ (9)$$

Where;

δ = elastic deformation of the pile

P = applied load

L = pile length

E = elastic modulus of the pile's material

A = cross sectional area of the pile

The following section explain the different methods which are used to extrapolate the failure load from non-failed load test;

1.1. DAVISSON'S CRITERION

Davisson (1972) defined the ultimate pile load is the load corresponding to the pile head settlement which exceeds the elastic compression of the pile by a displacement equal to 0.15 inches (3.8 mm) plus the pile diameter (in inches) divided by 120;

$$X = 0.15 + B/120 \qquad \ldots\ldots \quad Eq.\ (10)$$

Where;

X = offset displacement of the elastic compression line

B = diameter of the pile in inches

The Davisson's criterion line is parallel to the line of the elastic compression. The intersection of Davisson's line with the load - settlement curve provides the ultimate capacity of the pile. This method has the advantage of being deterministic, while being able to consider the pile geometry and properties. Figure 17 illustrate the use of the Davisson's criterion method to determine the pile's failure load.

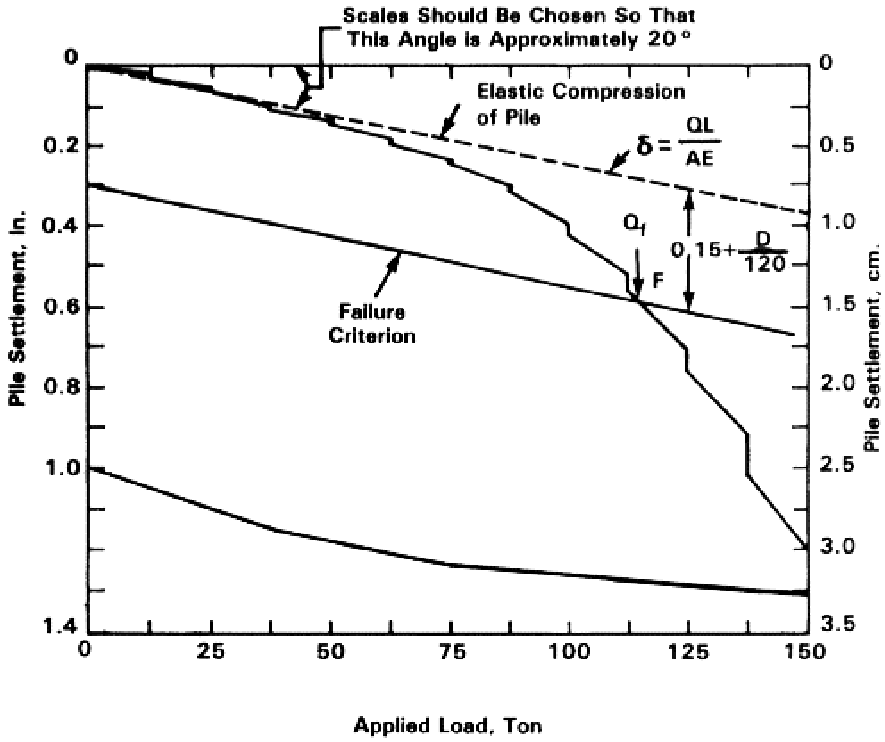

Figure 17. Davisson's Criterion Method

1.2. SHAPE OF THE CURVE

The shape of the curve is an approximation method to determine the failure load or the ultimate pile capacity from non-failure load test. The failure range is defining for load-settlement curve that exhibit rapid settlement with slightly increased loads. The piles that experience non-plunging failure, are difficult to analyze using this method because of the uniform changes in the slope of the lines drawn tangent to the curve. Figure 18 illustrates the use of the shape of the curve method to determine the range of the ultimate pile capacity from non-failure static load test.

1.3. LIMITED TOTAL SETTLEMENT METHOD

The limited total settlement method is an approximation method to calculate or determine the pile ultimate capacity from non-failure load test. The ultimate pile capacity by this method is defined as the load corresponding to the settlement of 1.0 inch and 0.1 times the pile diameter (Terzaghi, 1942). The disadvantage of this method is that it is not applicable in many cases. for example, the elastic deformation of any long steel pile may exceed 1.0 inch and/or 0.1B (pile diameter) without any plastic deformation in the soil.

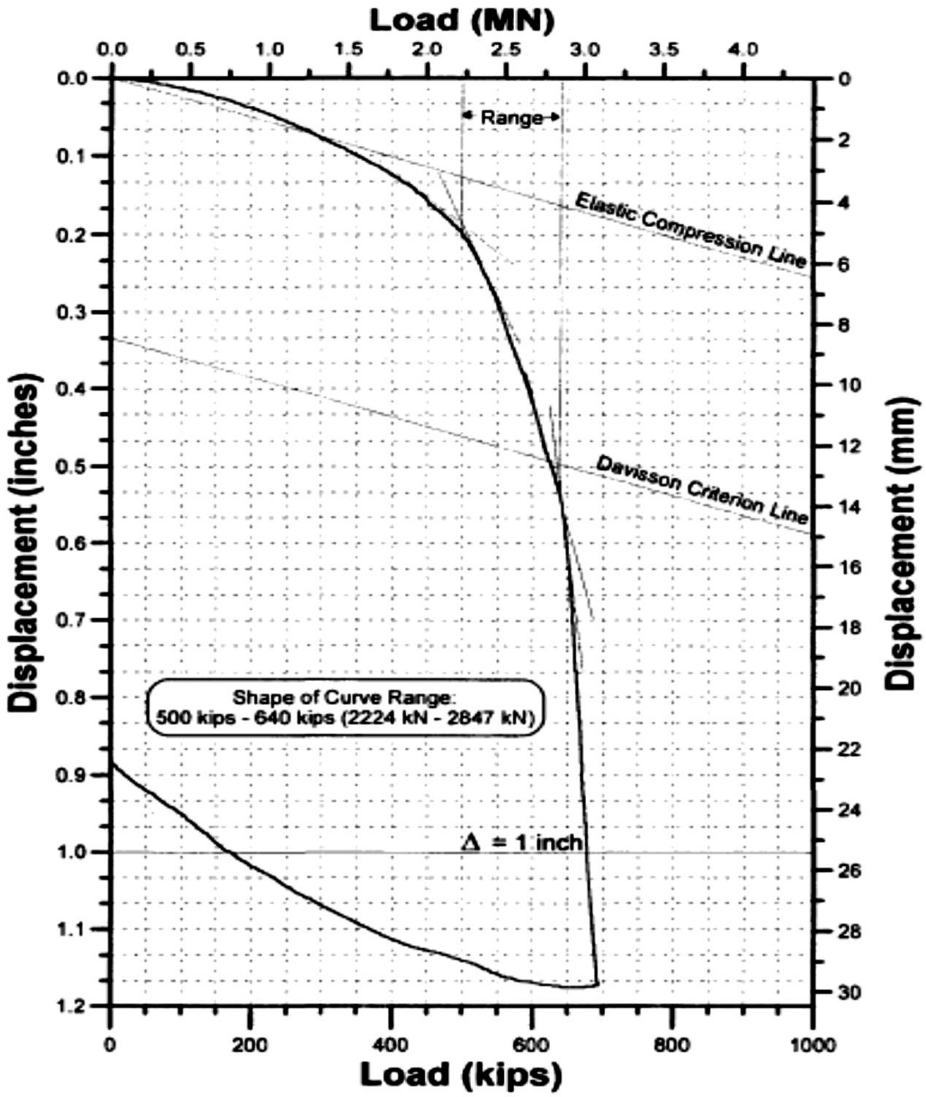

Figure 18. Shape of The Curve Method

1.4. DEBEER'S LOG-LOG METHOD

DeBeer (1970) defines that the ultimate pile capacity as the load which is corresponding to the intersection between the two curves of load - settlement data plotted by using a logarithmic scale. the following figure shows the use of this method to determine the pile ultimate capacity.

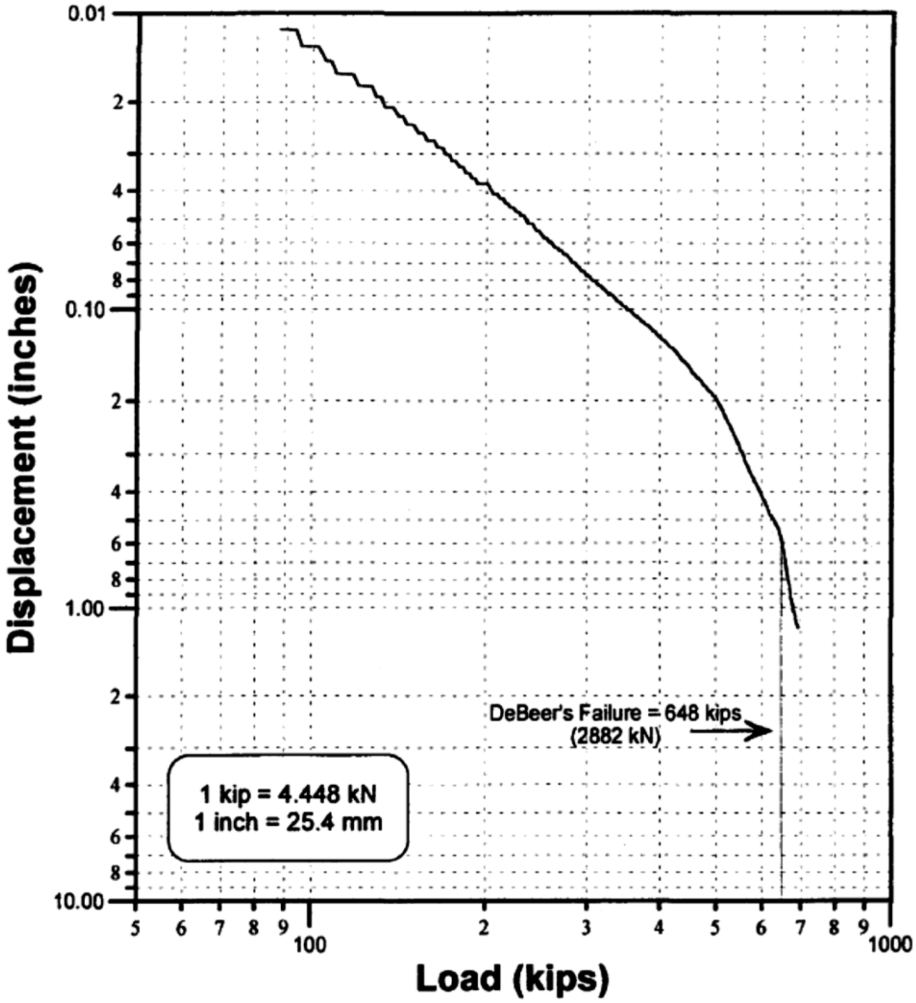

Figure 19. Determine the Failure Load According to DeBeer's Method

1.5. BRINCH-HANSEN'S METHOD

Brinch-Hansen (1963) defined that the ultimate pile capacity obtained from the results of non-failure static load test, this assumes that hyperbolic relationships exist between the loads and the displacements. They proposed two methods 90% and 80% criteria. The first criteria define the ultimate pile capacity as the load which is associated with twice the movement of the pile head as obtained for 90% of the load. The 80% method defines the ultimate pile capacity is the load which is corresponding to four times the movement of the pile head as obtained for 80% of the load (Fellenius, 1989). The following equation explain the use of Brinch-Hansen's method to determine the ultimate pile capacity;

$$Q_u = \frac{1}{2\sqrt{C1+C2}} \qquad \text{..... Eq. (11)}$$

$$\delta_u = \frac{C2}{C1} \qquad \text{..... Eq. (12)}$$

Where;

Q_u = ultimate pile capacity

δ_u = pile displacement at failure

C1 and C2 is the slop and y-intercept respectively, of the straight line obtained by plotting the load-displacement using Y-axis as $\sqrt{\delta}/Q$ and X-axis of Δ, where Δ is the pile displacement and Q is the corresponding load.

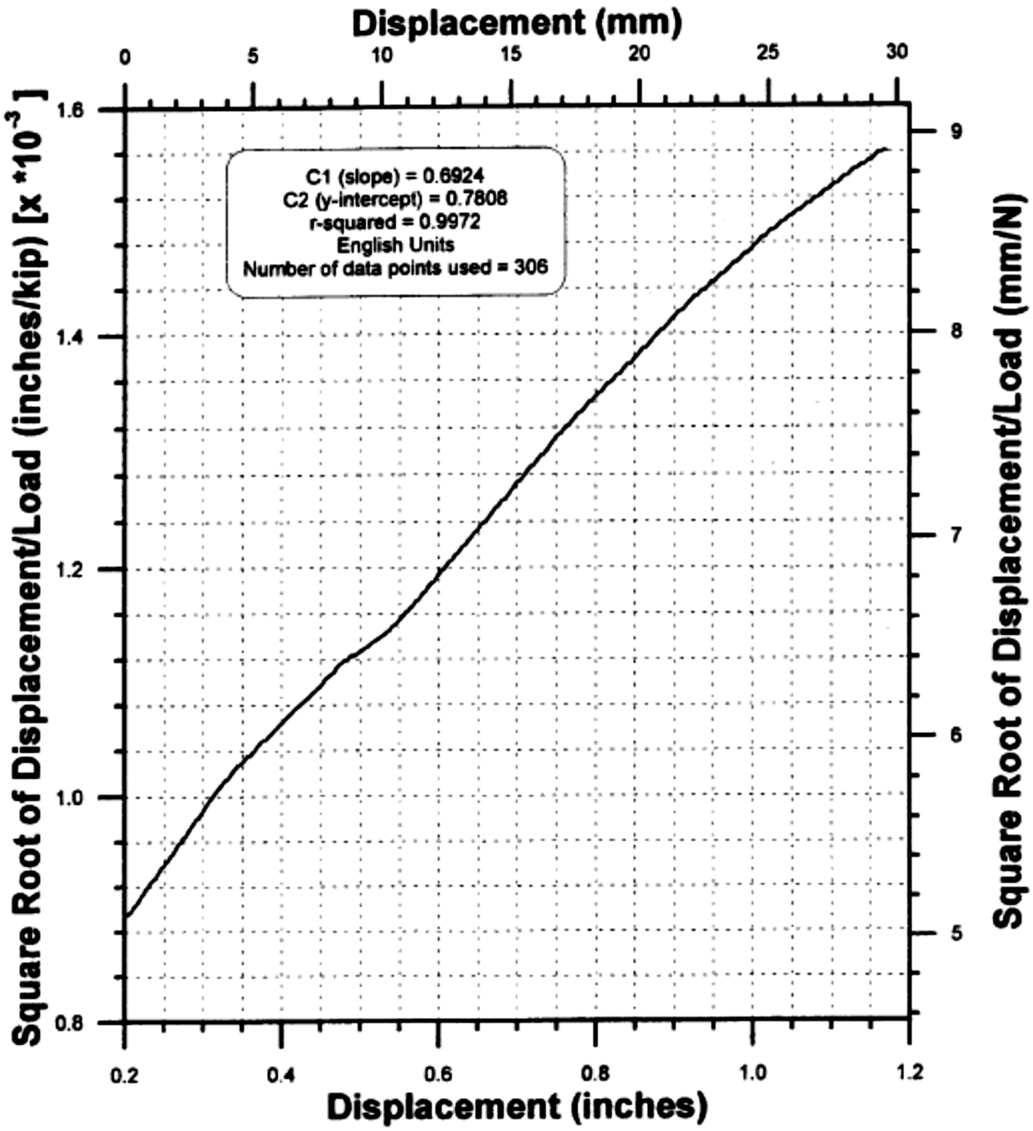

Figure 20. Determine the Failure Load According to Brinch-Hansen Method

1.6. CHIN'S METHOD *(the used method in this research)*

Chin's method (Chin and Vail, 1973) is the most developed method to predict the ultimate pile capacity from the results of non-failure static load test. It is assumed that the load-settlement relationship is hyperbolic, and the ultimate pile capacity can be predicted by plotting a curve between the settlement (Δ) / load (P) in the vertical axis and the settlement (Δ) in the horizontal axis. Then plot the best fit line through the data points. The ultimate pile capacity is derived from the inverse slopes of this line.

$$\frac{\Delta}{Q} = C_1\Delta + C_2 \qquad \text{..... } \textit{Eq. (13)}$$

$$Q_u = \frac{1}{C_1} \qquad \text{..... } \textit{Eq. (14)}$$

Where;

Q_u = ultimate pile capacity

Δ = pile displacement

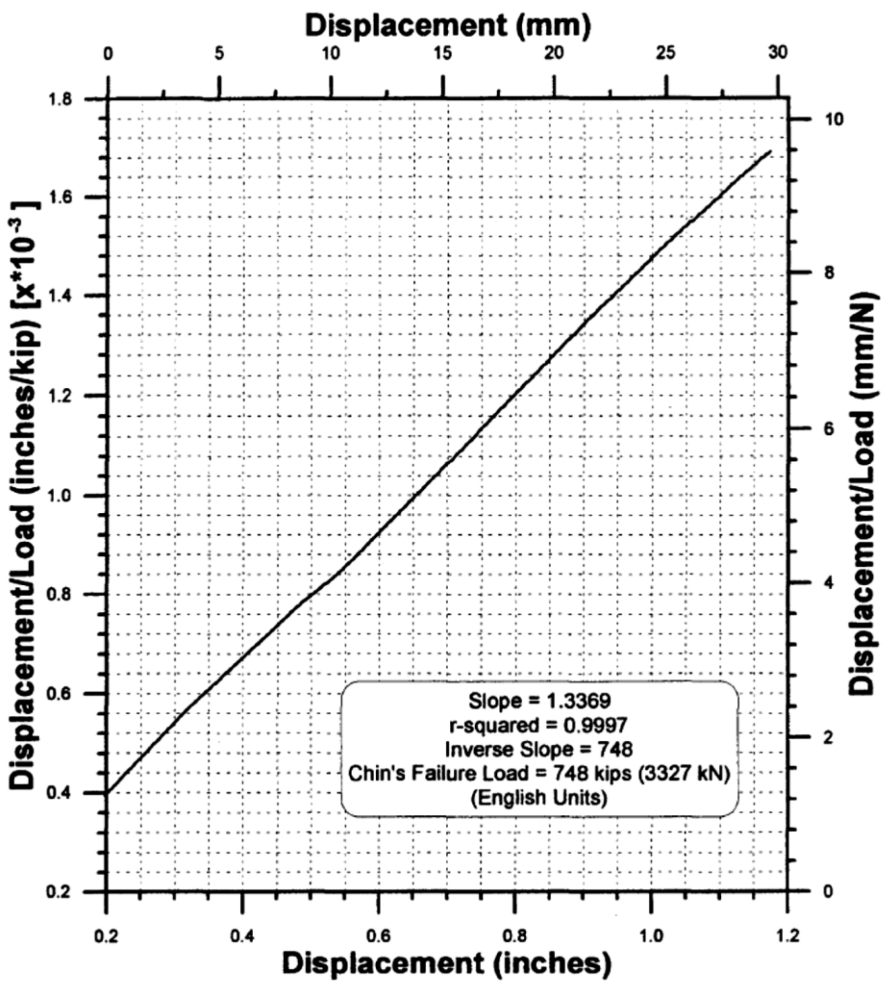

Figure 21. Determine the Failure Load According to Chin's Method

PREDICTION OF PILE CAPACITY FROM NON-DESTRUCTIVE BI-DIRECTIONAL STATIC LOAD TEST (BDSLT)

The bi-directional static load test as stated in the **BS 8004** code and **ASTM D5780** is applied to the piles foundation by dividing the pile to more than one element and each element is tested separately or in combination. For example, the following figure is showing a single level loading arrangement, effectively two independent elements are loaded simultaneously and produce two separate sets of results.

The bi-directional loading test using **Osterberg cells (O-Cells)** recently became a common for different types of pile loading tests, especially when the pile is having a high load test more than 10 MN or where it is not convenient to perform a traditional static load test due to site conditions or lack of space at site.

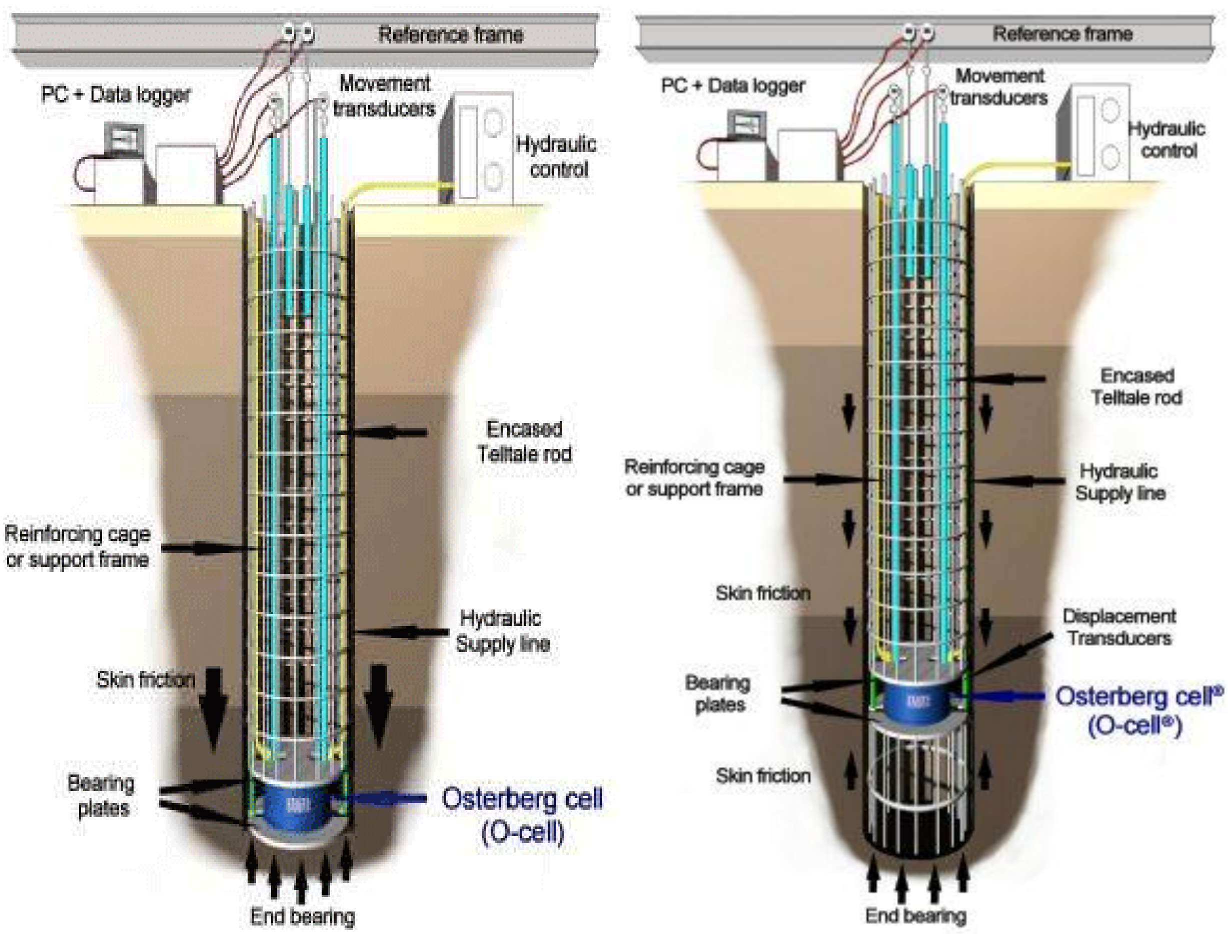

Figure 22. Bi-directional single level load test

The O-Cell is a hydraulic bearing plates installed during the installation of the proposed pile which will be tested. The fixation of O-Cell to be placed during the installation of the pile's reinforcement at a specific level as per the test procedure and specification. The bearing plates are applying the test load in two directions, the upward direction is against the pile skin friction capacity and the downward direction against either pile end bearing capacity alone or pile end bearing capacity with part of skin friction capacity based on the level of the bearing plates.

The using of bi-directional load test became more common nowadays, this is because of the significant development in the piling equipment which gives the geotechnical engineers the ability to use piles having a high compression capacity equal to or more than 10 MN. Moreover, the development in the field of high-rise buildings construction is considered as a challenge to the engineers to find a suitable foundation system which can transfer the structure reactions to the soil hard strata, because of that the required piles capacities increased and the top down static load test (kentledge load test) became not preferable compared to bi-directional static load test in terms of cost and time.

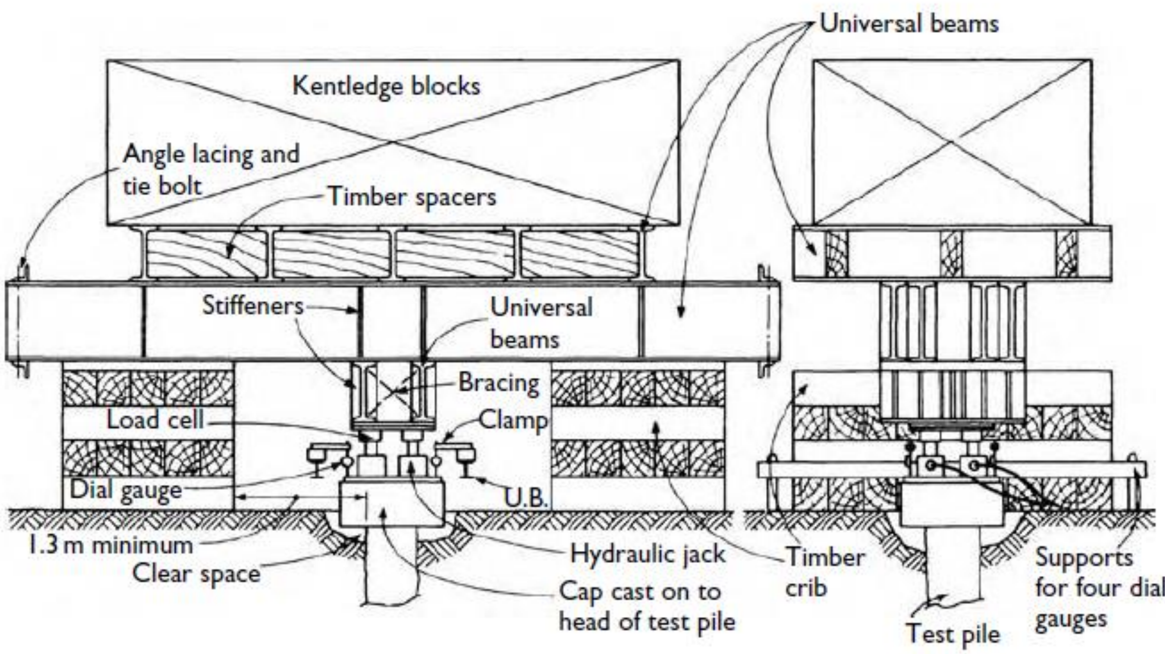

Figure 23. Static load test on pile using kentledge method

The following items show the main differences between the top down static load test (Kentledge load test) and the bi-directional static load test;

A. HIGH LOAD TEST

The value of test load is a very critical factor to choose the pile test type. Especially if the load test is higher than 10 MN, the using of top down load test is not considered as practical option. In terms of bi-directional load test, there are two factors which can make it preferable compared to top down static load test;

1. The cost and time saving in terms of test installation, erection of Kentledge, anchors and the required reaction system.
2. A significant development in terms of safety installation where the loading system at the pile head is not required.

In addition to these two factors, there are some specific factors can be the reason to choose the bi-directional static load test such as the lack of space at site around the testing pile.

Figure 24. Installation of multiple O-Cells

B. LOAD TRANSFER TECHNIQUE

In the top-down static load test the whole test load is transferred to the soil layers through the skin friction between the pile material and the soil layers and the end bearing at the pile toe level as one unit. On the other hand, the test load in case of bi-directional load test is transferred to the soil based on the test arrangement. For example, the single level bi-directional test has two segments. The upper segment resists the test load by the skin friction between the pile material and the upper soil layers which are around the upper pile segment. The lower segment resists the test loading by the end bearing or end bearing with partial skin friction based on the O-Cell level compared to the pile toe level.

EQUIVALENT TOP-DOWN STATIC LOADED LOAD-SETTLEMENT CURVE FROM THE RESULTS OF A BI-DIRECTIONAL STATIC LOAD TEST (BDSLT)

The BDSLT is used as alternative solution to the top-down static load test in some specific cases. But the test results should be analyzed to generate the load versus settlement curve which is used to understand the pile behavior during the loading test. To estimate the load-settlement curve from a BDSLT, there are some assumption should be taken into consideration as follows;

1. The upper skin friction (side shear) load-movement curve resulting from the upward movement of O-Cell is equal to the settlement of the pile head in a conventional top-down static load test.
2. The part of the pile shaft below the O-Cell has the same load-movement behavior as the downward pile movement in a conventional top-down static load test. The subsequent movement curve in the BDSLT refers to the combined lower skin friction and end bearing movement of the entire length of pile shaft below the O-Cell level (2nd segment)
3. The pile is considered as rigid body, but the elastic deformation of the pile is considered in the estimation of the load-settlement curve as a correction procedure.

PROCEDURE A

This procedure complies with the above assumptions, to construct the equivalent load-settlement curve the following steps should be followed;

I. Select an arbitrary pile's movement such as the 0.40 inches to give point 4 on the pile shaft skin friction (side shear) load-movement curve in figure 25.
II. Record the corresponding load to the 0.40 inches’ movement which is 2,090 tons in this example. Because it is initially assumed that the pile is rigid body, the top of the pile moves downward the same as the bottom of the pile.
III. Similarly find out the corresponding load to the same value of the movement in the end bearing load movement curve which is 1,060 tons.

IV. Adding these two loads will give the total load of 3,150 tons due to side shear plus end bearing at the same movement and thus gives point 4 on the figure 26 load-settlement curve for an equivalent top-down static load test. The above steps can be used to obtain all the points in figure 26, and generate the best hyperbolic curve fitting these points which is the equivalent top-down static load-settlement curve.

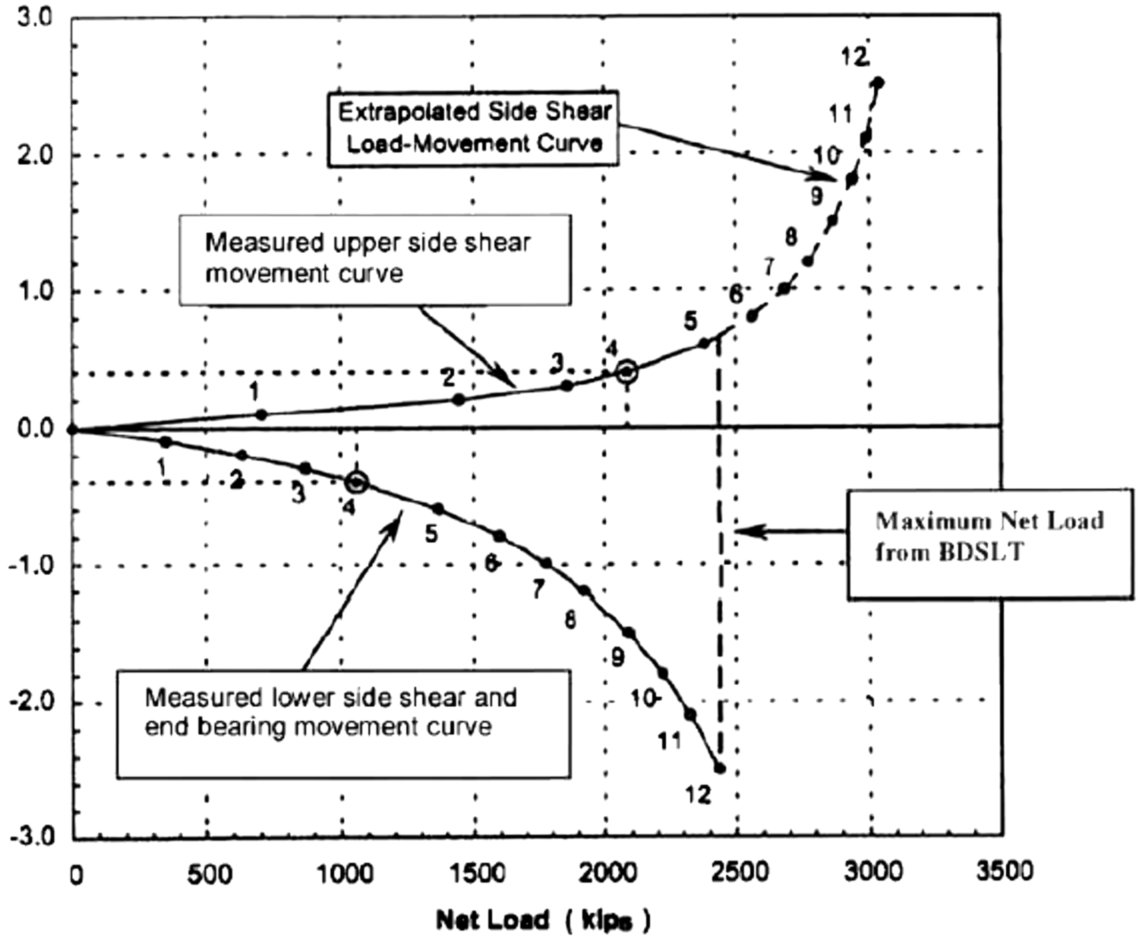

Figure 25. BDSLT results

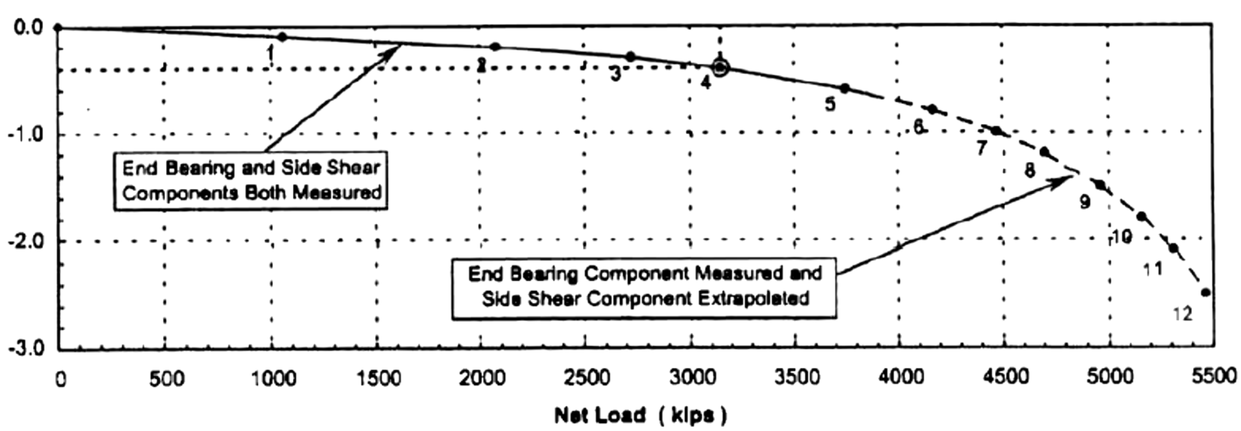

Figure 26. The equivalent top-down static load test curve

PROCEDURE B

This procedure is to estimate the elastic deformation of the pile and to modify the proposed load - settlement curve from the previous procedure. Figure 27 gives the equations which are used to determine the elastic deformation of the pile that occur in the BDSLT. Figure 28 gives the equations for the elastic deformation of pile that occur in the equivalent top-down static load test (TST). Subtracting the BDSLT from TLT compression gives the desired additional elastic compression at the top of the pile. Then this value is added to the rigid equivalent curve obtained from procedure A to obtain the final corrected equivalent load-settlement curve.

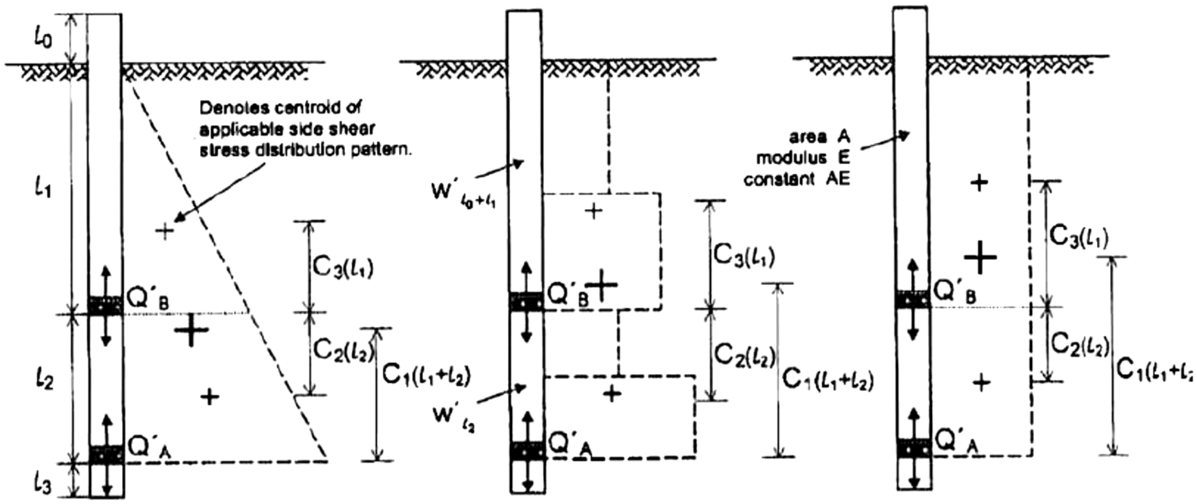

1-Stage Single Level Test (Q'_A only): $\delta_{BDSLT} = \delta_{\uparrow l1} + \delta_{\downarrow l2}$

$C_1 = \frac{1}{3}$	Centroid Factor = C_1	$C_1 = \frac{1}{2}$
$\delta_{\uparrow(l_1+l_2)} = \frac{1}{3}\frac{Q'_{\uparrow A}(l_1+l_2)}{AE}$	$\delta_{\uparrow(l_1+l_2)} = C_1\frac{Q'_{\uparrow A}(l_1+l_2)}{AE}$	$\delta_{\uparrow(l_1+l_2)} = \frac{1}{2}\frac{Q'_{\uparrow A}(l_1+l_2)}{AE}$

Net Loads:

$Q'_{\uparrow A} = Q_{\uparrow A} - W'_{l_0+l_1+l_2}$ $\quad Q'_{\uparrow B} = Q_{\uparrow B} - W'_{l_0+l_1}$ $\quad Q'_{\downarrow B} = Q_{\downarrow B} + W'_{l_2}$

W' = pile weight, bouyant where below water table

Figure 27. Theoretical elastic deformation in BDSLT based on pattern of skin friction stress development

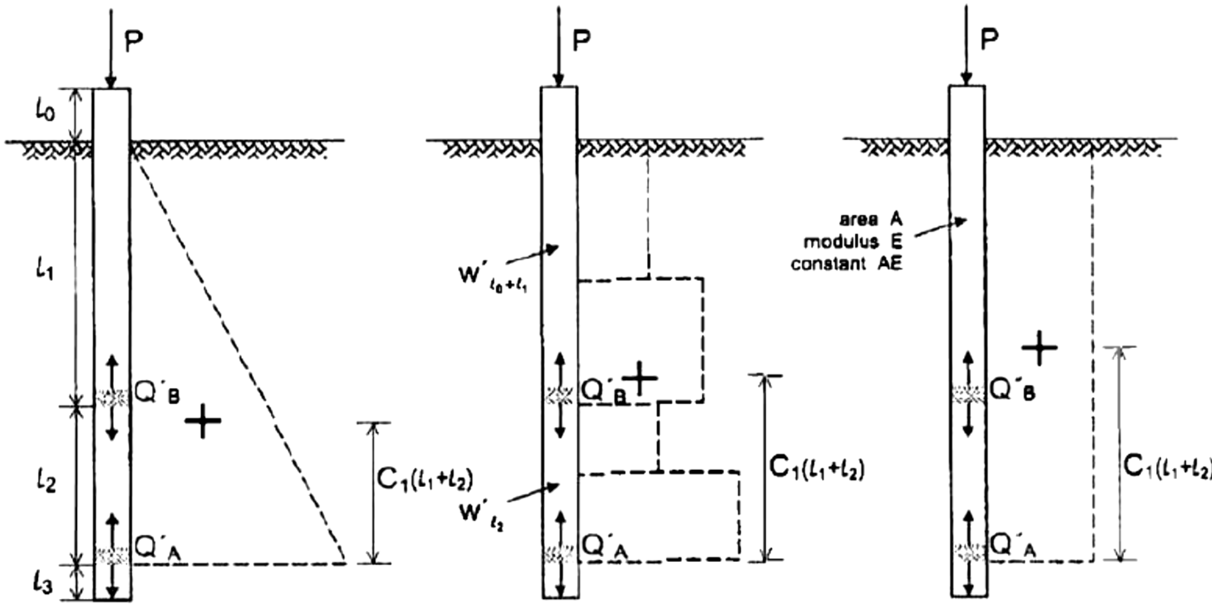

Top Loaded Test: $\delta_{TLT} = \delta_{\downarrow \ell_0} + \delta_{\downarrow \ell_1+\ell_2}$

$\delta_{\downarrow \ell_0} = \dfrac{P\ell_0}{AE}$	$\delta_{\downarrow \ell_0} = \dfrac{P\ell_0}{AE}$	$\delta_{\downarrow \ell_0} = \dfrac{P\ell_0}{AE}$
$C_1 = \dfrac{1}{3}$	Centroid Factor = C_1	$C_1 = \dfrac{1}{2}$
$\delta_{\downarrow \ell_1+\ell_2} = \dfrac{(Q'_{\downarrow A} + 2P)}{3} \dfrac{(\ell_2 + \ell_2)}{AE}$	$\delta_{\downarrow \ell_1+\ell_2} = [(C_1)Q'_{\downarrow A} + (1 - C_1)P]\dfrac{(\ell_1 + \ell_2)}{AE}$	$\delta_{\downarrow \ell_1+\ell_2} = \dfrac{(Q'_{\downarrow A} + P)}{2} \dfrac{(\ell_1 + \ell_2)}{AE}$

Net and Equivalent Loads:

$Q'_{\downarrow A} = Q_{\downarrow A} - W'_{\ell_0+\ell_1+\ell_2}$ $\quad P_{single} = Q'_{\downarrow A} + Q'_{\uparrow A}$ $\quad P_{multi} = Q'_{\downarrow A} + Q'_{\uparrow B} + Q'_{\downarrow B}$

Figure 28. Theoretical elastic deformation in top-down static load test based on pattern of skin friction stress development

LONG / MEGA PILING SYSTEM FOR HIGH-RISE BUILDINGS

In the last two decades there was a significant development in terms of high-rise buildings construction. The developed countries are competing with each other to build higher buildings which are used as icon for each country. In consequence, the engineers have been subjected to different challenges, to achieve the structural stability of the high-rise buildings. One of the major types of these challenges is the foundation system of high-rise building. The most used foundation system is the piled raft foundation system, the piles depth in this case can be reach 40 to 60 m which is considered as long piles. The definition of long piles is these piles which are having a depth equal to or more than 20 to 25 m. This chapter will discuss some aspect of design and construction of long bored pile foundation system and brief about the pile's bearing behavior.

INTRODUCTION

Because of rapid growth of the global economy in the last two decades, numerous developed countries in different regions have been built high-rise buildings, its height reaches to more than 600 to 700 m. Nowadays, there is an existing building located in Dubai, UAE the building's height is reaches to almost 830 m (tallest building in the world) and it is consisting 163 floors. Also, there is a building under construction located in Jeddah, KSA the building's height will reach to almost 1,000 m and the building after the construction will be the tallest building in the world.

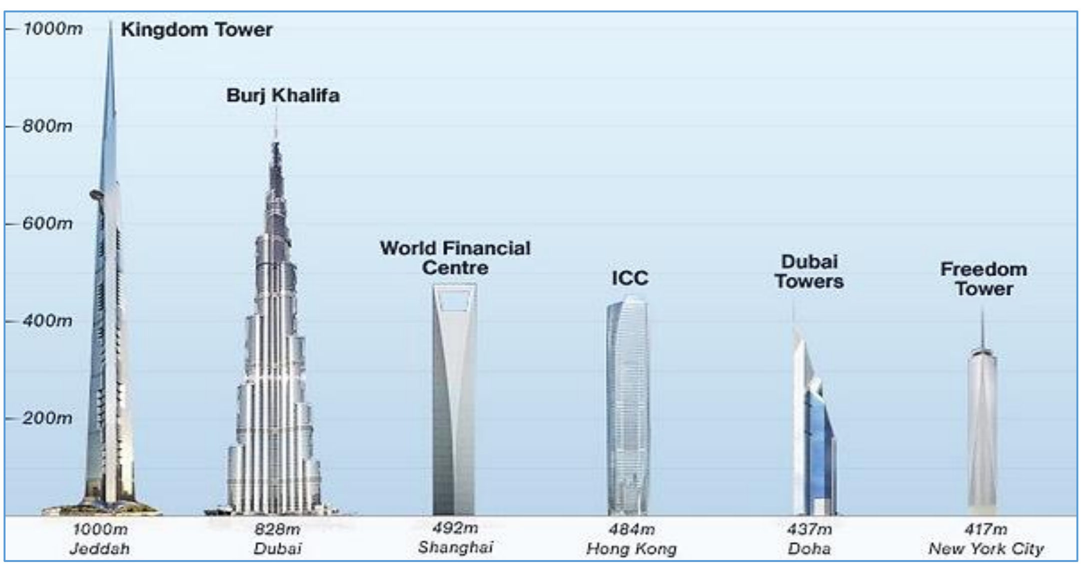

Figure 29. Tallest buildings in the world

Until now the experience of the design and construction of super-long piles is very limited and still the methods used are the traditional methods which are based on the old practical tests which have been done on short piles. Therefore, geotechnical engineers are being forced to develop these traditional design methods to match the current situation of the developed construction methods and the developed drilling techniques. The following sections in this chapter will give a simple idea about the super-long piles in terms of construction and design.

BEARING BEHAVIORS OF LONG PILE

Long piles mainly represent the piles with depth larger than 35 m and slenderness ratio (L/D) larger than 30, Where L is the pile depth and D is the pile diameter. Both theoretical studies and engineering practices show that the long piles behaviors are different from short piles. This is because there are many soil layers around the piles shaft, this leads to complex behavior in terms of pile shaft resistance of long piles compare to short piles. Furthermore, because of the large pile length and high slenderness ratio of the long bored pile, the stiffness of pile-soil system is relatively small. This influences the bearing characteristics of the long piles. With reference to the analysis of practical load tests results (Zhang and Liu, 2009), the basic bearing behaviors of long piles summarized in the following steps:

1. The pile load - settlement curve has no significant change in the slope, in case of the pile tip is post grouted.
2. In case of ultimate bearing load, the settlement of the pile head is mainly caused by pile shaft compression, especially the upper half of pile shaft. In addition, the pile shaft presents large plastic deformation under high load.
3. The pile shaft friction in the top soil layers is mobilized before that in the deep layers.
4. The mobilization of the pile shaft friction is dependent on the support condition at the pile tip. Therefore, the pile tip resistance and pile shaft friction can be increased significantly in case of the support condition is improved by post grouting at pile tip.

CHAPTER 2 – RESEARCH METHODOLOGY

The main purpose of the research is to compare between the theoretical, practical and numerical pile compression capacities. The research concentrate on the piles which had been installed in Dubai. And the research methodology is summarized in the following procedure;

1. Selection of **three** different cases of study (project) and collection of all required data which are required to determinate the pile capacities like;
   A. Project piling drawing including all the information about the pile such as pile cutoff level, pile toe level, pile diameter and the demanded pile capacity.
   B. Project soil investigation report including all the information about the soil layers' classifications and the recommendations about the piles foundation.
   C. The results of pile's static load test results, this is to predict the practical pile capacity by using Chin's method (see Section 1.6) in case of non-destructive static load test.
2. The first step is to extract the value of the theoretical pile compression capacity of the selected pile type in each case of study from the piles recommendation in the soil investigation report. The selected compression capacity is calculated based on the theoretical equations which are mentioned in chapter 1, equations 5, 6 and 7.

Table No. 9: Allowable Working Loads in Compression (Cut off level +3.30 DMD)

Toe Level of Piles (m DMD)	Allowable Working Loads in Compression (kN)				
	Pile Diameter (m)				
	0.60m	0.75m	0.90m	1.00m	1.20m
-16.00	1,866	2,332	2,799	3,110	3,732
-16.50	2,021	2,526	3,031	3,368	4,042
-17.00	2,176	2,720	3,263	3,626	4,351
-17.50	2,331	2,913	3,496	3,884	4,661
-29.00	5,251	6,564	7,877	8,752	10,502
-29.50	5,441	6,801	8,161	9,068	10,882
-30.00	5,630	7,038	8,446	9,384	11,261
-30.50	5,820	7,275	8,730	9,700	11,640
-31.00	6,010	7,512	9,015	10,016	12,020

Figure 30. Sample of piles recommendation in the soil investigation report

3. The practical pile capacity of the selected pile from each case of study will be estimated by using Chin's method (see Section 1.6). Chin's method is the most developed method to predict the ultimate pile capacity from the results of non-failure static load test. The used data to plot the Chin's curve are based on the actual results of pile's static load test by using one of the following techniques the first is kentledge load test or the second which is the bidirectional static load test.
4. For numerical pile capacity, a finite element model for the selected pile type from each case will be modeled by using PLAXIS 2D software to get the piles compression capacity. All the soil parameters which will be used in the numerical model will be extracted from the soil investigation report of each case.
5. Finally, a Comparison between theoretical, practical and numerical pile capacity of each case will be done and will be discussed in details.

CASES OF STUDY

Three cases of study have been chosen to be used in this research, this section will cover each case of study's description and the selected pile details.

CASE 1 _ AL HABTOOR RESIDENCE

Al Habtoor residence project is consisting 40 floors tower and two numbers of 60 floors towers over a common podium situated on a 25,000 m^2 plot. The project is to have one basement for parking with an additional 3 parking floors within the podium. The ground floor of the podium includes retail spaces whilst the top of the podium is landscaped with facilities for tenants.

Figure 31. Al Habtoor residence

The project is located on plot No. 3450106 at Burj Khalifa and business bay areas in Dubai.

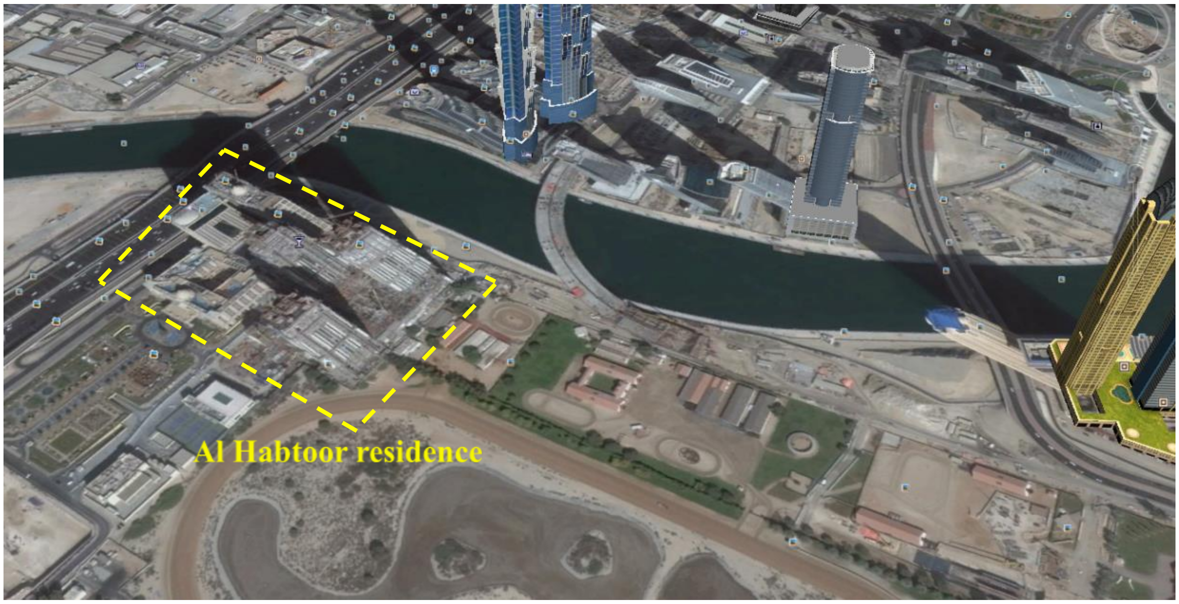

Figure 32. Al Habtoor residence location

PILE DETAIL

The selected pile from this case of study details are as the following table;

Table 6. Pile details

Pile Details			
Pile C.O.L [m]	Pile Toe Level [m]	Pile Length [m]	Pile Diameter [mm]
-4.85	-57.0	52.15	1,500

Cut off Level DMD (m)	Toe Elevations DMD (m)	Tentative Compressive Working Pile Capacities (Tons)*																	
		600mmϕ			750mmϕ			900mmϕ			1200mmϕ			1500mmϕ			1750mmϕ		
		Total Capacity	Friction	End Bearing	Total Capacity	Friction	End Bearing	Total Capacity	Friction	End Bearing	Total Capacity	Friction	End Bearing	Total Capacity	Friction	End Bearing	Total Capacity	Friction	End Bearing
-4.0 to -6.0	-21.0	234	199	35	303	249	54	376	299	78	536	398	138	714	498	216	875	581	294
	-25.0	322	265	58	421	331	90	527	397	130	760	530	230	1022	662	360	1262	772	490
	-29.0	422	365	58	546	456	90	677	547	130	960	730	230	1272	912	360	1554	1064	490
	-33.0	472	438	35	601	547	54	734	656	78	1013	875	138	1310	1094	216	1570	1276	294
	-38.0	529	494	35	672	618	54	819	741	78	1126	988	138	1451	1235	216	1735	1441	294
	-41.0	563	528	35	714	660	54	870	792	78	1194	1056	138	1536	1320	216	1834	1540	294
	-45.0	653	596	58	835	745	90	1023	894	130	1422	1192	230	1850	1490	360	2228	1738	490
	-49.0	752	680	72	962	850	113	1182	1020	162	1648	1360	288	2150	1700	450	2595	1983	613
	-54.0	897	812	85	1148	1015	133	1409	1218	191	1964	1624	340	2561	2030	531	3091	2369	723
	-57.0	979	894	85	1251	1118	133	1533	1341	191	2128	1789	340	2767	2236	531	3331	2608	723
-10.0	-57.0	933	848	85	1193	1060	133	1463	1272	191	2036	1696	340	2651	2120	531	3196	2473	723

Figure 33. Piles recommendations as per project's soil investigation report

SOIL LAYERS' CLASSIFICATIONS

Reference to the soil investigation report from M/S Al Hai & Al Mukaddam REF: SR/1305101-2. REV 01, the soil layers' classifications are as per the following table;

Table 7. Soil layers' classifications

No.	Soil Layer	Layer Depth [m]	Soil parameters
1	Silty Sand and Calcrenite	3.15	E = 30,000 KN/m2 γsat = 18.5 KN/m3 γun sat = 18.5 KN/m3 $\varphi = 34^o$ υ = 0.3
2	Very Weak Sandstone	15.0	E = 200,000 KN/m2 γsat = 19.0 KN/m3 γun sat = 19.0 KN/m3 $\varphi = 40^o$ υ = 0.3
3	Calcisiltite and Gonglomerate	69.0	E = 400,000 KN/m2 γsat = 19.5 KN/m3 γun sat = 19.5 KN/m3 $\varphi = 40^o$ υ = 0.3

The modulus of elasticity (*E*) of each soil layer was missing in the project soil investigation report. Therefore, it has been estimated by using the following table of typical modulus of elasticity values for different soil types.

Table 8. Typical values of modulus of elasticity for different types of soils

No.	Type of Soil	*E* [N/mm^2]
1	Silty Sand	7 – 21
2	Loose Sand	10 – 24
3	Dense Sand	48 – 81
4	Shale & Rock	144 – 14,400

CASE 2 _ BLUEWATER HOSPITALITY

The project is located on reclaimed island (blue water island) of the coast of Dubai opposite to Jumeriah Beach Residence and Dubai Marina. The island has been reclaimed using dredged sand compacted using vibro compaction technique. The project is Bluewater island development; it consists of the following structures;

Table 9. Bluewater Hospitality Buildings' Details

Building	Occupancy	Building Details
Luxury Hotel	Hotel	Basement+ Basement mezzanine+ Ground+ Mezzanine+ 3 typical floors+ roof+ top roof
Family Hotel	Hotel	Basement+ Basement mezzanine+ Ground+ Mezzanine+ 2 typical floors+ roof+ top roof
Serviced apartment SA1	Residential	Partial Basement-2 + Basement-1 + Ground + Mezzanine+ 6 typical floors+ roof + top roof
Serviced apartment SA2	Residential	2 Basements+ Ground+ Mezzanine+ 7 typical floors+ roof + top roof
Beach Club	Club	Basement+ Ground + roof
Event Venu	Public	Basement+ Ground + Mezzanine + roof

Figure 34. Proposed Bluewater Hospitality Development

PILE DETAIL

The selected pile from this case of study details are as the following table;

Table 10. Pile Details.

Pile Details			
Pile C.O.L [m]	Pile Toe Level [m]	Pile Length [m]	Pile Diameter [mm]
+3.375 DMD	-31.0 DMD	34.375	900

Toe Level of Piles (m DMD)	Allowable Working Loads in Compression (kN)				
	Pile Diameter (m)				
	0.60m	0.75m	0.90m	1.00m	1.20m
-16.00	1,866	2,332	2,799	3,110	3,732
-16.50	2,021	2,526	3,031	3,368	4,042
-17.00	2,176	2,720	3,263	3,626	4,351
-17.50	2,331	2,913	3,496	3,884	4,661
-18.00	2,473	3,091	3,709	4,122	4,946
-18.50	2,607	3,259	3,911	4,345	5,214
-19.00	2,741	3,426	4,112	4,569	5,482
-19.50	2,875	3,594	4,313	4,792	5,751
-20.00	2,981	3,726	4,471	4,968	5,962
-20.50	3,067	3,834	4,601	5,112	6,135
-21.00	3,154	3,943	4,731	5,257	6,308
-21.50	3,241	4,051	4,861	5,401	6,481
-22.00	3,337	4,171	5,005	5,561	6,673
-22.50	3,439	4,299	5,159	5,732	6,878
-23.00	3,542	4,427	5,312	5,903	7,083
-23.50	3,644	4,555	5,466	6,073	7,288
-24.00	3,765	4,707	5,648	6,276	7,531
-24.50	3,900	4,874	5,849	6,499	7,799
-25.00	4,034	5,042	6,051	6,723	8,067
-25.50	4,168	5,210	6,252	6,946	8,336
-26.00	4,302	5,377	6,453	7,170	8,604
-26.50	4,436	5,545	6,654	7,393	8,872
-27.00	4,570	5,713	6,855	7,617	9,140
-27.50	4,704	5,880	7,056	7,840	9,409
-28.00	4,872	6,090	7,308	8,120	9,743
-28.50	5,061	6,327	7,592	8,436	10,123
-29.00	5,251	6,564	7,877	8,752	10,502
-29.50	5,441	6,801	8,161	9,068	10,882
-30.00	5,630	7,038	8,446	9,384	11,261
-30.50	5,820	7,275	8,730	9,700	11,640
-31.00	6,010	7,512	9,015	10,016	12,020

Figure 35. Piles recommendations as per project's soil investigation report

SOIL LAYERS' CLASSIFICATIONS

Reference to the soil investigation report from M/S Al Hai & Al Mukaddam REF: SD 14000067-Rev 0, the soil layers' classifications are as per the following table;

Table 11. Soil layers' classifications

No.	Soil Layer	Layer Depth – m Elevation of Engineering Parameters bottom of each layer (m DMD)		Engineering Parameters				
		Avg. Thick - m	To	Unit Wt, KN/m^3	E - MPa	Poison Ratio	C' - KPa	Ø^o
1	Silty fine sand	13.00	-10.00	18	25	0.35	0	34
2	Dense to very dense sand	0.7	-10.70	18	50	0.35	0	36
3	Calacrenite / Sandstone	3.3	-14.00	22	200	0.3	70	32
4		2.0	-16.00	22	200	0.3	100	32
5		2.0	-18.00	22	200	0.3	80	32
6		2.0	-20.00	22	200	0.3	60	32
7		2.0	-22.00	22	75	0.3	20	27
8		2.0	-24.00	22	75	0.3	27	27
9		4.0	-28.00	22	150	0.3	60	32
10		5.0	-33.00	22	250	0.3	120	32
11		5.0	-38.00	22	250	0.3	130	32
12	Sandstone	5.0	-43.00	22	400	0.3	85	34

CASE 3 _ MERSA AL SEEF (GREEK PHASE 3, 4)

The project is development of Dubai creek over an area equal to approximately 1.80 KM. The development includes hotel, retail, marina, underground car parks canal and ...etc. It covers marine, infrastructure and environmental design elements. The project site is located along Dubai creek on the Bur Dubai side.

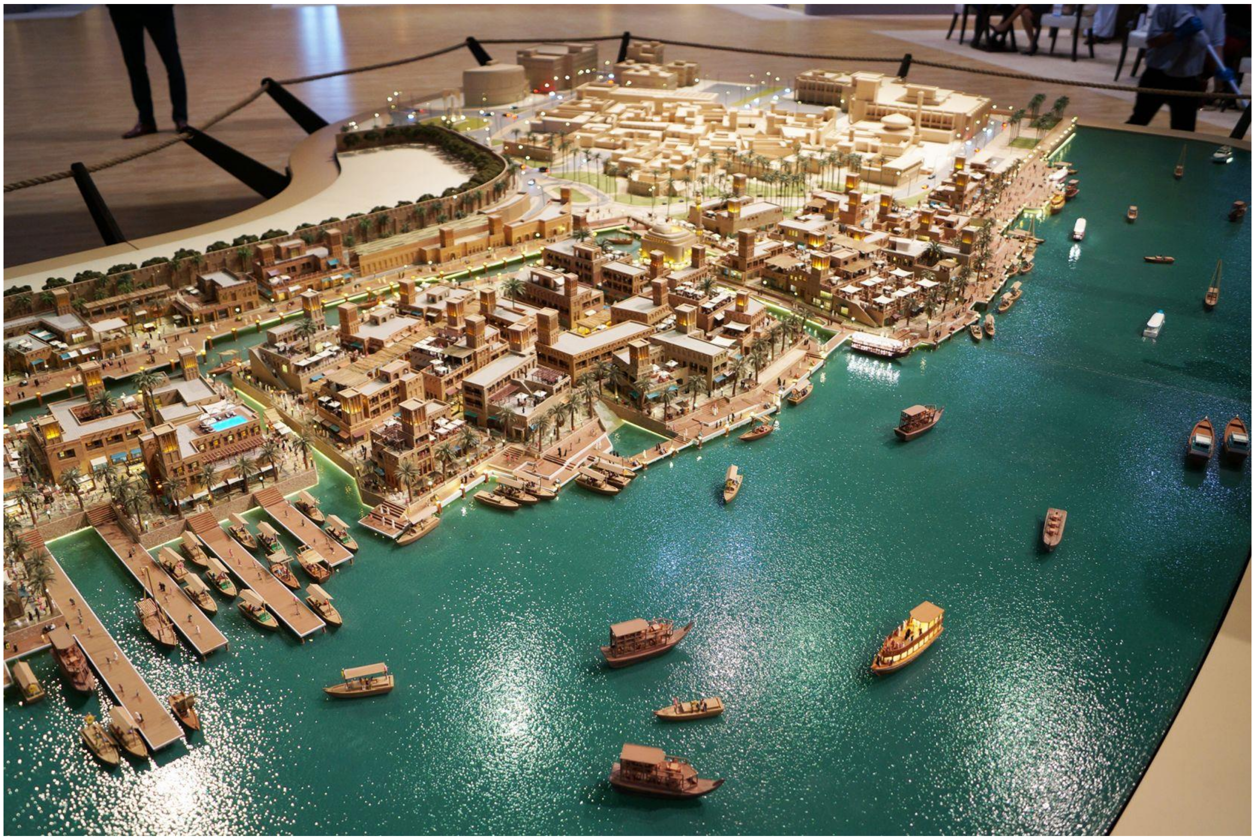

Figure 36. Mersa Al Seef Development

PILE DETAIL

The selected pile from this case of study details are as the following table;

Table 12. Pile Details

Pile Details				
Pile C.O.L - m	Pile Platform Level	Pile Toe Level - m	Pile Length - m	Pile Diameter - mm
- 3.175 DMD	+3.00 DMD	-30.80 DMD	27.80	1,200

Table No. 1: Allowable Working Loads in Compression

Toe Level of Piles (m DMD)	Allowable Working Loads in Compression (kN)			
	Pile Diameter (m)			
	0.75m	0.90m	1.00m	1.20m
-15	3,029	3,635	4,039	4,847
-16	3,428	4,114	4,571	5,485
-17	3,827	4,593	5,103	6,124
-18	4,227	5,072	5,635	6,762
-19	4,626	5,551	6,167	7,401
-20	5,025	6,030	6,700	8,040
-21	5,424	6,509	7,232	8,678
-22	5,756	6,907	7,674	9,209
-23	6,021	7,225	8,028	9,633
-24	6,286	7,543	8,381	10,058
-25	6,551	7,861	8,735	10,482
-26	6,816	8,179	9,088	10,906
-27	7,081	8,497	9,442	11,330
-28	7,346	8,816	9,795	11,754
-29	7,611	9,134	10,149	12,178
-30	7,876	9,452	10,502	12,602

Figure 37. Piles recommendations as per project's soil investigation report

SOIL LAYERS' CLASSIFICATIONS

Reference to the soil investigation report from M/S Arab Center REF: SD 14000057-01-Rev 02, the soil layers' classifications are as per the following table;

Table 13. Soil layers' classifications

No.	Soil Layer	Layer Depth – m Elevation of Engineering Parameters bottom of each layer (m DMD)		Engineering Parameters				
		Avg. Thick - m	To	Unit Wt, KN/m^3	E - MPa	Poison Ratio	C' - KPa	Ø°
1	Silty, gravely, fine sand	5.0	-2.0	18	25	0.35	0.5	35
2	Silty, gravely, fine sand	2.0	-4.0	18	35	0.35	0.5	36
3	Silty Sand	1.0	-5.0	18	50	0.35	5.0	38
4	Silty Sand	3.0	-8.0	18	60	0.33	5.0	40
5	CALCARENITE / Cal. SANDSTONE	13.5	-21.5	22	300	0.3	85	36
6	CALCARENITE / Cal. SANDSTONE	13.5	-35.0	22	400	0.3	35	33

CHAPTER 3 – RESEARCH RESULTS

This chapter will cover the explanation of the used methods to calculate the theoretical, practical and numerical piles capacities for the three cases of studies which mentioned in chapter (3). For the theoretical pile capacity of each pile type in each case of study, the value will be extracted from the foundation recommendations in the soil investigation report. These values are calculated based on the theoretical equations which discussed in chapter (1) for sand and rock soil layers. For the practical pile capacity, the pile capacity will be calculated from the static load test results by using an empirical method to detect the compression pile capacity from non-destructive static load test "Chin's Method" (see Section 1.6). The numerical pile capacity will be estimated by using a finite element model represent the concrete pile and the surrounding soil layers, the software which will be used is PLAXIS 2D, the model will be modeled by using axisymmetric option and the material will be modeled by using Mohr-Coulomb option.

Finally, a comparison between theoretical, practical and numerical pile compression capacities of each case of study will be stated in this chapter and will be discussed in details in the following chapter.

NUMERICAL ANALYSIS PROCEDURE

Finite element software will be used to model the selected pile of each case of study, the software which will be used is PLAXIS 2D version 8.6. The pile model will be modeled by using axisymmetric option and the materials which represent the pile and the surrounded soil layers will be modeled by using Mohr-Coulomb option. Prescribed settlement will be applied to the pile head and the force – settlement curve will be plotted to predict the numerical pile capacity.

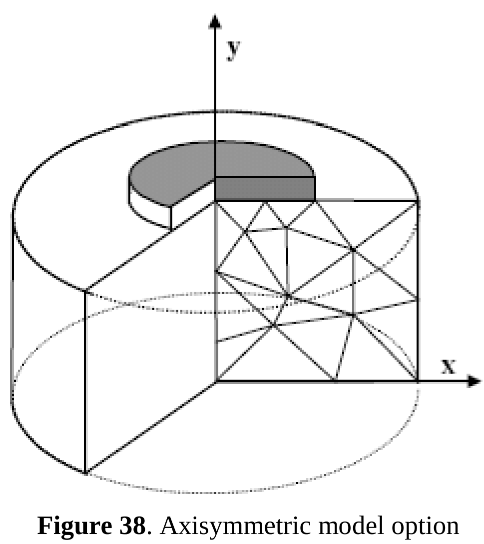

Figure 38. Axisymmetric model option

The major aspects in the modeling process are the graphical boundaries, soil layers' classification and parameters and the pile material - soil layers' friction angle. These factors will be discussed in details in the following sections;

GRAPHICAL BOUNDARIES

The following figure shows the model's graphical boundaries which should be followed in the modeling process.

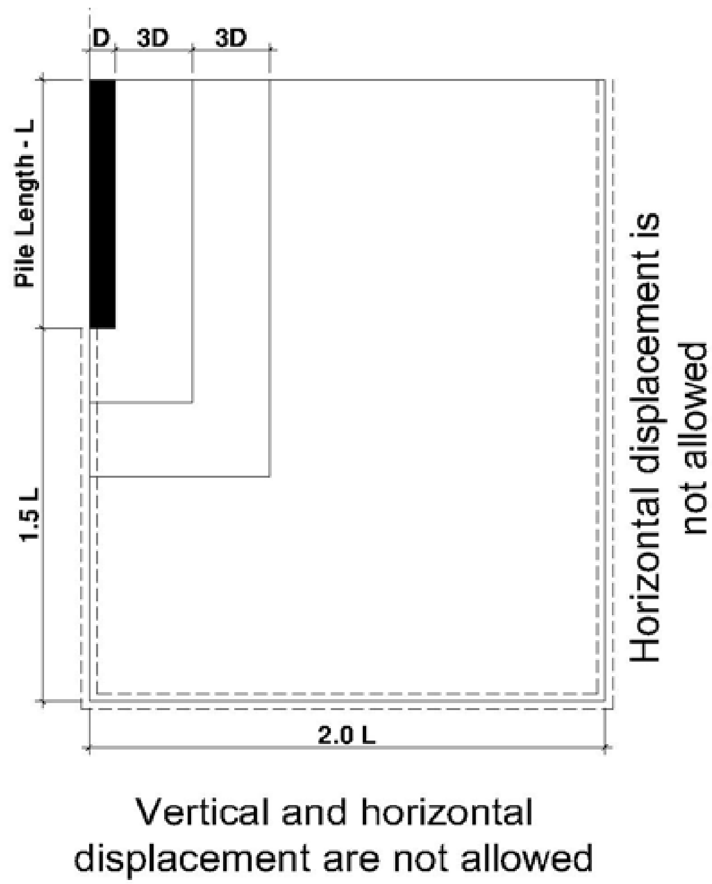

Figure 39. Graphical boundaries for the pile model

The boundaries are as follows;

- D is the pile radius.
- Two layers of mesh transition, each layer width is equal to 3D.
- L is the pile depth.
- The model dimensions are equal to 2.5L for the model depth and 2.0L for the model width.
- The horizontal and vertical displacement of the model edge are not allowed.

SOIL LAYERS’ CLASSIFICATION AND PARAMETERS

For the soil layers' classifications and the soil parameters which will be used in the numerical model will be estimated or derived from the soil investigation report of each case of study. soil layers' modulus of elasticity, cohesion, soil unit weight and the angle of internal friction of each layer are the major important factors which should be identified and used in the pile model.

PILE - SOIL FRICTION RELATIONSHIP

One of the important factors which has a significant impact on the pile skin friction resistance is the pile - soil interface condition. This factor depends on the following properties;

A. Soil layers’ classification.
B. Pile material.
C. The installation technique, for example the using of bentonite slurry in the pile installation has a negative impact on the skin friction resistance compared to the other techniques like bored pile or CFA technique. This is because the using of bentonite slurry generates a smooth surface between the pile and the surrounding soil.

Generally, the reduction factor of skin friction resistance due to interface condition has a value between 1.0 to 0.5, in this research the used reduction factor for sand soil layers is 0.8 and the value of the rock soil layers is 0.9 (see Table 2).

CASE 1 _ AL HABTOOR RESIDENCE

A. THEIORTICAL PILE CAPACITY (CASE 1)

Reference to the soil investigation report from M/S Al Hai & Al Mukaddam REF: SR/1305101-2. REV 01 (see Appendix 2), the compression capacity of the pile with diameter equal to 1,500 mm and the toe level is -57.0 m from the cut off level - 4.00 to - 6.00 m is **27,670 KN** (refer to Table 6 and Figure 33). This compression capacity is calculated by using set of theoretical equations which discussed in chapter 1 for sand and rock soil layers.

B. PRACTICAL PILE CAPACITY (CASE 1)

Bi-directional static loading test has been done to the selected pile PTP03 (see Appendix 2), the test has been done by M/S HSSG (piling contractor) and was monitoring by M/S Arab Center (specialist soil laboratory). The purpose of the bi-directional static loading test on instrumented pile was to evaluate the following criteria;

- Load settlement behavior of the tested pile under a test load equal to 250% of the working load.
- Load transfer and distribution along pile shaft during the compression load test.
- Skin friction along pile shaft during the compression load test.

The following steps are showing the procedure to calculate the pile compression capacity using Chin's method and the results from the bi-directional static load test;

1. Collecting the date and the results from the bi-directional static load test.

Table 14. Al Habtoor Residence _ Bi-directional static load test results

Load - P [KN]	Settlement - S [mm]	Settlement / Load [mm/KN]
0	0	0
10000	1.12	0.000112
20000	2.24	0.000112
30000	3.4	0.000113333
40000	4.87	0.00012175
50000	7	0.00014
60000	10.52	0.000175333

2. Plot Chin's diagram.

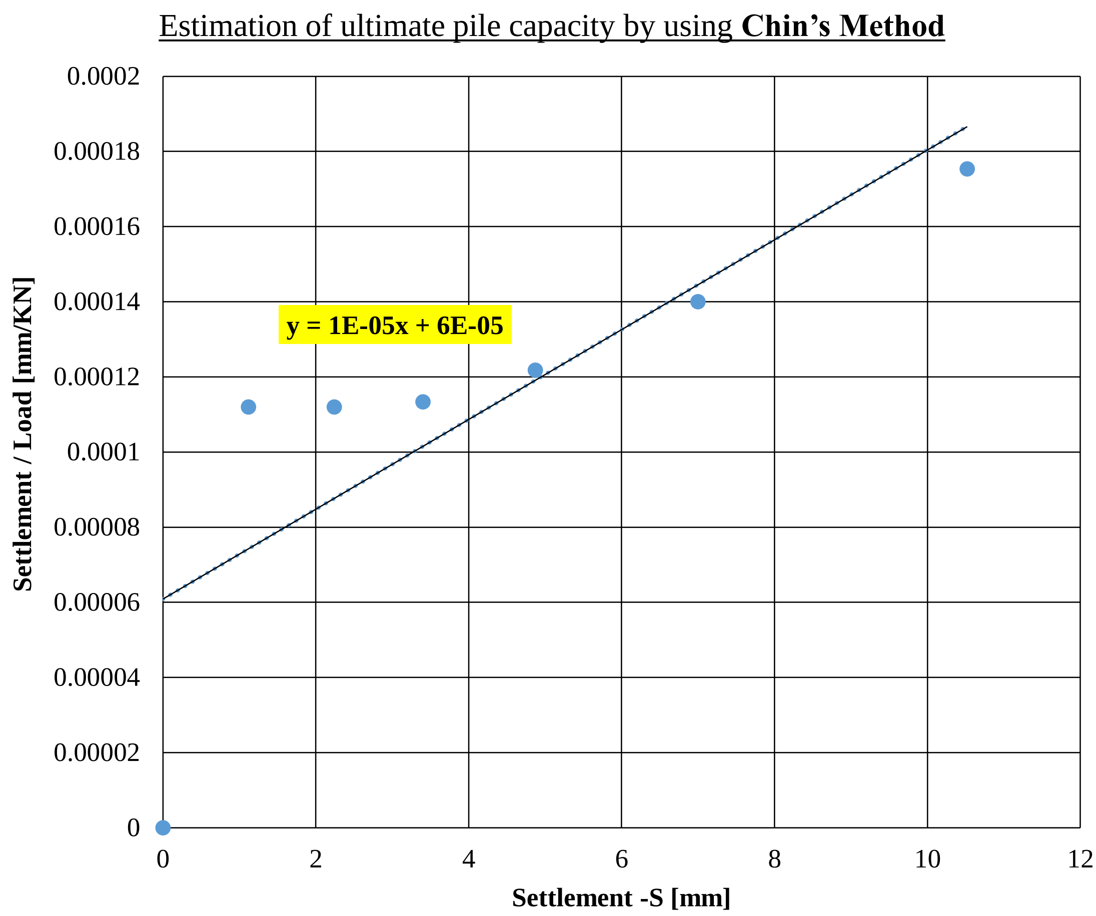

Figure 40. Chin's Diagram

3. Evaluating the practical pile capacity by using Chin's method.

From the previous figure, the equation which represent the best fit line through the data points is;

$$\frac{\Delta}{Q} = C_1\Delta + C_2 = Y = 1E - 05x + 6E - 05 \quad \ldots.. \quad \textit{Eq. (15)}$$

$$Q_u = \frac{1}{C_1} = \frac{1}{1E{-}05} = 100{,}000 \text{ KN} \quad \ldots.. \quad \textit{Eq. (16)}$$

$$Q = \frac{100{,}000}{F.O.S} = \frac{100{,}000}{2.5} = 40{,}000 \text{ KN} \quad \ldots.. \quad \textit{Eq. (17)}$$

From the previous equations, the estimated practical compression pile capacity by using Chin's method is **<u>40,000 KN</u>**.

C. NUMERICAL PILE CAPACITY (CASE 1)

A finite element software (PLAXIS 2D) has been used to model the pile and the surrounded soil layers. The different soil parameters and coefficients which are used in the numerical model such as soil's modulus of elasticity, soil's unit weight and the angle of internal friction are extracted or estimated based on the soil classification in the soil investigation report (see Table 7). The following steps are showing the procedure which has been used to model the pile by using PLAXIS 2D software;

1. The pile has been modeled by using PLAXIS 2D software, the model has been modeled by using axisymmetric option and the materials which represent the soil layers have been modeled by using Mohr-Coulomb option.

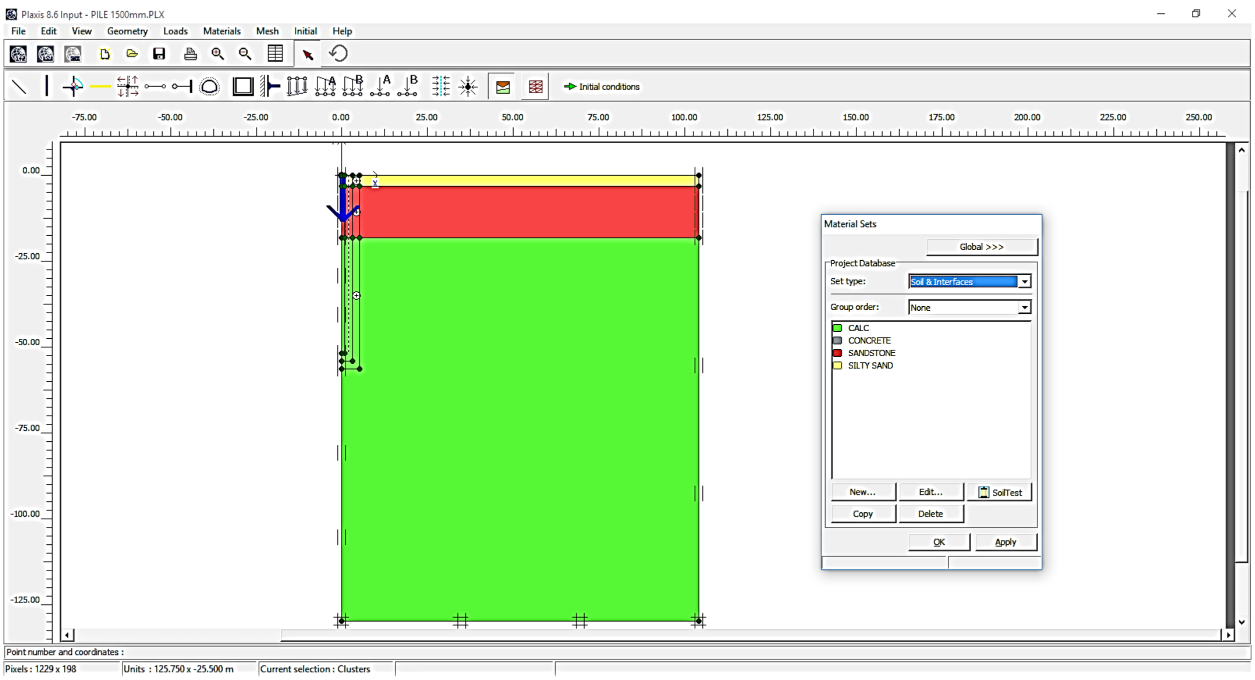

Figure 41. Pile Model by Using PLAXIS 2D

2. Prescribed settlement has been applied to the pile head, this is to plot the relationship between the radial compression pile capacity in the horizontal axis and the pile settlement in the vertical axis. From this relationship curve, the value of numerical pile capacity has been calculated based on the British standard BS **8004: 1986** recommendation. The ultimate pile capacity defined as that load which produce a settlement of the pile head equal to **10%** of the pile diameter or pile width.

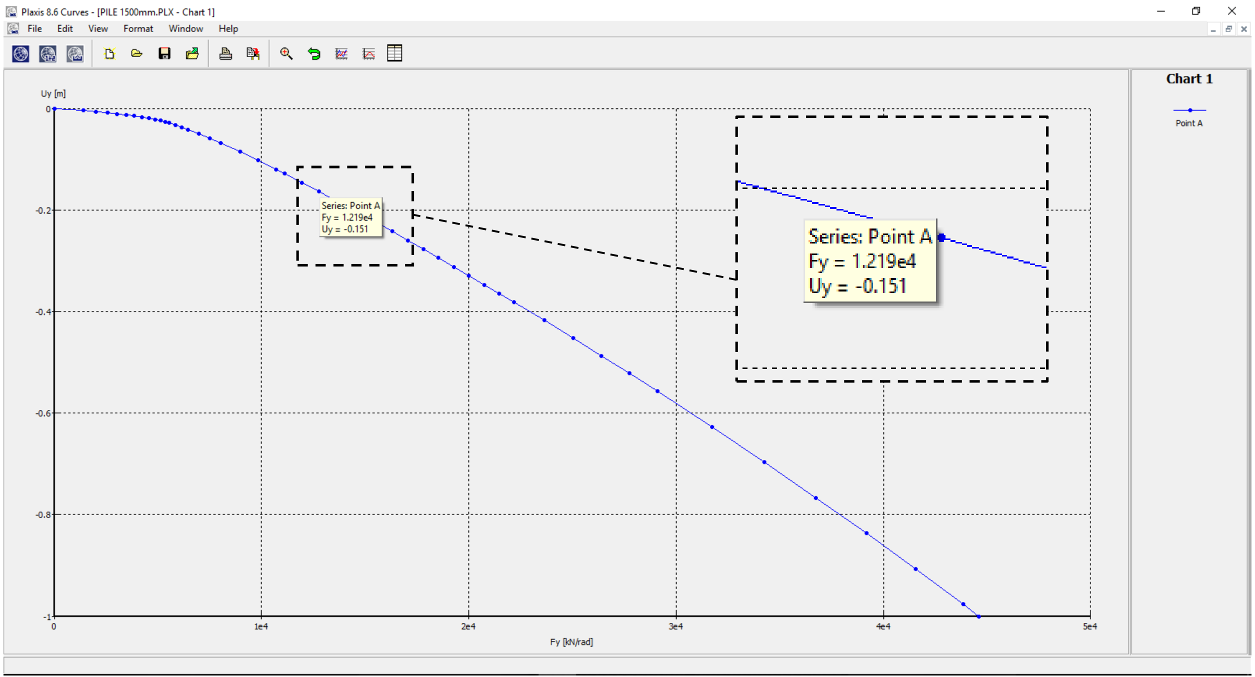

Figure 42. Pile Load - Settlement Relationship Curve

3. Calculating the numerical pile capacity by using the load - settlement relationship curve as follow;

    - 10% of the pile diameter = 150 mm = 0.15 m
    - From the previous figure, F_y = 12,190 KN/rad at displacement equal to 150 mm

$$Q_U = F_y \times 2\pi = 12{,}190 \times 2\pi = 76{,}553\ KN \qquad \text{….. } Eq.\ (18)$$

$$Q = \frac{Q_U}{F.O.S} = \frac{76{,}553}{2} = 38{,}277\ KN \qquad \text{….. } Eq.\ (19)$$

From the previous equations, the calculated numerical compression pile capacity by using PLAXIS 2D is **<u>38,277 KN</u>**.

CASE 2 _ BLUEWATER HOSPITALITY

A. THEIORTICAL PILE CAPACITY (CASE 2)

Reference to the soil investigation report from M/S Arab Center REF: SD14000067.REV00 (see Appendix 2), the compression capacity of the pile with diameter equal to 900 mm and the toe level is -31.0 m from the cut off level +3.375 m is **9,015 KN** (refer to Table 10 and Figure 35). This compression capacity is calculated by using set of theoretical equations which discussed in chapter 1 for sand and rock soil layers.

B. PRACTICAL PILE CAPACITY (CASE 2)

Static load test has been done to the selected pile PTP02 (see Appendix 2), the test has been done by M/S Swiss Boring (piling contractor) and was monitoring by M/S Arab Center (specialist soil laboratory). The purpose of the static load test (Kent ledge blocks method) on instrumented pile was to evaluate the following criteria;

- Load settlement behavior of the tested pile under a test load equal to 250% of the working load.
- Load transfer and distribution along pile shaft during the compression load test.
- Skin friction along pile shaft during the compression load test.

The following steps are showing the procedure which is used to calculate the pile compression capacity by using Chin's method and the results from the static load test;

1. Collecting the date and the results from the static load test.

Table 15. Bluewater Hospitality _ Static load test results

Load - P [KN]	Settlement -S [mm]	Settlement / Load [mm/KN]
0	0.793	0
2240	1.100	0.000491071
4490	2.960	0.000659243
6780	4.850	0.000715339
8970	7.060	0.000787068
11210	8.935	0.000797056
13460	11.000	0.000817236
15690	12.900	0.00082218
17940	14.850	0.000827759
20180	16.800	0.000832507
22430	19.100	0.000851538

2. Plot Chin's diagram.

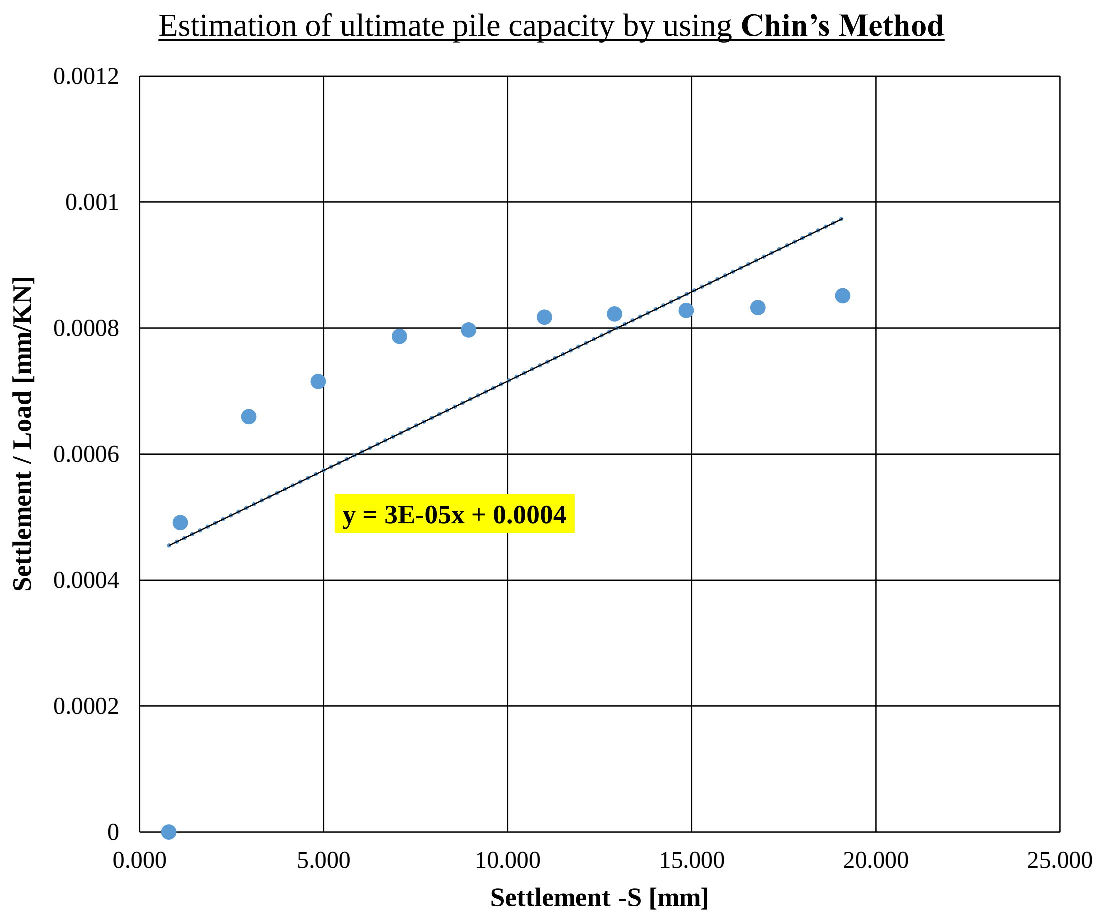

Figure 43. Chin's Diagram

3. Evaluating the practical pile capacity by using Chin's method.

From the previous figure, the equation which represent the best fit line through the data points is;

$$\frac{\Delta}{Q} = C_1\Delta + C_2 = Y = 3E - 05x + 0.0004 \qquad \text{.....} \quad \textit{Eq. (20)}$$

$$Q_u = \frac{1}{C_1} = \frac{1}{3E{-}05} = 33{,}333.33 \text{ KN} \qquad \text{.....} \quad \textit{Eq. (21)}$$

$$Q = \frac{33{,}333.33}{F.O.S} = \frac{33{,}333.33}{2.5} = 13{,}333.33 \text{ KN} \qquad \text{.....} \quad \textit{Eq. (22)}$$

From the previous equations, the estimated practical compression pile capacity by using Chin's method is **<u>13,333.33 KN</u>**.

C. NUMERICAL PILE CAPACITY (CASE 2)

A finite element software (PLAXIS 2D) has been used to model the pile and the surrounded soil layers. The different soil parameters and coefficients which are used in the numerical model such as soil's modulus of elasticity, soil's unit weight and the angle of internal friction are extracted or estimated based on the soil classification in the soil investigation report (see Table 11). The following steps are showing the procedure which has been used to model the pile by using PLAXIS 2D software;

1. The pile has been modeled by using PLAXIS 2D software, the model has been modeled by using axisymmetric option and the materials which represent the soil layers have been modeled by using Mohr-Coulomb option.

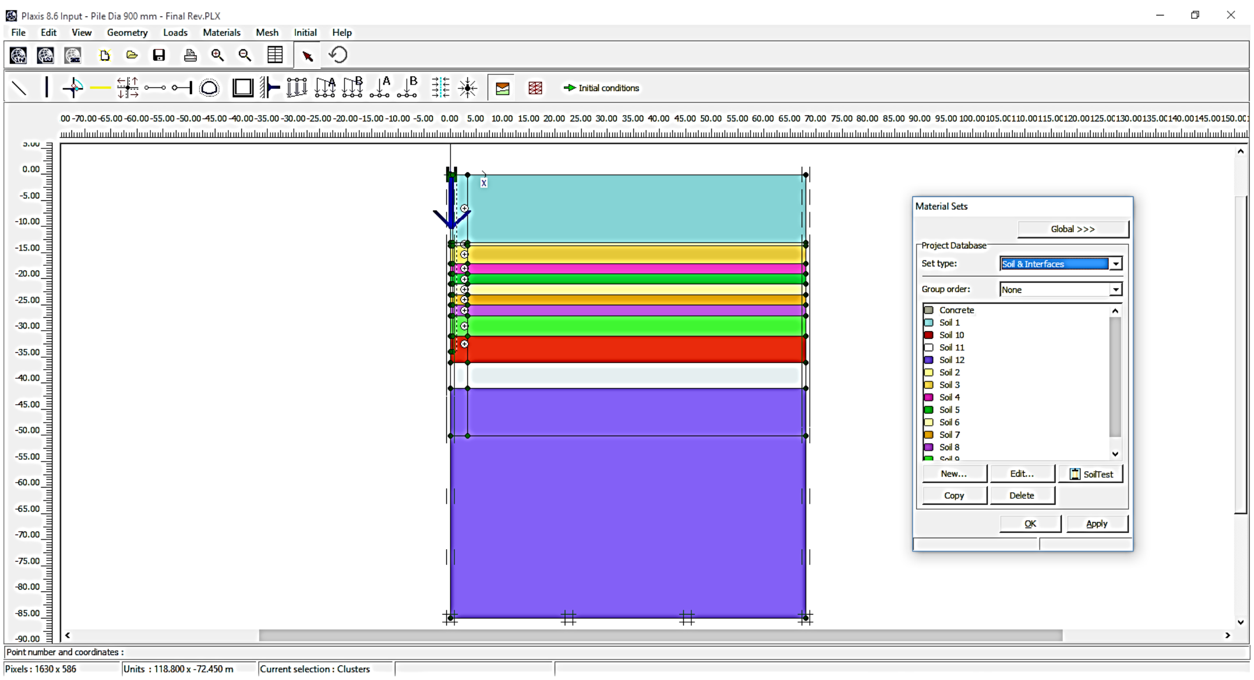

Figure 44. Pile Model by Using PLAXIS 2D

2. Prescribed settlement has been applied to the pile head, this is to plot the relationship between the radial compression pile capacity in the horizontal axis and the pile settlement in the vertical axis. From this relationship curve, the value of numerical pile capacity has been calculated based on the British standard BS **8004: 1986** recommendation. The ultimate pile capacity defined as that load which produce a settlement of the pile head equal to **10%** of the pile diameter or pile width.

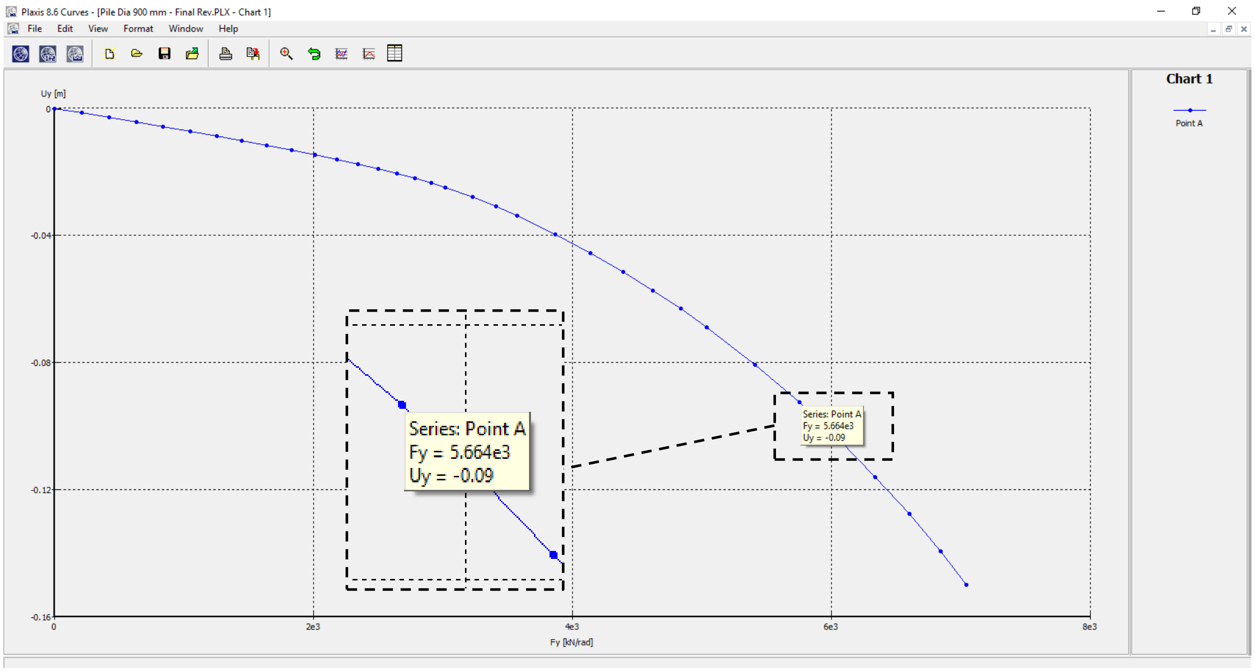

Figure 45. Pile Load - Settlement Relationship Curve

3. Calculating the numerical pile capacity by using the load - settlement relationship curve as follow;

    - 10% of the pile diameter = 90 mm = 0.09 m
    - From the previous figure, F_y = 5,664 KN/rad at displacement equal to 90 mm

$$Q_U = F_y \times 2\pi = 5{,}664 \times 2\pi = 35{,}570\ KN \qquad \text{….. } Eq.\ (23)$$

$$Q = \frac{Q_U}{F.O.S} = \frac{35{,}570}{2} = 17{,}784\ KN \qquad \text{….. } Eq.\ (24)$$

From the previous equations, the calculated numerical compression pile capacity by using PLAXIS 2D is **17,784 KN**.

CASE 3 _ MERSA AL SEEF (GREEK PHASE 3, 4)

A. THEIORTICAL PILE CAPACITY (CASE 3)

Reference to the soil investigation report from M/S Arab Center REF: SD14000057-01.REV 02, the compression capacity of the pile with diameter equal to1200 mm and the toe level is -30.80 m from the cut off level -3.175 m is **12,600 KN** (refer to Table 12 and Figure 37). This compression capacity is calculated by using set of theoretical equations which discussed in chapter 1 for sand and rock soil layers.

B. PRACTICAL PILE CAPACITY (CASE 3)

Bi-directional static loading test has been done to the selected pile PTP03 (see Appendix 2), the test has been done by M/S STRAINSTALL (specialist soil laboratory). The purpose of the bi-directional static loading test on instrumented pile was to evaluate the following criteria;

- Load settlement behavior of the tested pile under a test load equal to 250% of the working load.
- Load transfer and distribution along pile shaft during the compression load test.
- Skin friction along pile shaft during the compression load test.

The following steps are showing the procedure to calculate the pile compression capacity by using Chin's method and the results from the bi-directional static load test;

1. Collecting the date and the results from the bi-directional static load test.

Table 16. MERSA AL SEEF (GREEK PHASE 3, 4) _ bi-directional static load test results

Load - P [KN]	Settlement -S [mm]	Settlement / Load [mm/KN]
0	0.000	0
5000	1.540	0.000308
10000	3.220	0.000322
15000	4.840	0.000322667
20000	6.520	0.000326
25000	8.460	0.0003384
30000	10.540	0.000351333
35000	13.790	0.000394

2. Plot Chin's diagram.

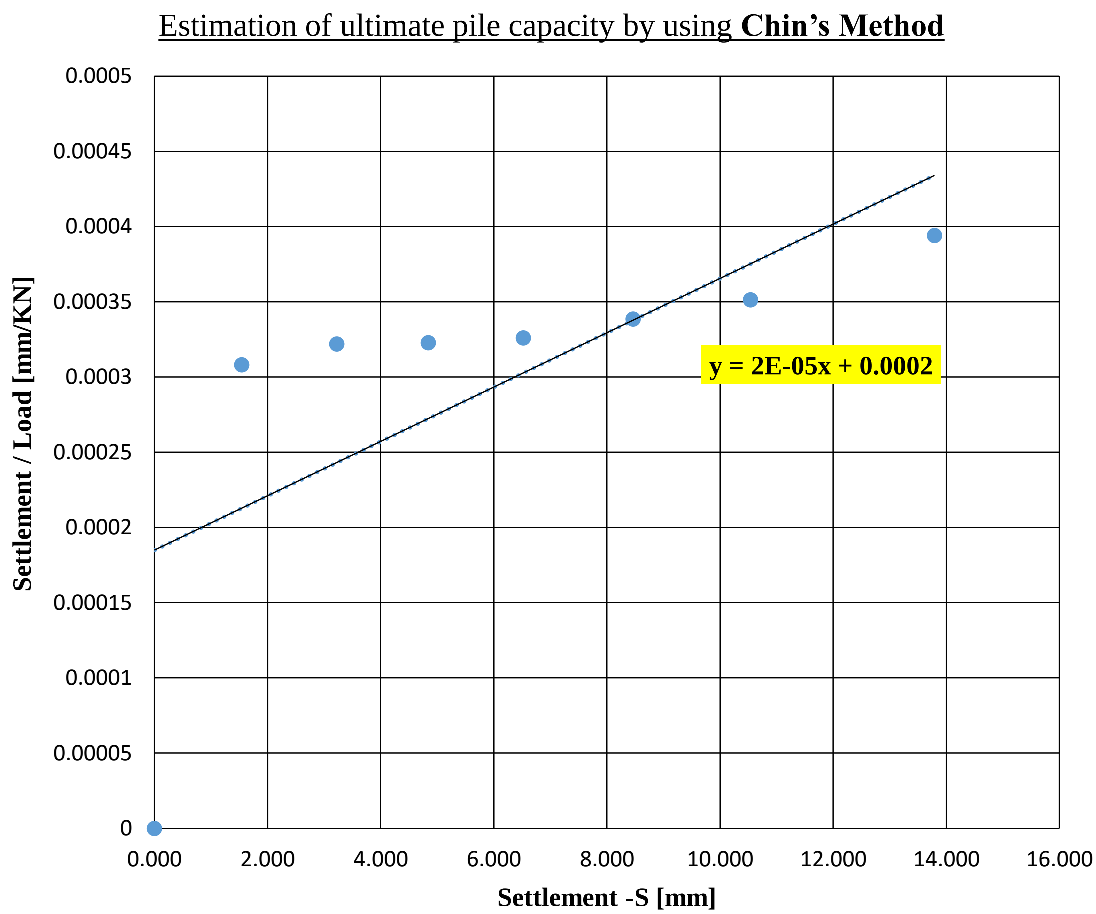

Figure 46. Chin's Diagram

3. Evaluating the practical pile capacity by using Chin's method.

From the previous figure, the equation which represent the best fit line through the data points is;

$$\frac{\Delta}{Q} = C_1\Delta + C_2 = Y = 2E - 05x + 0.0002 \qquad \text{.....} \quad \textit{Eq. (25)}$$

$$Q_u = \frac{1}{C_1} = \frac{1}{2E{-}05} = 50{,}000 \text{ KN} \qquad \text{.....} \quad \textit{Eq. (26)}$$

$$Q = \frac{50{,}000}{F.O.S} = \frac{50{,}000}{2.5} = 20{,}000 \text{ KN} \qquad \text{.....} \quad \textit{Eq. (27)}$$

From the previous equations, the estimated practical compression pile capacity by using Chin's method is **20,000 KN**.

C. NUMERICAL PILE CAPACITY (CASE 3)

A finite element software (PLAXIS 2D) has been used to model the pile and the surrounded soil layers. The different soil parameters and coefficients which are used in the numerical model such as soil's modulus of elasticity, soil's unit weight and the angle of internal friction are extracted or estimated based on the soil classification in the soil investigation report (see Table 13). The following steps are showing the procedure which has been used to model the pile by using PLAXIS 2D software;

1. The pile has been modeled by using PLAXIS 2D software, the model has been modeled by using axisymmetric option and the materials which represent the soil layers have been modeled by using Mohr-Coulomb option.

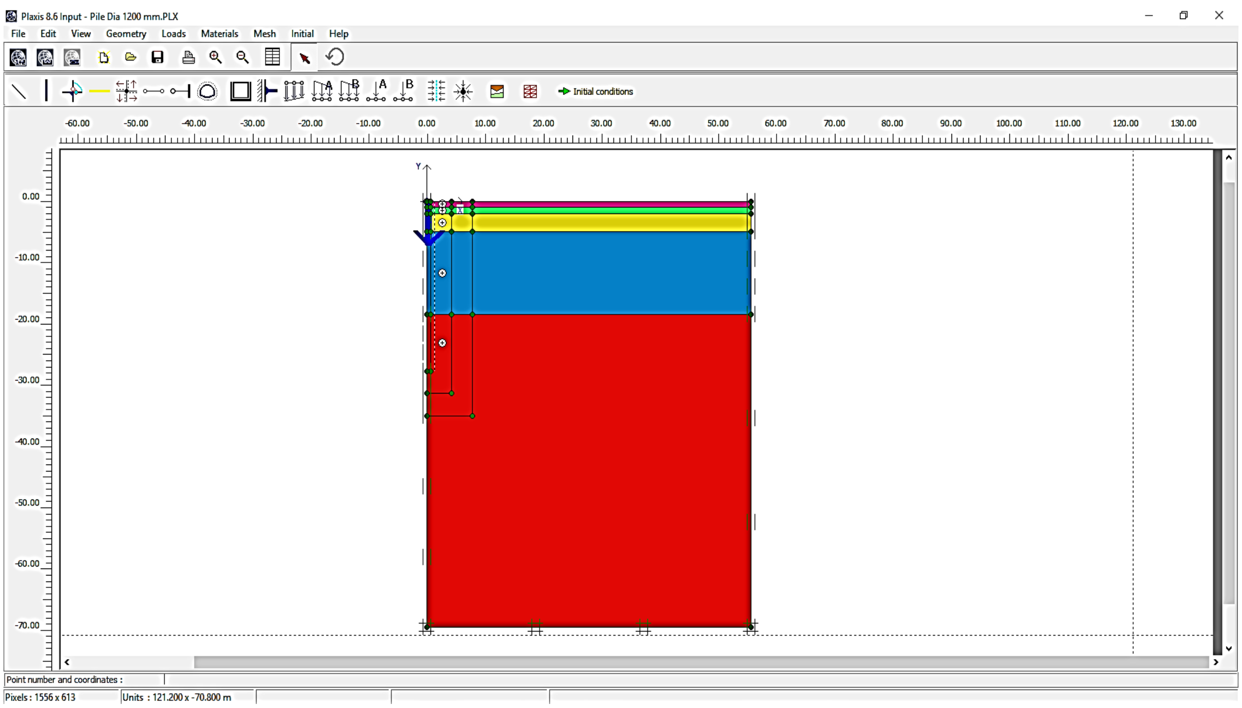

Figure 47. Pile Model by Using PLAXIS 2D

2. Prescribed settlement has been applied to the pile head, this is to plot the relationship between the radial compression pile capacity in the horizontal axis and the pile settlement in the vertical axis. From this relationship curve, the value of numerical pile capacity has been calculated based on the British standard BS **8004: 1986** recommendation. The ultimate pile capacity defined as that load which produce a settlement of the pile head equal to **10%** of the pile diameter or pile width.

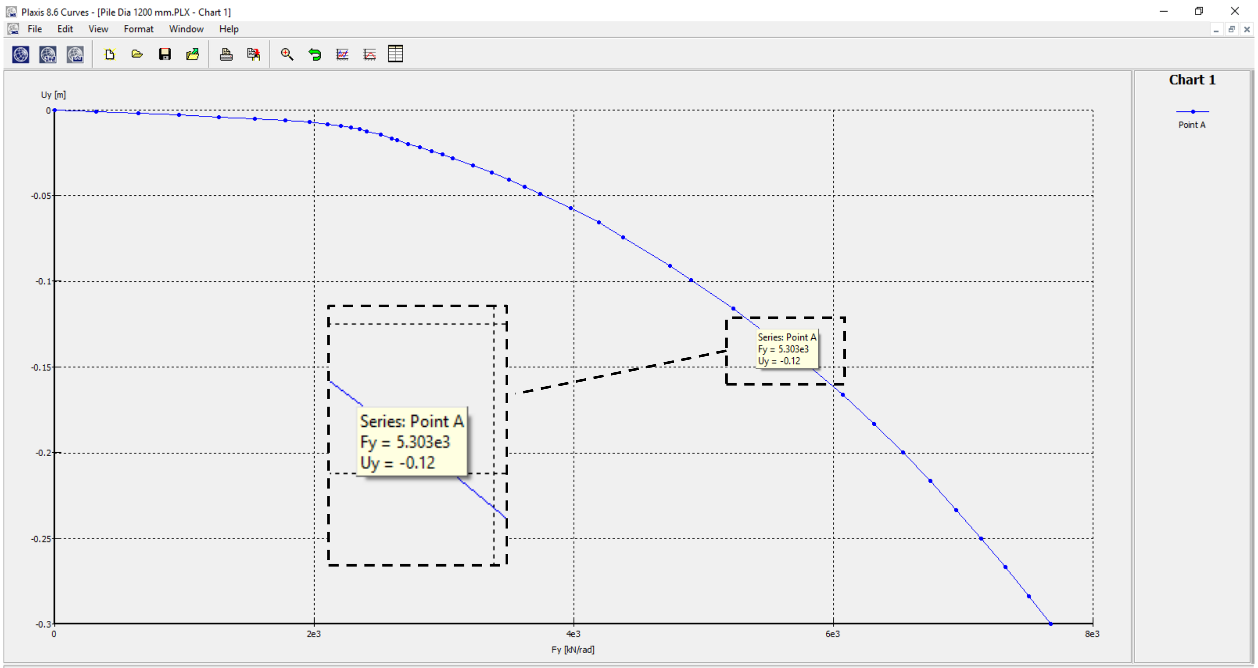

Figure 48. Pile Load - Settlement Relationship Curve

3. Calculating the numerical pile capacity by using the load - settlement relationship curve as follow;
   - 10% of the pile diameter = 120 mm = 0.12 m
   - From the previous figure, F_y = 5,303 KN/rad at displacement equal to 120 mm

$$Q_U = F_y \times 2\pi = 5{,}303 \times 2\pi = 33{,}333\ KN \qquad \ldots\ldots \quad Eq.\ (28)$$

$$Q = \frac{Q_U}{F.O.S} = \frac{33{,}333}{2} = 16{,}666\ KN \qquad \ldots\ldots \quad Eq.\ (29)$$

From the previous equations, the calculated numerical compression pile capacity by using PLAXIS 2D is **16,666 KN**.

CHAPTER 4 – CONCLUSION AND RECOMMENDATIONS

This chapter will discuss the results of the three cases of study which stated in the previous chapter. Each case of study has three different pile's compression capacity values, theoretical, practical and numerical capacity. The main purpose of this research is to compare between the theoretical and practical compression pile capacities, in addition a finite element model has been used to calculate the numerical pile capacity, this is to assist in the comparison between the theoretical and practical capacities.

This chapter will be divided to four main sections, the first section is "results discussion" this section will discuss the results of each case of study separately to identify the relation and differences between the three values of pile's compression capacity in each case of study. The second section will be "research conclusion" this section will summarize the end result of this research and the final relation between the theoretical, practical and numerical pile capacities based on the results of the three cases of study. The third section is "research recommendations" this section will cover an important aspect which is the final recommendations in respect to the research results. Finally, the fourth section is "further research" this section will discuss the development process which can be done in the main research to improvement the results further.

RESULTS DISCUSSION

In this section, the results of the research will be discussed for each case of study. In each case of study, there are three different values of pile's compression capacity. The theoretical pile capacity calculated based on the theoretical equations which discussed in chapter 2. The practical pile capacity estimated based on the results of practical static load test by using an empirical method (Chin's Method). Finally, the numerical pile's capacity estimated by using a finite element software (Plaxis 2D). The three values of pile capacity will be discussed separately for each case of study.

CASE 1 _ AL HABTOOR RESIDENCE

The following table and chart represent the relation between theoretical, practical and numerical pile's compression capacities which calculated in details in the previous chapter;

Table 17. Theoretical, practical and numerical pile capacities _ Case 1

ID	Theoretical Capacity [KN]	Practical Capacity [KN]	Numerical Capacity [KN]
1	**27,670**	**40,000**	**38,277**

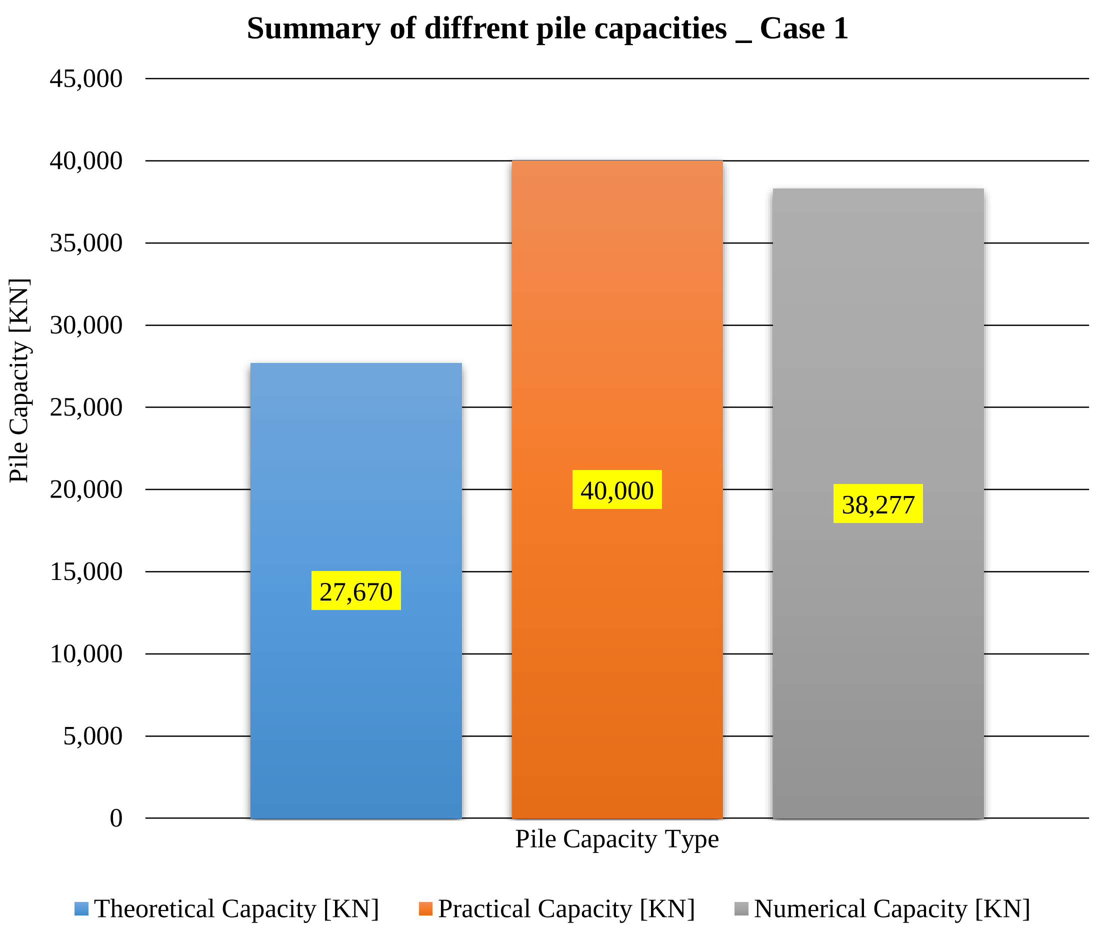

Figure 49. Pile Capacities _ Case 1

From the previous table and chart, it can be summarized that the practical pile capacity is greater than the theoretical capacity by almost 144 %. And the numerical capacity is greater than the theoretical capacity by 138 %. This mean that the estimated pile capacity by using the theoretical / empirical equations is less than the capacities which are estimated based on the practical static load test and the capacity which is calculated by using a finite element software by around 30 to 40 % which is considered as a significant impact.

CASE 2 _ BLUEWATER HOSPITALITY

The following table and chart represent the relation between theoretical, practical and numerical pile's compression capacities which calculated in details in the previous chapter;

Table 18. Theoretical, practical and numerical pile capacities _ Case 2

ID	Theoretical Capacity [KN]	Practical Capacity [KN]	Numerical Capacity [KN]
1	**9,015**	**13,333**	**17,784**

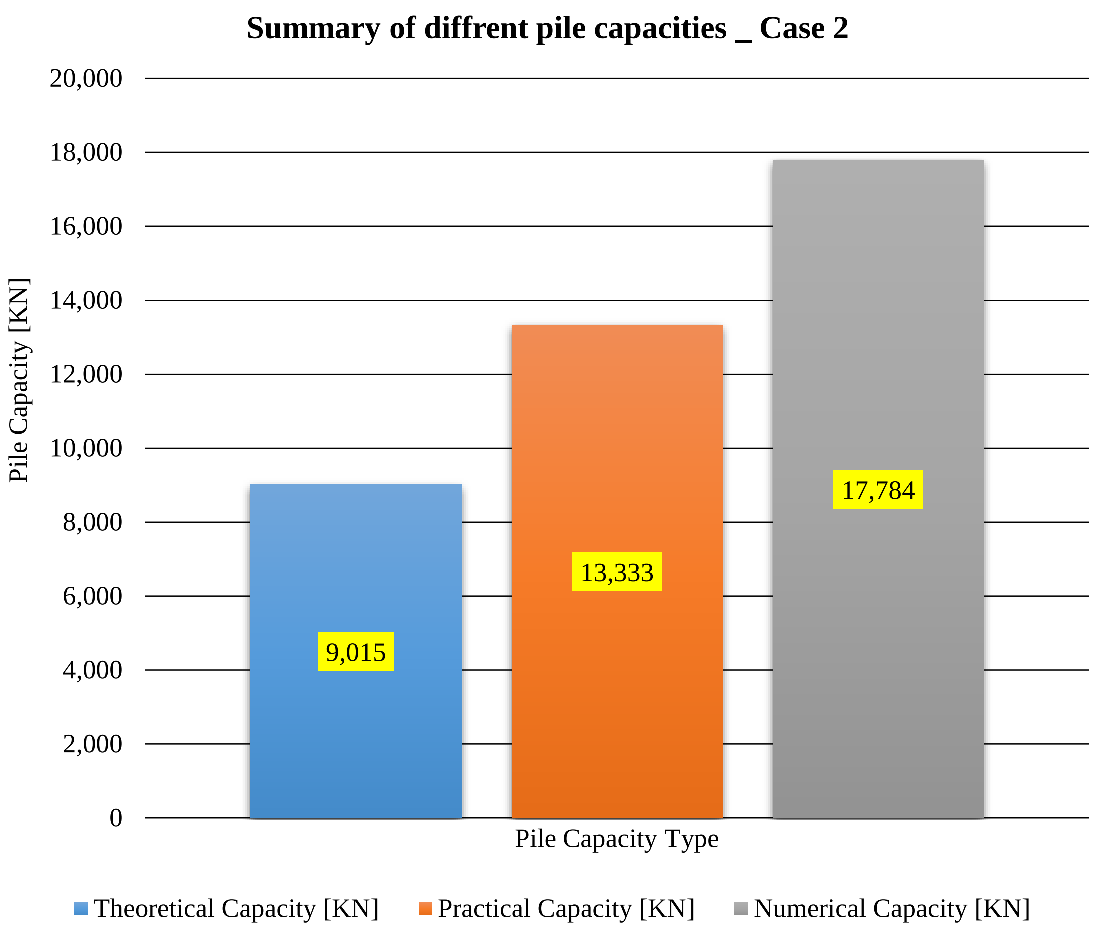

Figure 50. Pile Capacities _ Case 2

From the previous table and chart, it can be summarized that the practical pile capacity is greater than the theoretical capacity by almost 147 %. And the numerical capacity is greater than the theoretical capacity by 197 %. This mean that the estimated pile capacity by using the theoretical / empirical equations is less than the capacities which are estimated based on the practical static load test and the capacity which is calculated by using a finite element software by around 40 to 90 % which is considered as a significant impact.

CASE 3 _ MERSA AL SEEF (GREEK PHASE 3, 4)

The following table and chart represent the relation between theoretical, practical and numerical pile's compression capacities which calculated in details in the previous chapter;

Table 19. Theoretical, practical and numerical pile capacities _ Case 3

ID	Theoretical Capacity [KN]	Practical Capacity [KN]	Numerical Capacity [KN]
1	**12,600**	**20,000**	**16,666**

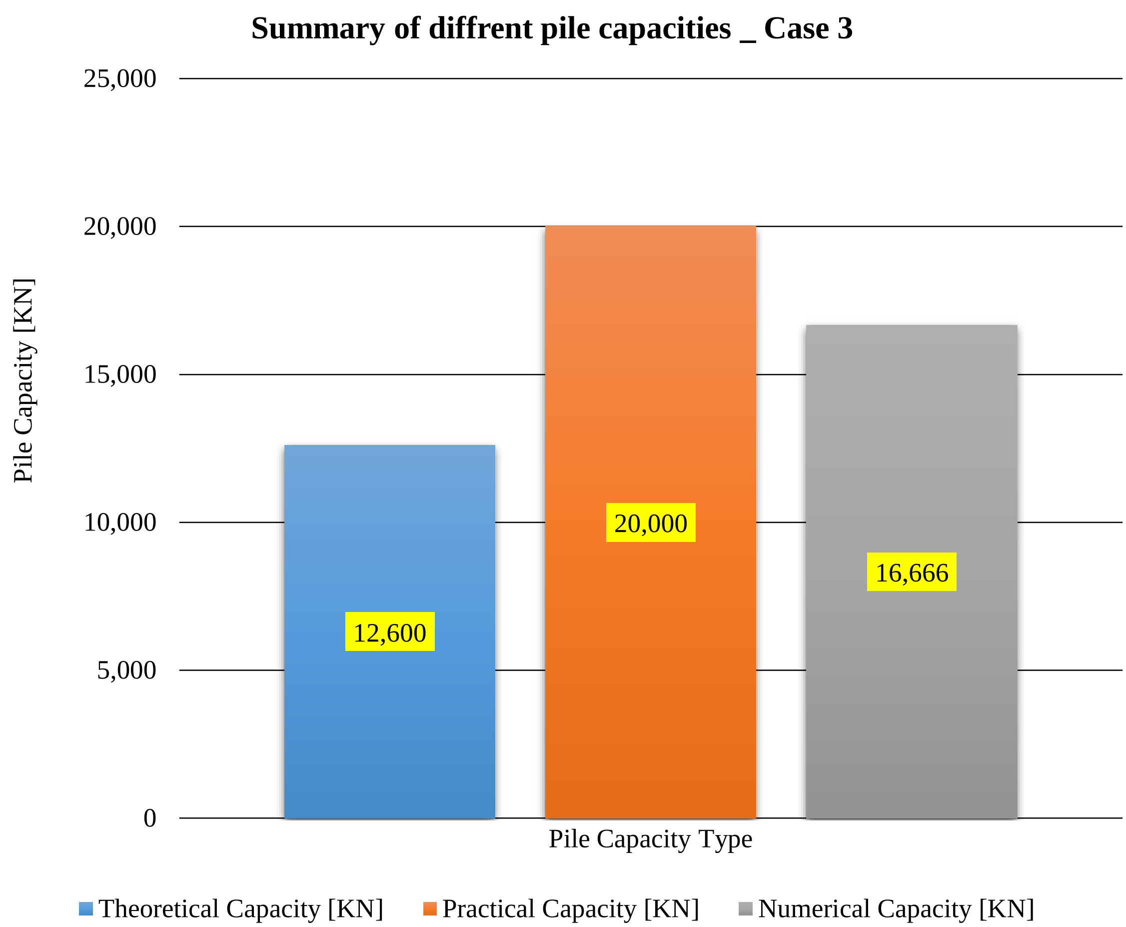

Figure 51. Pile Capacities _ Case 2

From the previous table and chart, it can be summarized that the practical pile capacity is greater than the theoretical capacity by almost 158 %. And the numerical capacity is greater than the theoretical capacity by 132 %. This mean that the estimated pile capacity by using the theoretical / empirical equations is less than the capacities which are estimated based on the practical static load test and the capacity which is calculated by using a finite element software by around 30 to 50 % which is considered as a significant impact.

RESEARCH CONCLUSION

As a conclusion of the research's results, it has been proved by using three different case of studies that the calculated theoretical pile capacity by using the old theoretical equations is less than the practical and numerical pile capacities which are calculated by using the results of static load test and a numerical model by a finite element software respectively.

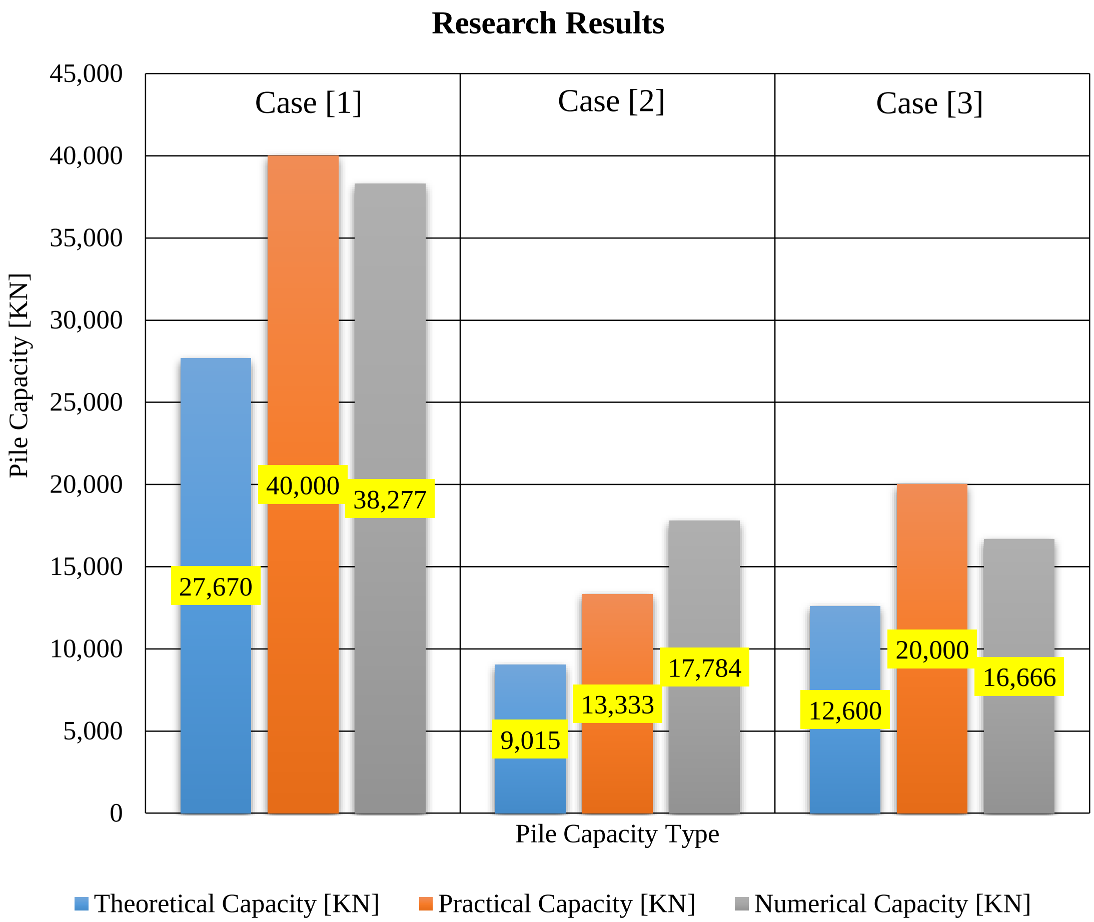

Figure 52. Research Results

It has been concluded from case 1 that the practical pile capacity is equal to 144% of the theoretical pile capacity and the numerical pile capacity is equal to 138% of the theoretical pile capacity. For case 2, the practical pile capacity is equal to 147% of the theoretical pile capacity and the numerical pile capacity is equal to 197% of the theoretical pile capacity. Same results in case 3 where the practical pile capacity is equal to 158% of the theoretical pile capacity and the numerical pile capacity is equal to 132% of the theoretical pile capacity.

Table 20. Research results

ID	Theoretical Capacity [KN]	Practical Capacity [KN]	Numerical Capacity [KN]	% (Practical / Theoretical)	% (Numerical / Theoretical)
Case 1	27,670	40,000	38,277	144%	138%
Case 2	9,015	13,333	17,784	147%	197%
Case 3	12,600	20,000	16,666	158%	132%

From the previous table, it can be summarized that the percent between the practical and theoretical pile capacities is ranged between 144 to 158% and the percent between the numerical and theoretical pile capacities is ranged between 132 to 138% (neglecting case 2 which is equal to 197% because it is exaggerated value). In conclusion, the research results have been provided an acceptable relation between the practical, numerical and theoretical pile capacities where it can be recommended as follows;

$$Practical\ Pile\ Capacity = 140\% \times Theoretical\ Pile\ Capacity \quad \ldots.. \quad Eq.\ (30)$$

$$Numerical\ Pile\ Capacity = 130\% \times Theoretical\ Pile\ Capacity \quad \ldots.. \quad Eq.\ (31)$$

RESEARCH RECOMMENDATIONS

The research has been analyzed three different cases of study for piling projects having been done in Dubai. The major soil classifications are sand soil for the first 2 to 4 m of N.G.L and different types of sandstone soil for the lower soil layers. The same conclusion has been proved from the results of the three cases of study, the major conclusion is that the theoretical equations which are used to calculate the compression pile capacity need more improvement to have results matching to the practical or numerical pile capacity.

Another aspect such as the constructability of deep piles and the sustainability, the research results provided the opportunity to achieve and improved these aspects. In terms of piles' constructability, the using of research results and recommendations like the improvement of theoretical equations will provide the ability to geotechnical designer to achieve the required pile capacity with less pile depth compared to the using of classical equations. Moreover, the demanded material to construct the deep piles will be decreased because of the decreasing of pile length, and this can be considered as sustainable practice.

Finally, the research recommendations can be summarized in the following points;

1. Proper soil investigation report for the project should be done at early stage and before the starting of the design stage, this is to identify the soil layers' classifications and different soil parameters.
2. Numerical model for the piles foundations should be done during the design stage to estimate the compression piles capacities, and this value should be compared to the calculated value by using the classical theoretical equations.
3. It is recommended to construct a single pile from each type, this is to test the pile and to identify the practical compression pile capacity.

4. The classical equation which are used to calculate the compression pile capacity should be improved to achieve results nearing from the practical and numerical results.
5. Applying this research results in practically will provide the ability to enhance the pile's constructability and the sustainability factor.
6. Applying the research results practically will provide to the engineers the ability to construct a higher rise building which is required deeper piles, this is due to the improving of the classical equations will end up with deep pile can be constructed practically.
7. Significant reduction in the proposed construction cost and time of the piling foundation in case of applying this research recommendation.

FURTHER RESEARCH

The research results defined the differences between the theoretical, practical and numerical pile capacity but unfortunately the research did not provide a specific difference between pile skin friction capacity and pile end bearing capacity in each case. This research methodology can be improved by using the numerical model. This by defining a non-soil material with very small stiffness value to cancel the end bearing resistance, this non-soil material will be assigned below the pile toe level to a distance equal to (2-3 times the Pile Diameter). The same concept which used before to estimate the numerical pile capacity will be used to calculate the pile capacity from the modified numerical model, but this value of pile capacity will present the numerical skin friction capacity. To get the value of numerical end bearing resistance, subtract the value of numerical skin friction from the value of numerical pile capacity which calculated before for the same case of study, the result will present the value of numerical end bearing resistance. In this case it can be easily to define the differences between the theoretical and numerical calculations, and the parameters of the theoretical equations can be improved accordingly.

THE METHODOLOGY

The further research will be applied in the following sections to the case 1 of study "Al Habtoor Residence", from figure 33 the theoretical pile capacity is equal to 27,670 KN. This value is a combination between the theoretical end bearing resistance 5,310 KN and the theoretical skin friction resistance 22,360 KN.

The numerical model has been developed to estimate the numerical skin friction resistance, this is by assigning a non-soil layer for a depth equal to (2 - 3 Pile Diameter). For the numerical end bearing resistance, it will be calculated by subtract the numerical skin friction resistance from the numerical pile capacity 38,277 KN.

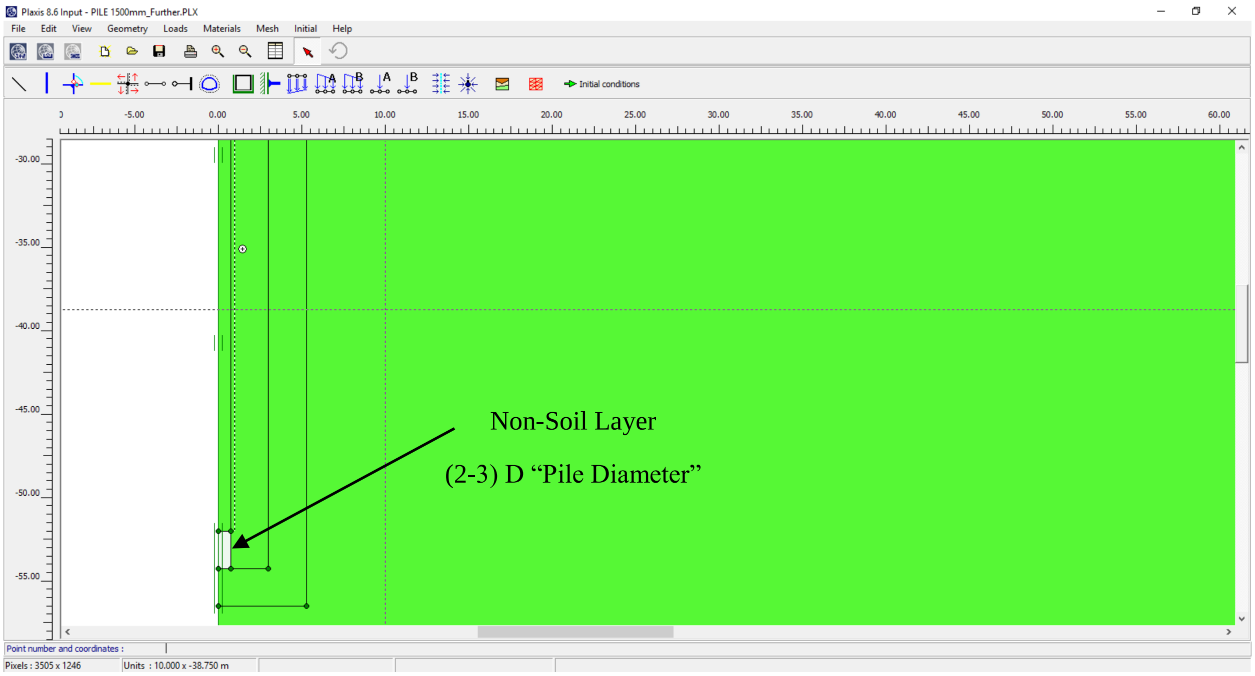

Figure 54. Modified Pile Model by Using PLAXIS 2D

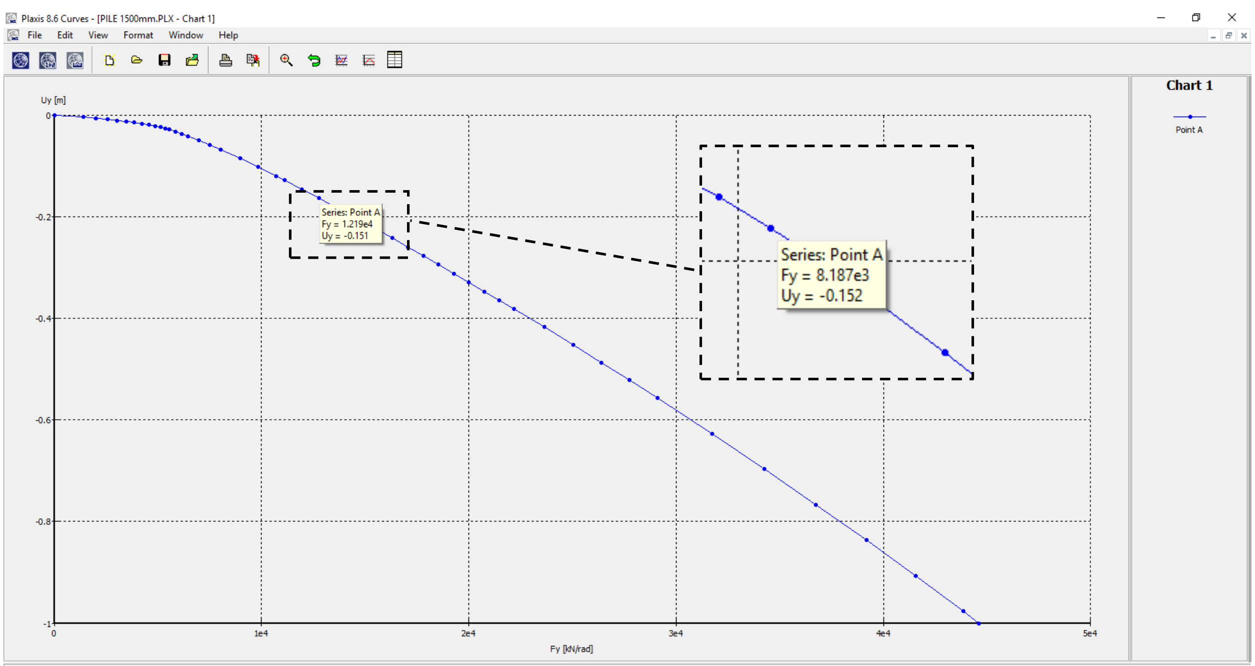

Figure 53. Modified Pile Load - Settlement Relationship Curve

Calculating the numerical pile capacity by using the load - settlement relationship curve as follow;

- 10% of the pile diameter = 150 mm = 0.15 m

- From the previous figure, F_y = 8,187 KN/rad at displacement equal to 120 mm

$$Q_{US} = F_y \times 2\pi = 8{,}187 \times 2\pi = 51{,}461\ KN \qquad \ldots\ldots \quad Eq.\ (32)$$

$$Q_S = \frac{Q_U}{F.O.S} = \frac{51{,}461}{2} = 25{,}730\ KN \qquad \ldots\ldots \quad Eq.\ (33)$$

From the previous equations, the calculated numerical skin friction compression pile capacity by using PLAXIS 2D is 25,730 KN. The numerical end bearing resistance will be;

$$Q_B = Q - Q_S = 38{,}277 - 25{,}730 = 12{,}547\ KN \qquad \ldots\ldots \quad Eq.\ (34)$$

The following table and figure summarized the results of the further research methodology;

Table 21. Further research results

CASE 1 _ AL HABTOOR RESIDENCE [Further Research]			
Theoretical Capacity [KN]		Numerical Capacity [KN]	
27,670		38,277	
% (Numerical / Theoretical)		138%	
Theoretical Skin Friction Capacity [KN]	Theoretical End Bearing Capacity [KN]	Numerical Skin Friction Capacity [KN]	Numerical End Bearing Capacity [KN]
22,360	5,310	25,730	12,547
% (Numerical / Theoretical)		115%	236%

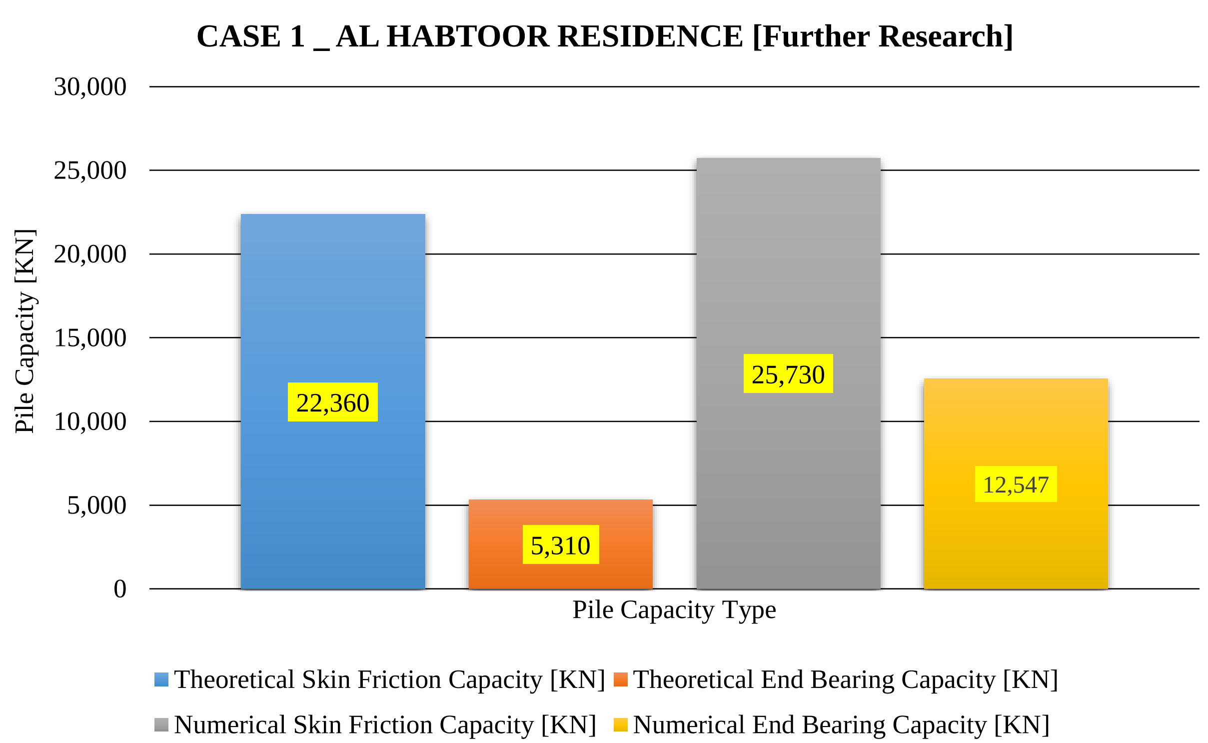

Figure 55. Further research results

REFERENCES

1. Baker, B. & Pawlikowski, J. (2015). The Design and Construction of the World's Tallest Building: The Burj Khalifa, Dubai. *Structural Engineering International*, vol. 25 (4), pp. 389-394.

2. Belloc, H. (1967). *On*. Freeport, N.Y.:Books for Libraries Press.

3. Brain, M. (n.d.). *The engineering book*.

4. Brinkgreve, R., Broere, W. & Al-Khoury, R. (2004). *PLAXIS: 2D, version 8*. Lisse:Balkema.

5. Esrig, M. & Bachus, R. (1991). *Deep foundation improvements*. Philadelphia, Pa:American Society for Testing and Materials.

6. Fu, F. (n.d.). *Advanced Modeling Techniques in Structural Design*.

7. Green, H. (1961). Long-Term Loading of Short-Bored Piles. *Géotechnique*, vol. 11 (1), pp. 47-53.

8. Hansbo, S. (1994). *Foundation engineering*. Amsterdam:Elsevier.

9. Huang, J., Zhang, J. & Chen, Z. (2011). Load-Transfer Properties of Extra-Long Piles Embedded into Deep Hard-Rock and High-Pressure Grouting Piles Set into Fragmental Rock. *Advanced Materials Research*, vol. 250-253, pp. 2501-2505.

10. Johnson, A. (2013). *Recommendations on Piling (EA Pfhle)*. Hoboken:Wiley.

11. Lee, M. (2015). *How did they build that?*. La Jolla, CA:Scobre Educational.

12. Lin, M. (2006). *Proceedings of the International Symposium on New Generation Design Codes for Geotechnical Engineering Practice - Taipei 2006*. Singapore:World Scientific.

13. Murthy, V. (2003). *Geotechnical engineering*. New York:Marcel Dekker.

14. Tomlinson, M. & Boorman, R. (2001). *Foundation design and construction*. Harlow [u.a.]:Prentice Hall.

15. Tomlinson, M. & Woodward, J. (n.d.). *Pile design and construction practice*.

16. Vesić, A. (1977). *Design of pile foundations*. Washington:Transportation Research Board, National Research Council.

17. Advances in structural engineering. (2011). Durnten-Zurich:TTP, Trans Tech Publications.

18. Bowles, J. (2007). Foundation analysis and design. Norwich, NY:Knovel.

19. British Standard code of practice for foundations (formerly CP 2004). (1986). London:British Standards Institution.

20. Chang, S., Bahar, S. & Zhao, J. (2013). Advances in civil engineering and building materals. Boca Raton, Fla.:CRC Press.

21. Chen, F. & Morris, M. (2001). Soil engineering. Boca Raton:CRC Press.

22. Cock, F. & Legrand, C. (1997). Design of axially loaded piles. Rotterdam [u.a.]:Balkema.

23. Design and construction of auger cast piles, and other foundation issues. (1994). Washington, D.C.:National Academy Press.

24. Hamza, M., Shahien, M. & El-Mossallamy, Y. (2009). Proceedings of the 17th International Conference on Soil Mechanics and Geotechnical Engineering. Amsterdam:IOS Press / Millpress Science Pub.

25. Madabhushi, G., Knappett, J. & Haigh, S. (2010). Design of pile foundations in liquefiable soils. London:Imperial College Press.

26. Orense, R., Chouw, N. & Pender, M. (2010). Soil-Foundation-Structure Interaction. Abingdon:CRC Press [Imprint].

27. Soil mechanics 2006. (2006). Washington:Transportation Research Board.

28. Terzaghi, K. (2007). Theoretical Soil Mechanics. Hoboken:Wiley [Imprint].

29. Young, F. (1982). Piles and foundations. London:Telford.

30. Zhao, Z., Chai, J. & Fan, C. (2014). Numerical Simulation Analysis of Bearing Performance of Extra-Long and Large-Diameter Single Pile. Advanced Materials Research, vol. 1065-1069, pp. 943-948.

31. Aoyama, H. (2001). Design of modern highrise reinforced concrete structures. London:Imperial College Press.

32. Belloc, H. (1967). On. Freeport, N.Y.:Books for Libraries Press.

33. Belloc, H. (1967). On. Freeport, N.Y.:Books for Libraries Press.

34. Bowles, J. (2007). Foundation analysis and design. Norwich, NY:Knovel.

35. Coduto, D., Kitch, W. & Yeung, M. (n.d.). Foundation design.

36. Crowther, C. (1989). Load testing of deep foundations. New York:Wiley.

37. Meyer, J. (1984). Analysis and design of pile foundations. New York, N.Y.:American Society of Civil Engineers.

38. Nash, P. (1989). Super structures. Ada, OK:Garrett Educational Corp.

39. Rao, N. (2011). Foundation Design: Theory and Practice. John Wiley & Sons.

40. Sabry, M. (2002). Shaft resistance of a single vertical or batter pile in sand subjected to axial compression or uplift loading. Ottawa:National Library of Canada = Bibliothèque nationale du Canada.

41. Wolf, J. & Deeks, A. (2004). Foundation vibration analysis. Amsterdam [u.a.]:Elsevier.

42. Wrana, B. (2015). Pile Load Capacity – Calculation Methods. Studia Geotechnica et Mechanica, vol. 37 (4).

43. Coduto, D., Kitch, W. & Yeung, M. (n.d.). Foundation design.

44. Deep Foundations on Bored and Auger Piles - BAP V. (2008). CRC Press.

45. Fleming, W. & Sliwinski, Z. (1986). The use and influence of bentonite in bored pile construction. London:CIRIA.

46. Gong, X., Fan, Q. & Xu, Y. (2011). Efficiency of Pile Groups of Large Diameter Bored Cast-in-Place Pile. Advanced Materials Research, vol. 261-263, pp. 1215-1219.

47. Wulandari, P. & Tjandra, D. (2015). Analysis of Piled Raft Foundation on Soft Soil Using PLAXIS 2D. Procedia Engineering, vol. 125, pp. 363-367.

48. 孙, 永. (2013). Based on PLAXIS Finite Element Software Analysis of Deep Foundation Pit. Hans Journal of Civil Engineering, vol. 02 (02), pp. 110-121.

Appendix [1] – Numerical Models Output

Numerical Models Output [Case 1]

REPORT

10/09/2017

User: Koxhiyoki Kabuto, Japan

Title: PILE 1500mm

Table of Contents

1. General Information

Table [1] units

Type	Unit
Length	m
Force	kN
Time	day

Table [2] Model dimensions

	min.	max.
X	0.000	104.000
Y	-130.000	0.000

Table [3] Model

Model	Axisymmetry
Element	15-Noded

2. Geometry

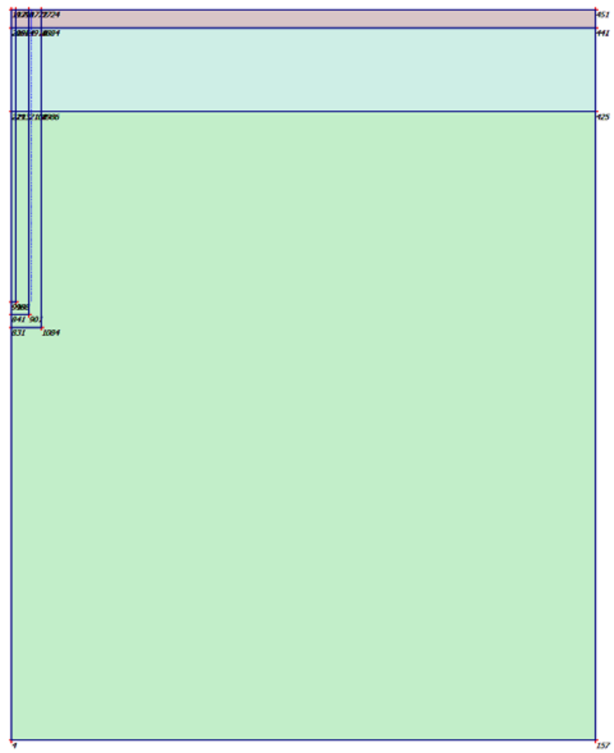

Fig. 1 Plot of geometry model with significant nodes

2.1. Clusters

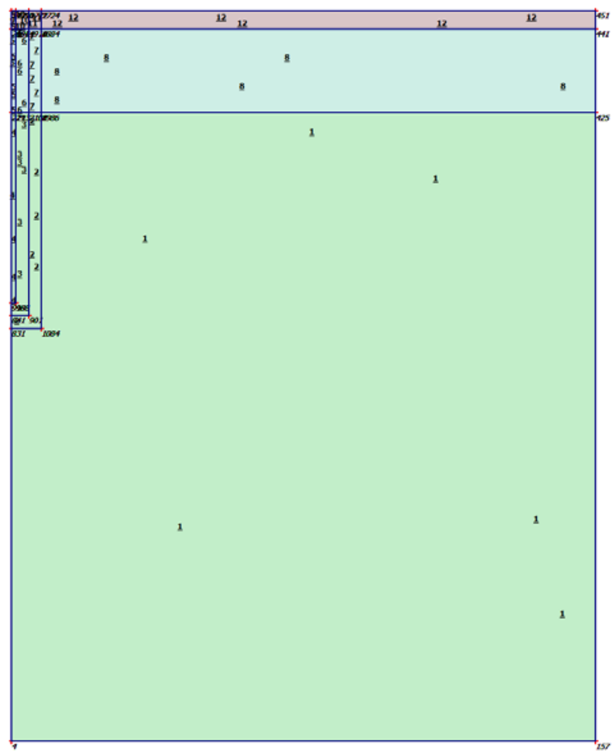

Fig. 2 Plot of geometry model with cluster numbers

3. Structures

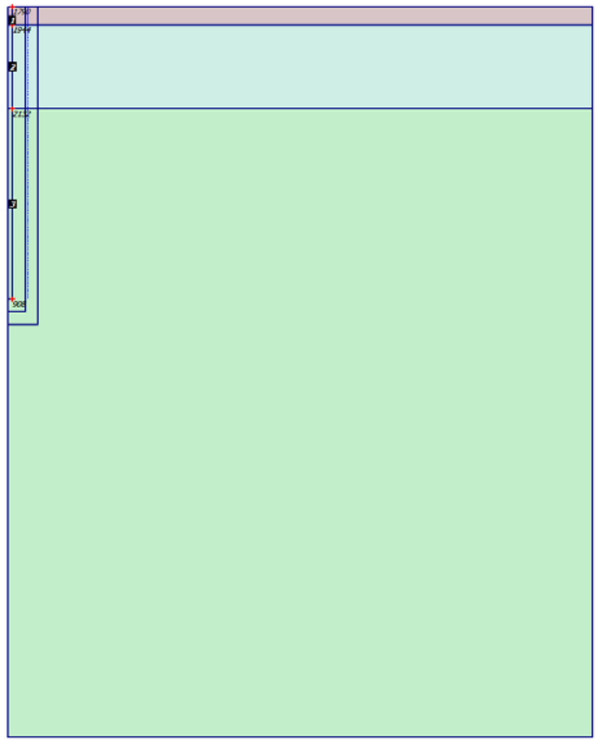

Fig. 3 Plot of geometry model with structures

Table [4] Interfaces

Interface no.	Data set	Nodes
1	SILTY SAND	1790, 1944.
2	SANDSTONE	1944, 2132.
3	CALC	2132, 908.

4. Mesh data

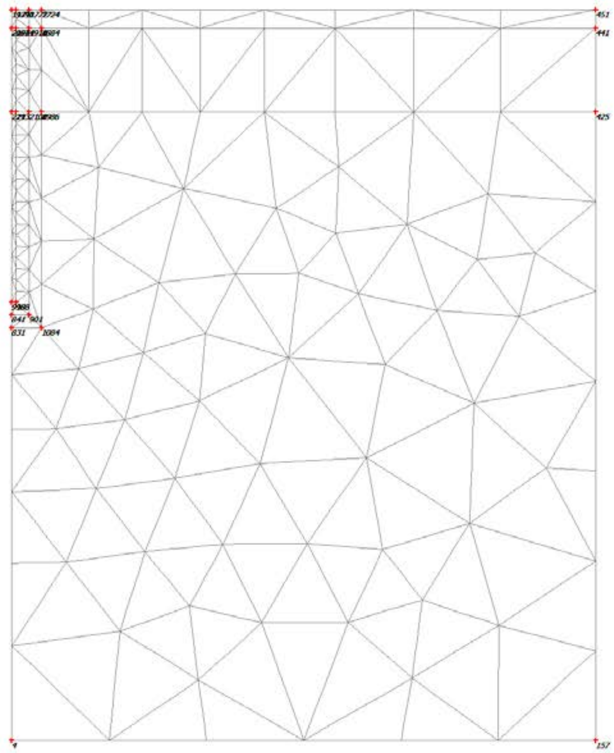

Fig. 4 Plot of the mesh with significant nodes

5. Material data

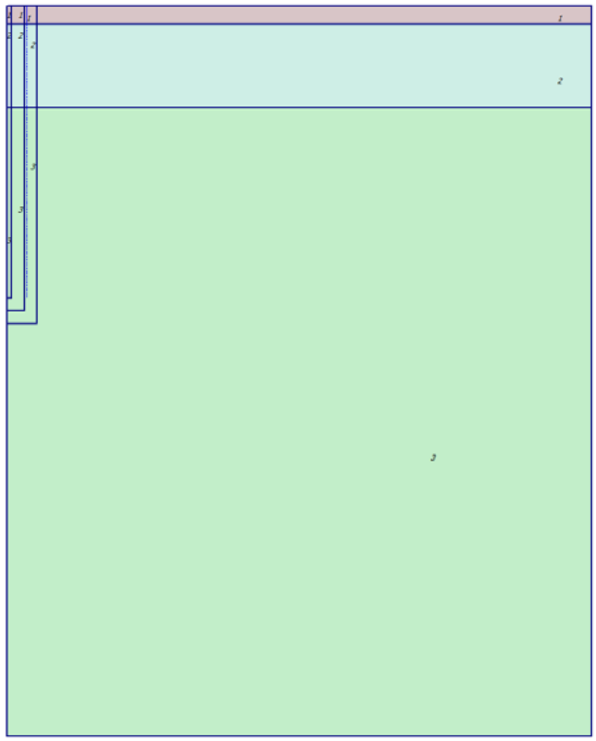

Fig. 5 Plot of geometry with material data sets

Table [5] Soil data sets parameters

Linear Elastic		4 CONCRETE
Type		Non-porous
γ_{unsat}	[kN/m³]	24.00
γ_{sat}	[kN/m³]	24.00
k_x	[m/day]	0.000
k_y	[m/day]	0.000
e_{init}	[-]	0.500
c_k	[-]	1E15

Linear Elastic		4 CONCRETE
E_{ref}	[kN/m²]	31992382.14
ν	[-]	0.200
G_{ref}	[kN/m²]	13329524.082
E_{oed}	[kN/m²]	35549632.653
E_{incr}	[kN/m²/m]	0.00
y_{ref}	[m]	0.000
R_{inter}	[-]	1.000
Interface permeability		Impermeable

Mohr-Coulomb		1 SILTY SAND	2 SANDSTONE	3 CALC
Type		Drained	Drained	Drained
γ_{unsat}	[kN/m³]	18.50	19.00	19.50
γ_{sat}	[kN/m³]	18.50	19.00	19.50
k_x	[m/day]	1.000	0.500	0.500
k_y	[m/day]	1.000	0.500	0.500
e_{init}	[-]	0.500	0.500	0.500
c_k	[-]	1E15	1E15	1E15
E_{ref}	[kN/m²]	30000.000	200000.000	400000.000
ν	[-]	0.300	0.300	0.300
G_{ref}	[kN/m²]	11540.645	76929.047	153857.001
E_{oed}	[kN/m²]	40356.820	269154.702	538323.312
c_{ref}	[kN/m²]	5.00	40.00	60.00
φ	[°]	34.00	40.00	40.00
ψ	[°]	5.00	10.00	10.00

Mohr-Coulomb		1 SILTY SAND	2 SANDSTONE	3 CALC
E_{inc}	[kN/m²/m]	0.00	0.00	0.00
y_{ref}	[m]	0.000	0.000	0.000
$c_{increment}$	[kN/m²/m]	0.00	0.00	0.00
$T_{str.}$	[kN/m²]	0.00	0.00	0.00
$R_{inter.}$	[-]	0.80	0.90	0.90
Interface permeability		Neutral	Neutral	Neutral

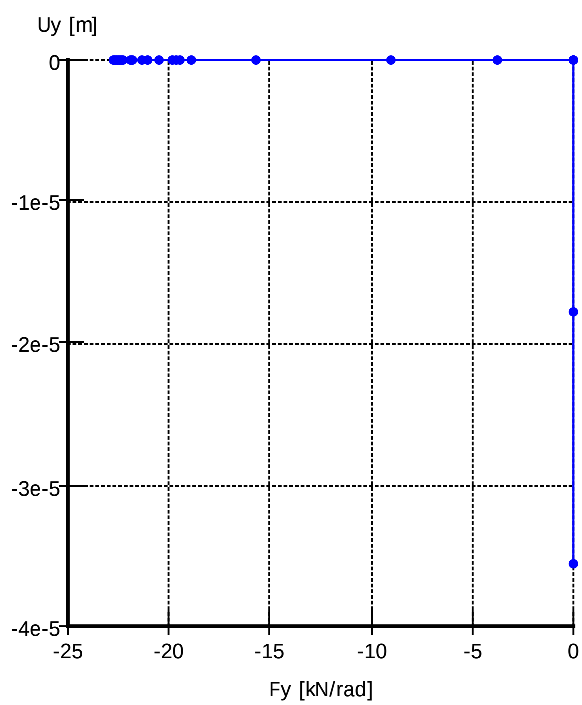

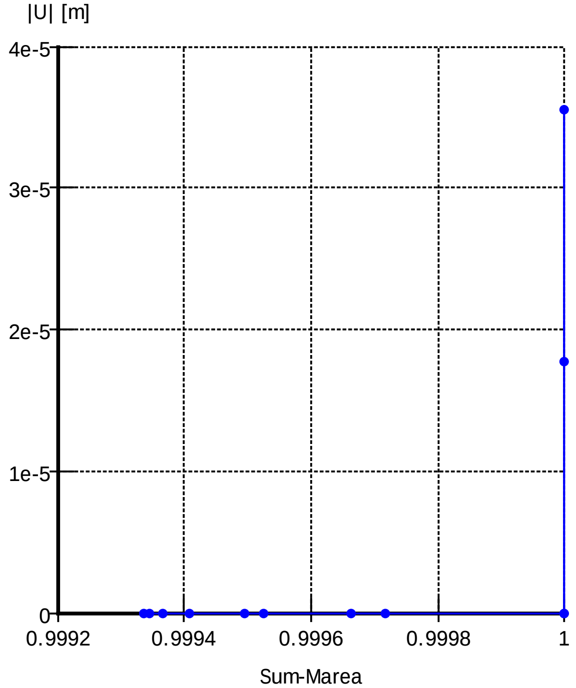
|U| [m]
4e-5
3e-5
2e-5
1e-5
0
0.9992
0.9994
0.9996
0.9998
1
Sum-Marea

Fig. 6

Fig. 7

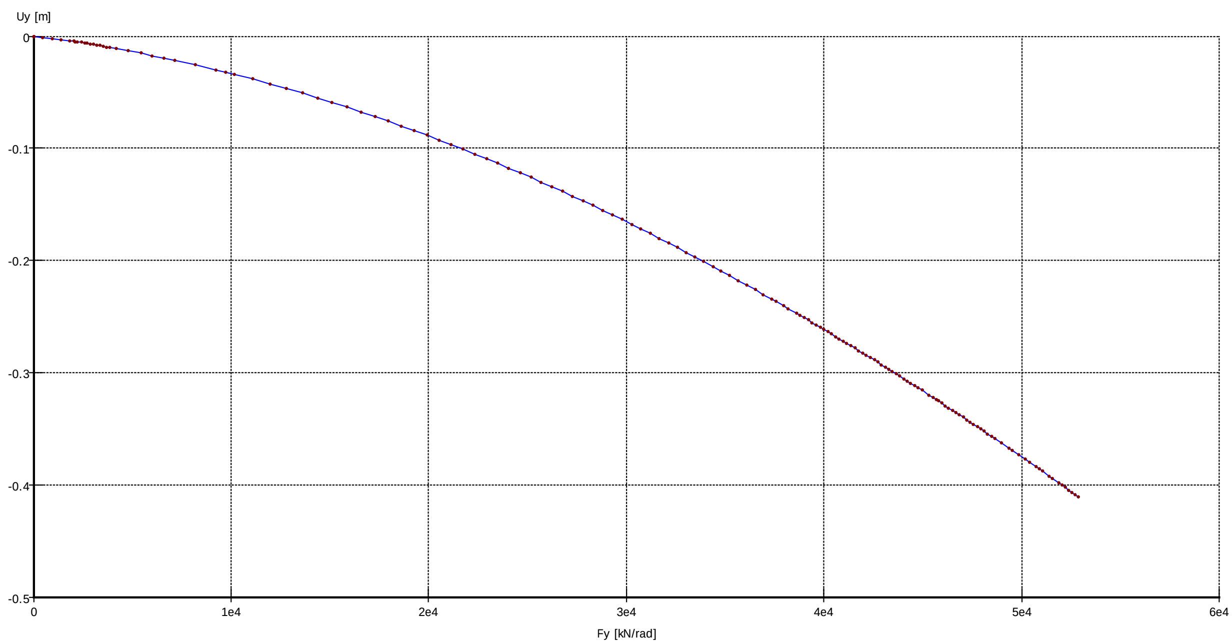
Uy [m]
0
-0.1
-0.2
-0.3
-0.4
-0.5
0
1e4
2e4
3e4
4e4
5e4
6e4
Fy [kN/rad]

Fig. 8

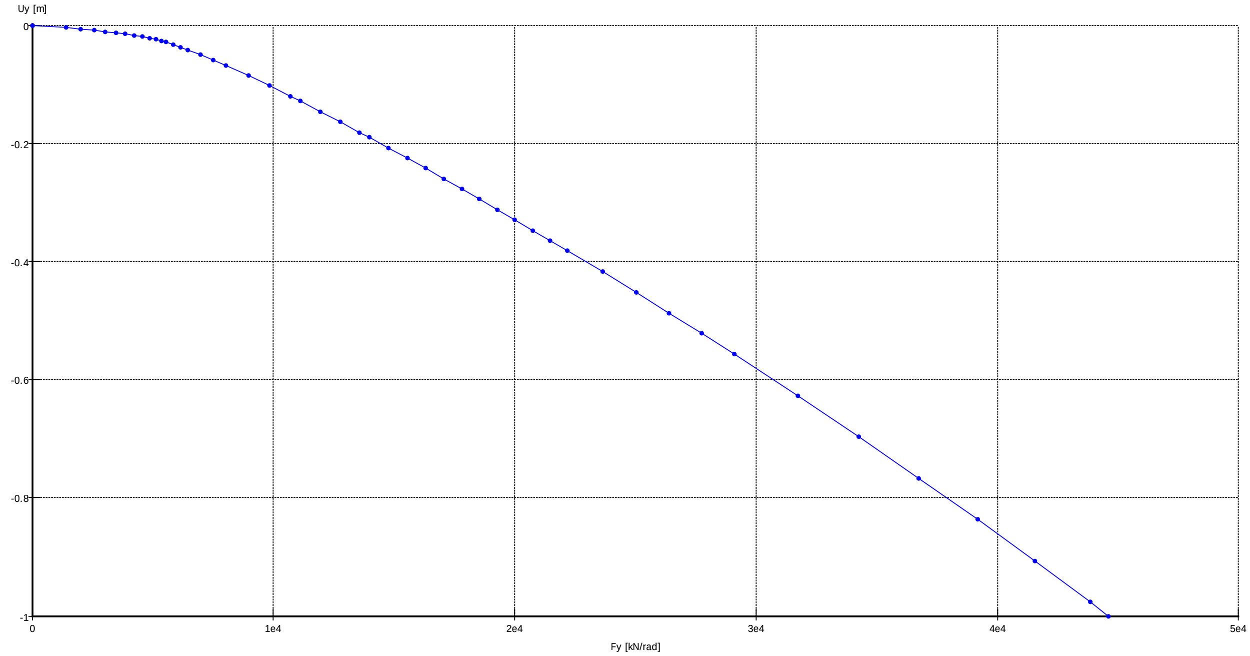

Fig. 9

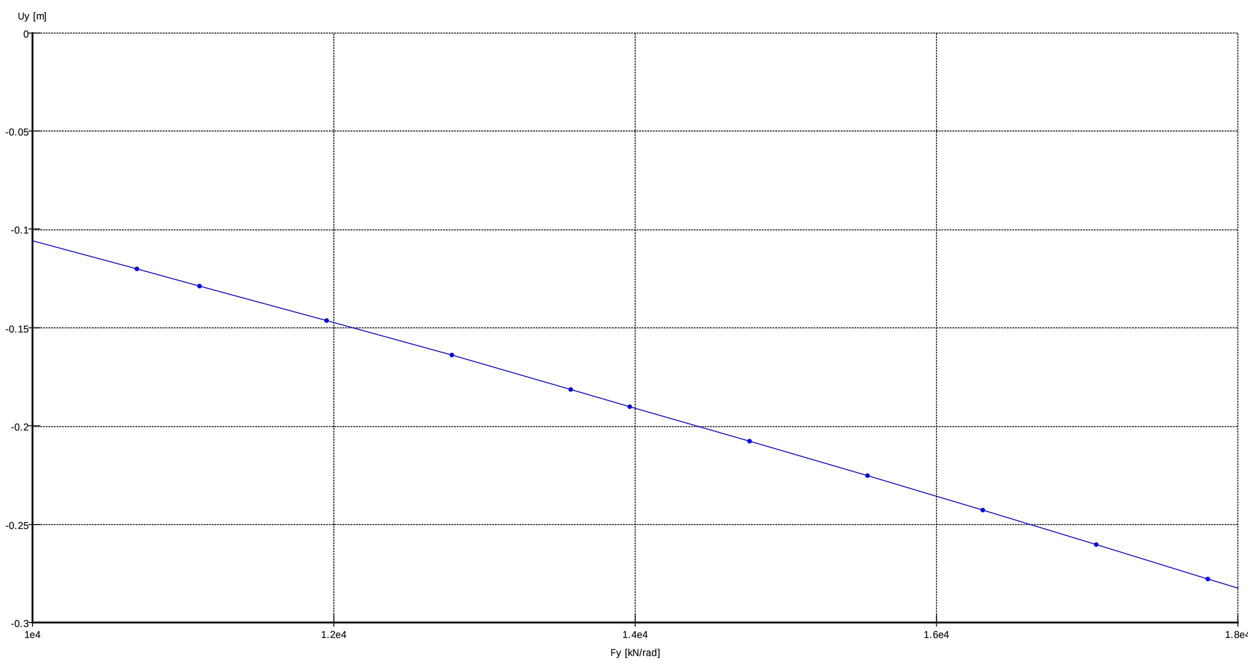

Fig. 10

Numerical Models Output [Case 2]

REPORT

10/09/2017

User: Koxhiyoki Kabuto, Japan

Title:

Table of Contents

1. General Information

Table [1] units

Type	Unit
Length	m
Force	kN
Time	day

Table [2] Model dimensions

	min.	max.
X	0.000	68.000
Y	-85.000	0.000

Table [3] Model

Model	Axisymmetry
Element	15-Noded

2. Geometry

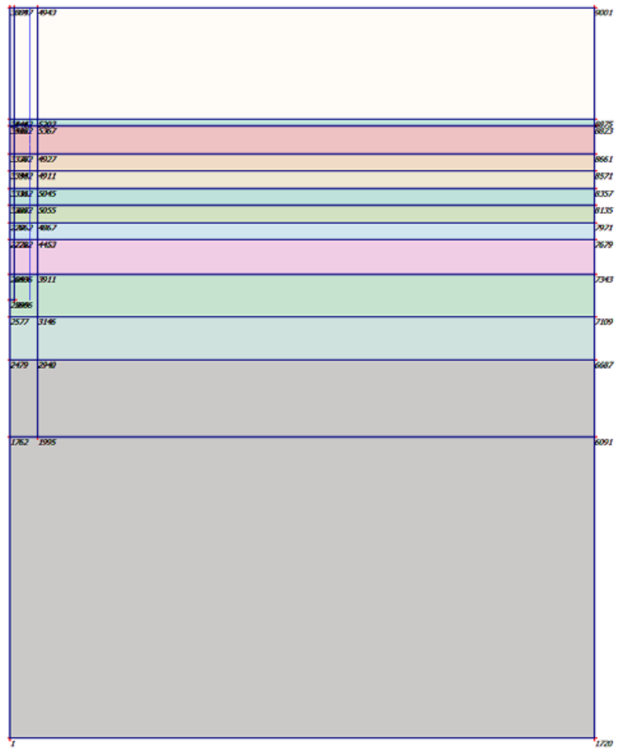

Fig. 1 Plot of geometry model with significant nodes

2.1. Clusters

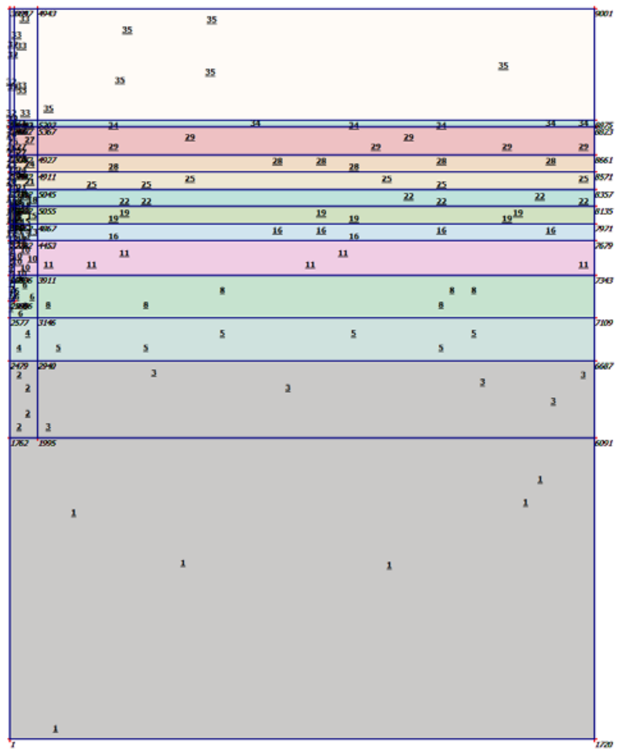

Fig. 2 Plot of geometry model with cluster numbers

3. Structures

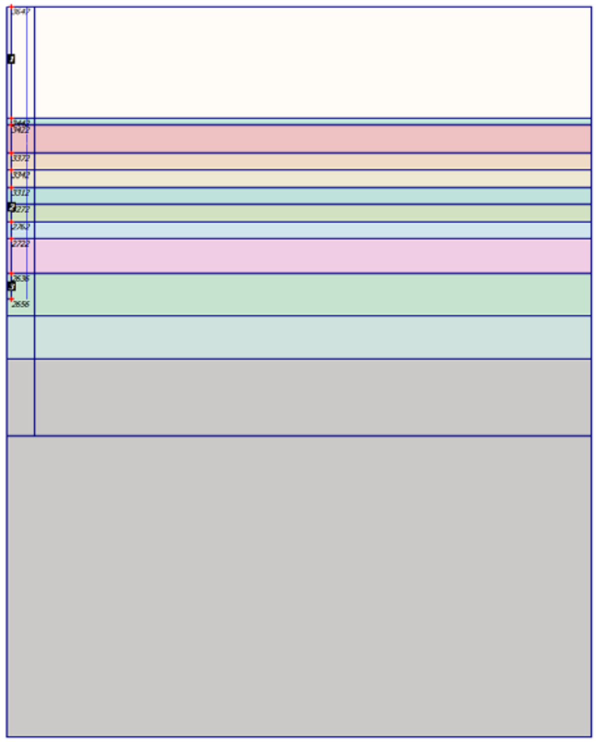

Fig. 3 Plot of geometry model with structures

Table [4] Interfaces

Interface no.	Data set	Nodes
1	Soil 1	3442, 3422.
	Soil 2	3647, 3442.
2	Soil 9	2722, 2636.
	Soil 7	2762, 2722.
	Soil 8	3272, 2762.
	Soil 7	3312, 3272.

Interface no.	**Data set**	**Nodes**
	Soil 6	3342, 3312.
	Soil 5	3372, 3342.
	Soil 4	3422, 3372.
3	Soil 10	2636, 2656.

4. Mesh data

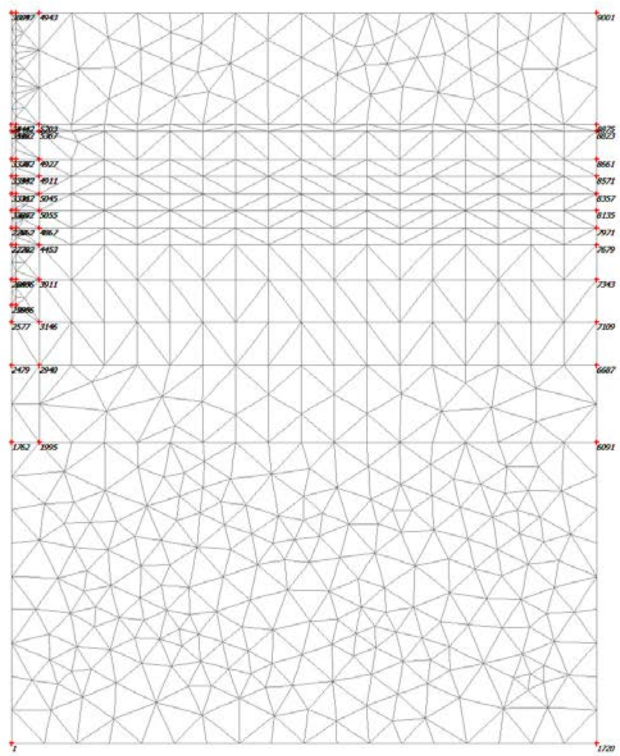

Fig. 4 Plot of the mesh with significant nodes

5. Material data

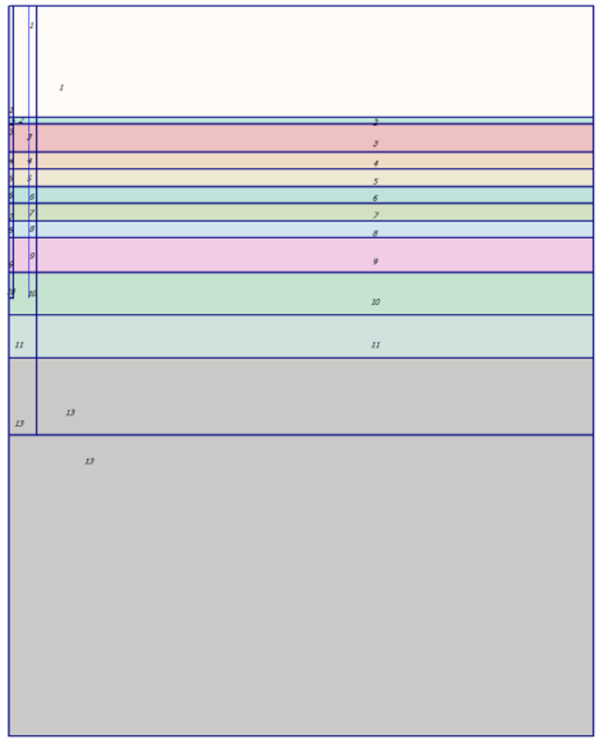

Fig. 5 Plot of geometry with material data sets

Table [5] Soil data sets parameters

Linear Elastic		**12** **Concrete**
Type		Non-porous
γ_{unsat}	[kN/m³]	24.00
γ_{sat}	[kN/m³]	24.00
k_x	[m/day]	0.000
k_y	[m/day]	0.000
e_{init}	[-]	0.500
c_k	[-]	1E15

Linear Elastic		12 Concrete
E_{ref}	[kN/m²]	32000000.00
ν	[-]	0.200
G_{ref}	[kN/m²]	13333333.333
E_{oed}	[kN/m²]	35555555.556
E_{incr}	[kN/m²/m]	0.00
y_{ref}	[m]	0.000
R_{inter}	[-]	1.000
Interface permeability		Impermeable

Mohr-Coulomb		1 Soil 1	2 Soil 2	3 Soil 3	4 Soil 4
Type		Drained	Drained	Drained	Drained
γ_{unsat}	[kN/m³]	18.00	18.00	22.00	22.00
γ_{sat}	[kN/m³]	18.00	18.00	22.00	22.00
k_x	[m/day]	0.000	0.000	0.000	0.000
k_y	[m/day]	0.000	0.000	0.000	0.000
e_{init}	[-]	0.500	0.500	0.500	0.500
c_k	[-]	1E15	1E15	1E15	1E15
E_{ref}	[kN/m²]	25000.000	50000.000	200000.000	199980.653
ν	[-]	0.350	0.350	0.300	0.300
G_{ref}	[kN/m²]	9259.259	18518.500	76922.158	76914.716
E_{oed}	[kN/m²]	40123.457	80247.396	269242.493	269216.447
c_{ref}	[kN/m²]	0.00	0.00	70.00	100.00
φ	[°]	34.00	36.00	32.00	32.00
ψ	[°]	4.00	6.00	0.00	0.00

Mohr-Coulomb		1 Soil 1	2 Soil 2	3 Soil 3	4 Soil 4
E_{inc}	[kN/m²/m]	1000.00	1000.00	1000.00	1000.00
y_{ref}	[m]	0.000	0.000	0.000	0.000
$c_{increment}$	[kN/m²/m]	5.00	5.00	0.00	0.00
$T_{str.}$	[kN/m²]	0.00	0.00	0.00	0.00
$R_{inter.}$	[-]	0.80	0.80	0.90	0.90
Interface permeability		Neutral	Neutral	Neutral	Neutral

Mohr-Coulomb		5 Soil 5	6 Soil 6	7 Soil 7	8 Soil 8
Type		Drained	Drained	Drained	Drained
γ_{unsat}	[kN/m³]	22.00	22.00	22.00	22.00
γ_{sat}	[kN/m³]	22.00	22.00	22.00	22.00
k_x	[m/day]	0.000	0.000	0.000	0.000
k_y	[m/day]	0.000	0.000	0.000	0.000
e_{init}	[-]	0.500	0.500	0.500	0.500
c_k	[-]	1E15	1E15	1E15	1E15
E_{ref}	[kN/m²]	200000.000	199980.653	75000.000	75000.000
ν	[-]	0.300	0.300	0.300	0.300
G_{ref}	[kN/m²]	76923.077	76914.716	28846.154	28846.154
E_{oed}	[kN/m²]	269230.769	269216.447	100961.538	100961.538
c_{ref}	[kN/m²]	80.00	60.00	20.00	27.00
φ	[°]	32.00	32.00	27.00	27.00
ψ	[°]	0.00	0.00	0.00	0.00
E_{inc}	[kN/m²/m]	1000.00	1000.00	1000.00	1000.00
y_{ref}	[m]	0.000	0.000	0.000	0.000

Mohr-Coulomb		5 Soil 5	6 Soil 6	7 Soil 7	8 Soil 8
$c_{increment}$	[kN/m²/m]	0.00	0.00	0.00	0.00
$T_{str.}$	[kN/m²]	0.00	0.00	0.00	0.00
$R_{inter.}$	[-]	0.90	0.90	0.90	0.90
Interface permeability		Neutral	Neutral	Neutral	Neutral

Mohr-Coulomb		9 Soil 9	10 Soil 10	11 Soil 11	13 Soil 12
Type		Drained	Drained	Drained	Drained
γ_{unsat}	[kN/m³]	22.00	22.00	22.00	22.00
γ_{sat}	[kN/m³]	22.00	22.00	22.00	22.00
k_x	[m/day]	0.000	0.000	0.000	0.000
k_y	[m/day]	0.000	0.000	0.000	0.000
e_{init}	[-]	0.500	0.500	0.500	0.500
c_k	[-]	1E15	1E15	1E15	1E15
E_{ref}	[kN/m²]	149982.587	250081.119	250000.000	400051.358
ν	[-]	0.300	0.300	0.300	0.300
G_{ref}	[kN/m²]	57685.100	96191.633	96153.846	153863.600
E_{oed}	[kN/m²]	201906.145	336563.722	336538.462	538560.090
c_{ref}	[kN/m²]	60.00	120.00	130.00	85.00
φ	[°]	32.00	32.00	32.00	34.00
ψ	[°]	0.00	0.00	0.00	0.00
E_{inc}	[kN/m²/m]	1000.00	1000.00	1000.00	1000.00
y_{ref}	[m]	0.000	0.000	0.000	0.000
$c_{increment}$	[kN/m²/m]	0.00	0.00	0.00	0.00
$T_{str.}$	[kN/m²]	0.00	0.00	0.00	0.00

Mohr-Coulomb		**9** **Soil 9**	**10** **Soil 10**	**11** **Soil 11**	**13** **Soil 12**
$R_{inter.}$	[-]	0.90	0.90	0.90	0.90
Interface permeability		Neutral	Neutral	Neutral	Neutral

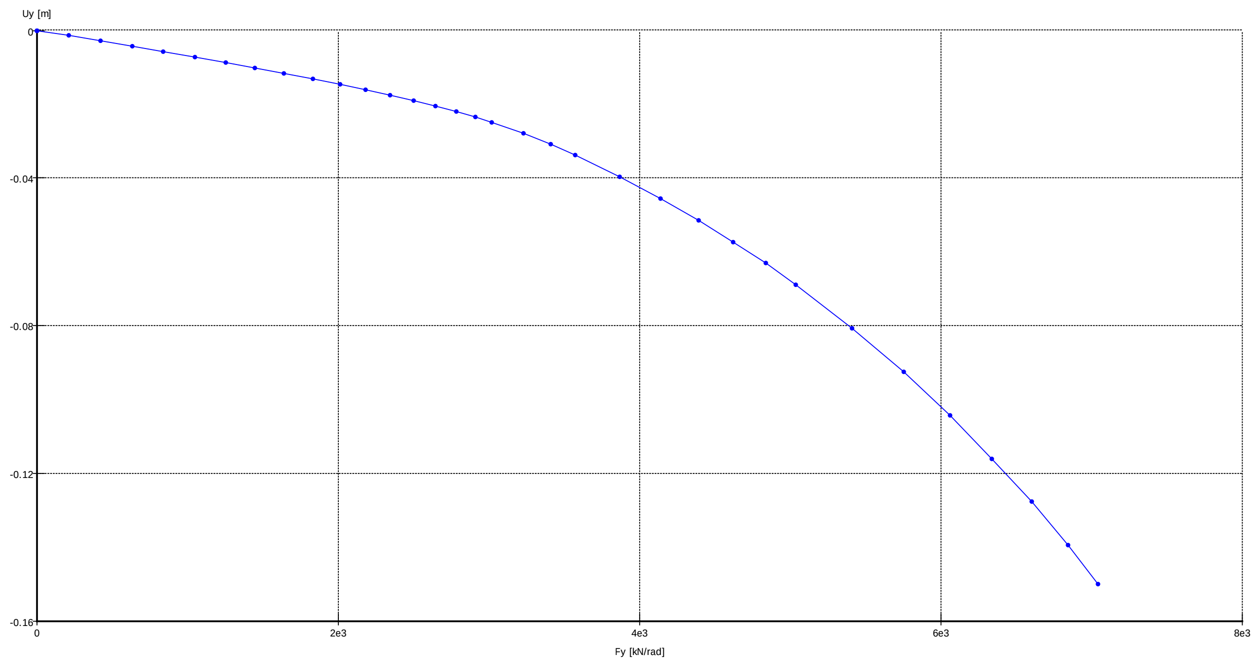

Fig. 6

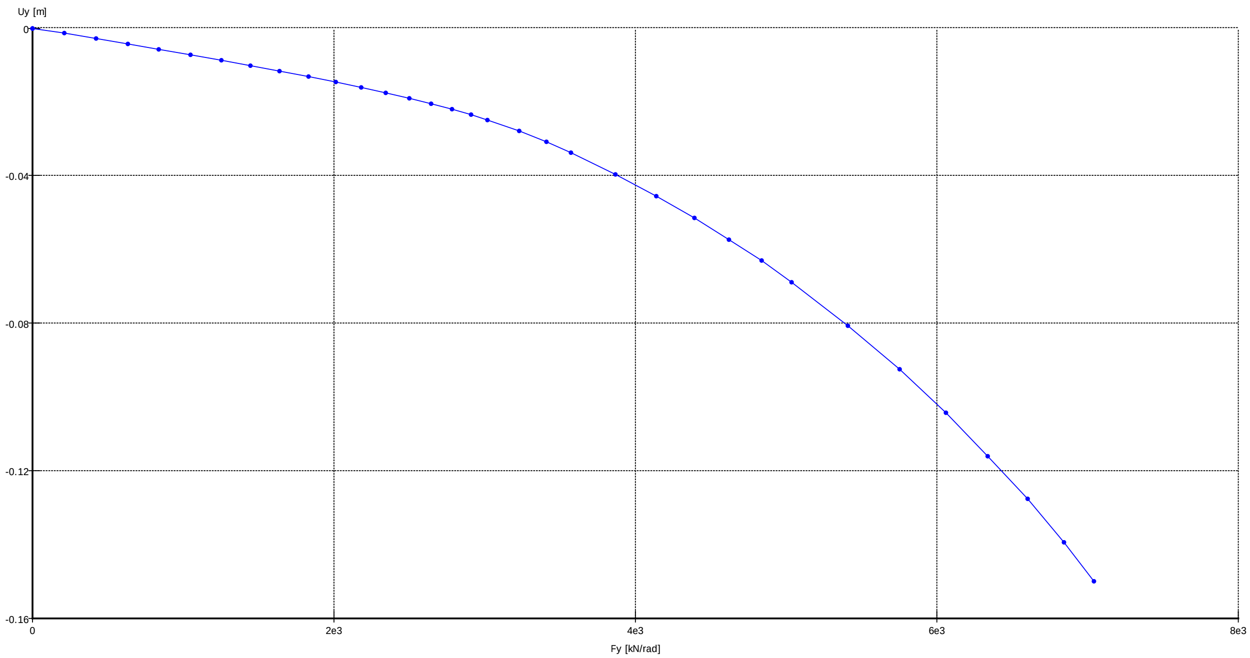

Fig. 7

Numerical Models Output [Case 3]

REPORT

10/09/2017

User: Koxhiyoki Kabuto, Japan

Title: Pile Dia 1200 mm

Table of Contents

1. General Information

Table [1] units

Type	**Unit**
Length	m
Force	kN
Time	day

Table [2] Model dimensions

	min.	**max.**
X	0.000	55.600
Y	-69.500	0.000

Table [3] Model

Model	Axisymmetry
Element	15-Noded

2. Geometry

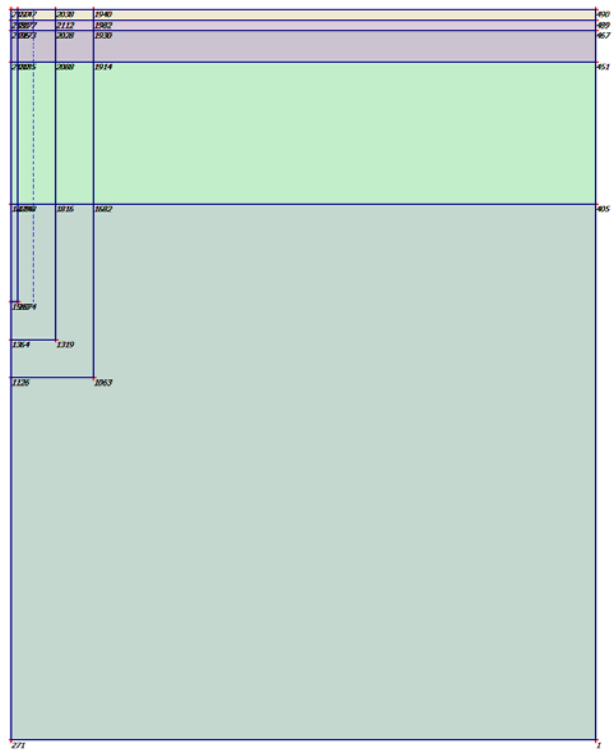

Fig. 1 Plot of geometry model with significant nodes

2.1. Clusters

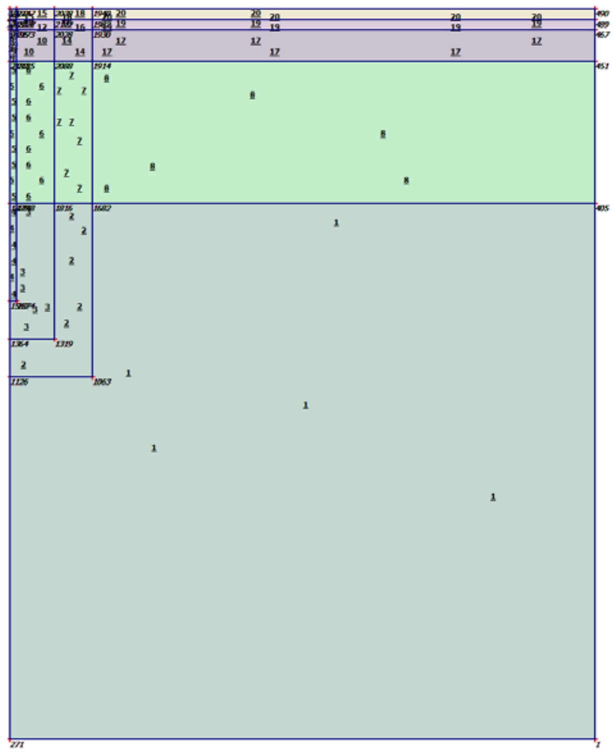

Fig. 2 Plot of geometry model with cluster numbers

3. Structures

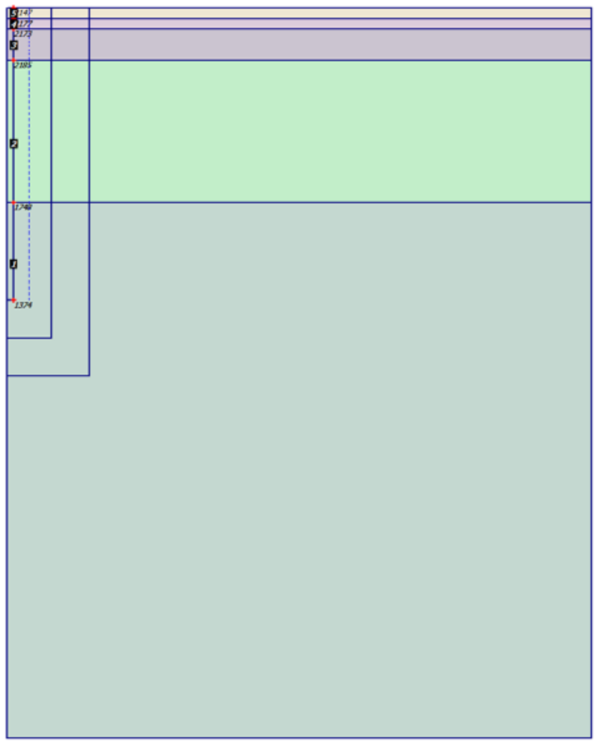

Fig. 3 Plot of geometry model with structures

Table [4] Interfaces

Interface no.	Data set	Nodes
1	CALCARENITE _ Layer 5	1748, 1374.
2	CALCARENITE _ Layer 4	2185, 1748.
3	Sand Soil _ Layer 2	2173, 2185.
4	Sand Soil _ Layer 1	2177, 2173.

Interface no.	Data set	Nodes
5	Sand Soil _ Layer 2	2147, 2177.

4. Mesh data

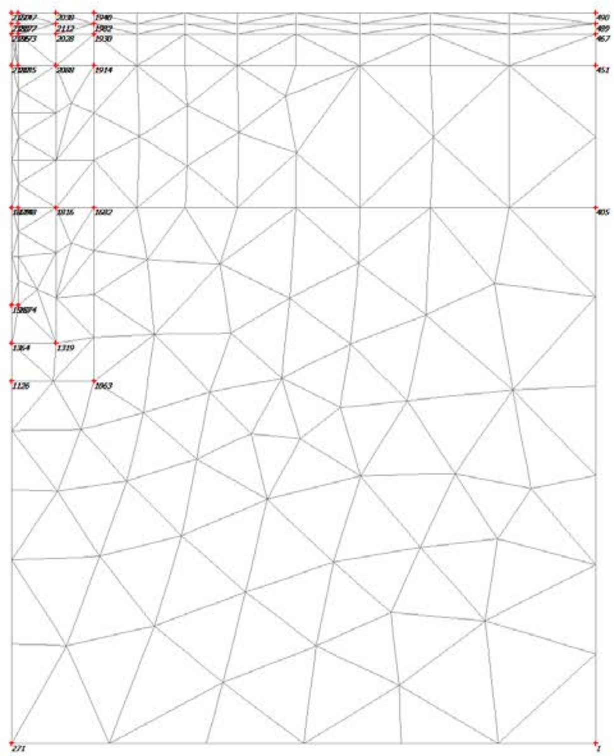

Fig. 4 Plot of the mesh with significant nodes

5. Material data

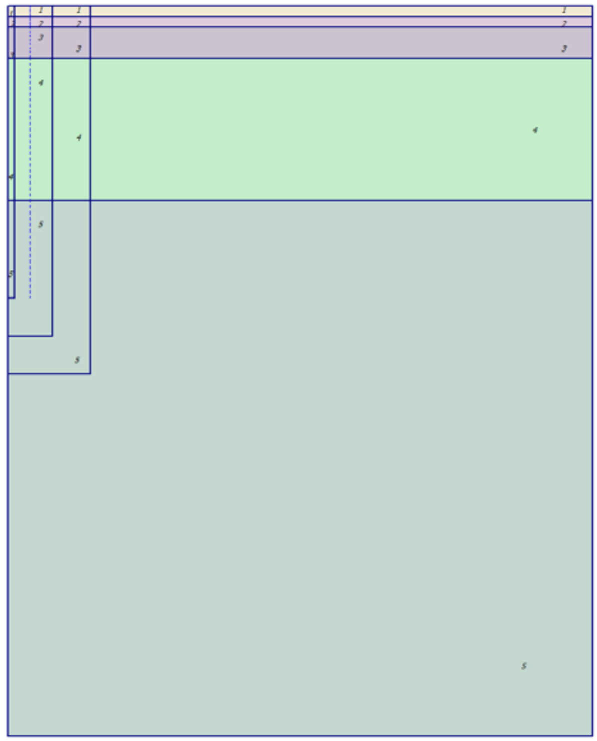

Fig. 5 Plot of geometry with material data sets

Table [5] Soil data sets parameters

Linear Elastic		**6** **Concrete**
Type		Non-porous
γ_{unsat}	[kN/m³]	24.00
γ_{sat}	[kN/m³]	24.00
k_x	[m/day]	0.000
k_y	[m/day]	0.000
e_{init}	[-]	0.500
c_k	[-]	1E15

Linear Elastic		**6** **Concrete**
E_{ref}	[kN/m²]	32000000.00
ν	[-]	0.200
G_{ref}	[kN/m²]	13332698.038
E_{oed}	[kN/m²]	35558097.545
E_{incr}	[kN/m²/m]	0.00
y_{ref}	[m]	0.000
R_{inter}	[-]	1.000
Interface permeability		Impermeable

Mohr-Coulomb		**1** **Sand Soil _ Layer 1**	**2** **Sand Soil _ Layer 2**	**3** **Sand Soil _ Layer 3**	**4** **CALCARENITE _ Layer 4**
Type		Drained	Drained	Drained	Drained
γ_{unsat}	[kN/m³]	18.00	18.00	18.00	22.00
γ_{sat}	[kN/m³]	20.00	20.00	20.00	22.00
k_x	[m/day]	0.000	0.000	0.000	0.000
k_y	[m/day]	0.000	0.000	0.000	0.000
e_{init}	[-]	0.500	0.500	0.500	0.500
c_k	[-]	1E15	1E15	1E15	1E15
E_{ref}	[kN/m²]	35000.000	50000.000	60000.000	300000.000
ν	[-]	0.350	0.350	0.330	0.300
G_{ref}	[kN/m²]	12962.963	18518.500	22555.146	115384.615
E_{oed}	[kN/m²]	56172.840	80247.396	88922.464	403846.154
c_{ref}	[kN/m²]	0.50	5.00	5.00	85.00
φ	[°]	36.00	38.00	40.00	36.00
ψ	[°]	6.00	8.00	10.00	0.00

Mohr-Coulomb		**1** **Sand Soil _ Layer 1**	**2** **Sand Soil _ Layer 2**	**3** **Sand Soil _ Layer 3**	**4** **CALCARENITE _ Layer 4**
E_{inc}	[kN/m²/m]	5000.00	5000.00	5000.00	10000.00
y_{ref}	[m]	0.000	0.000	0.000	0.000
$c_{increment}$	[kN/m²/m]	0.00	0.00	0.00	0.00
$T_{str.}$	[kN/m²]	0.00	0.00	0.00	0.00
$R_{inter.}$	[-]	0.80	0.80	0.80	1.00
Interface permeability		Neutral	Neutral	Neutral	Neutral

Mohr-Coulomb		**5** **CALCARENITE _ Layer 5**
Type		Drained
γ_{unsat}	[kN/m³]	22.00
γ_{sat}	[kN/m³]	22.00
k_x	[m/day]	0.000
k_y	[m/day]	0.000
e_{init}	[-]	0.500
c_k	[-]	1E15
E_{ref}	[kN/m²]	400000.000
ν	[-]	0.300
G_{ref}	[kN/m²]	153846.154
E_{oed}	[kN/m²]	538461.538
c_{ref}	[kN/m²]	35.00
φ	[°]	33.00
ψ	[°]	0.00
E_{inc}	[kN/m²/m]	1000.00

Mohr-Coulomb		**5** **CALCARENITE _ Layer 5**
y_{ref}	[m]	0.000
$c_{increment}$	[kN/m²/m]	0.00
$T_{str.}$	[kN/m²]	0.00
$R_{inter.}$	[-]	1.00
Interface permeability		Neutral

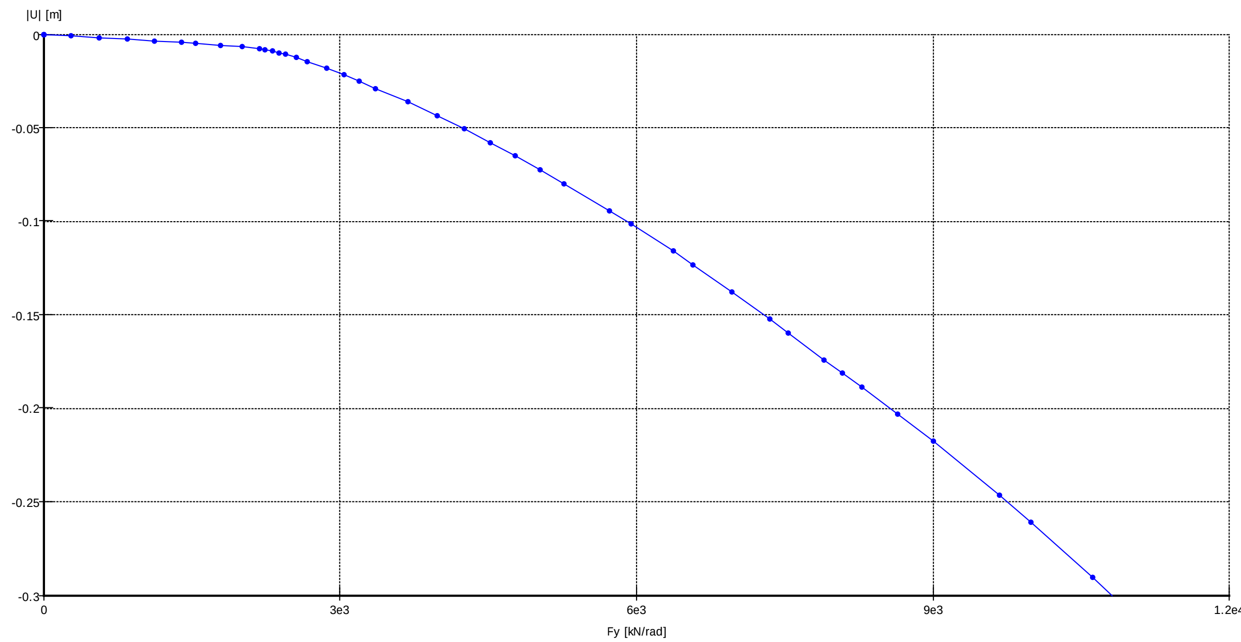

Fig. 6

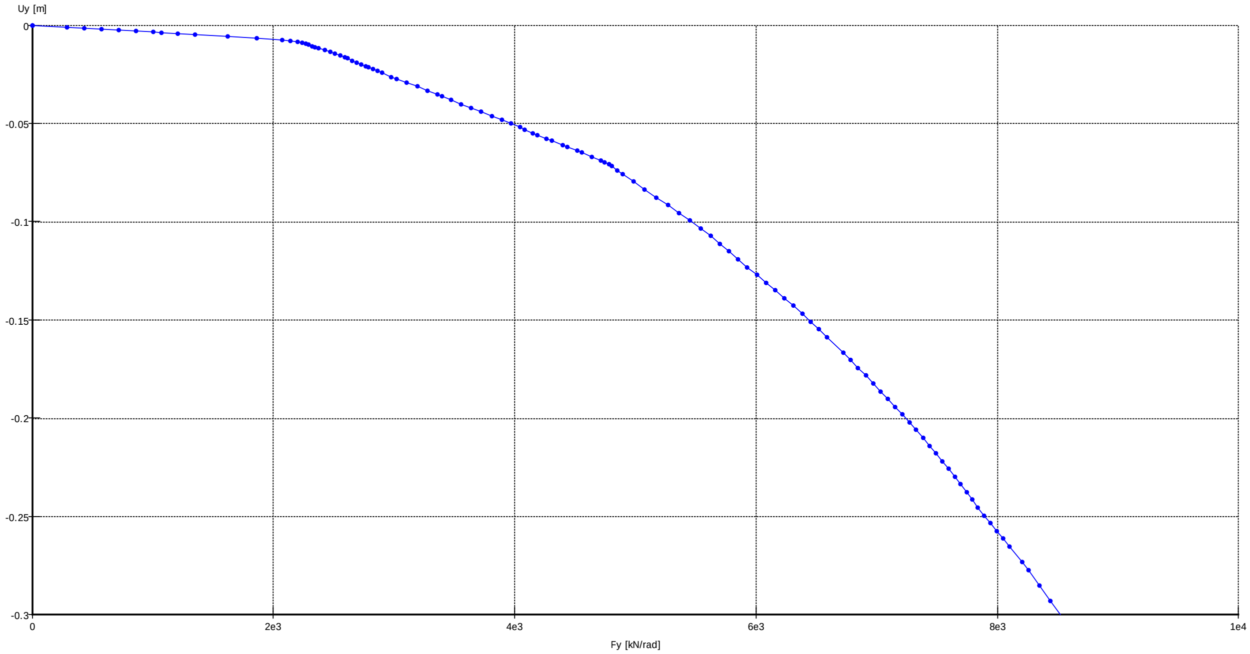
Uy [m]
0
-0.05
-0.1
-0.15
-0.2
-0.25
-0.3
0
2e3
4e3
6e3
8e3
1e4
Fy [kN/rad]

Fig. 7

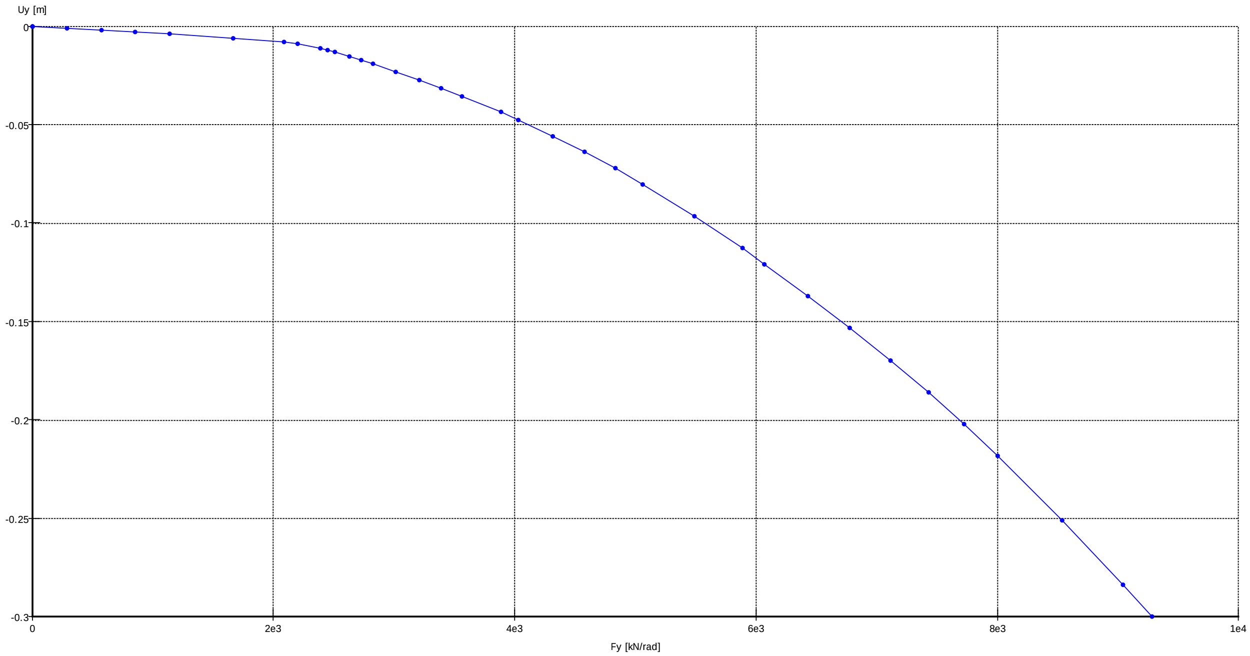
Uy [m]
0
-0.05
-0.1
-0.15
-0.2
-0.25
-0.3
0
2e3
4e3
6e3
8e3
1e4
Fy [kN/rad]

Fig. 8

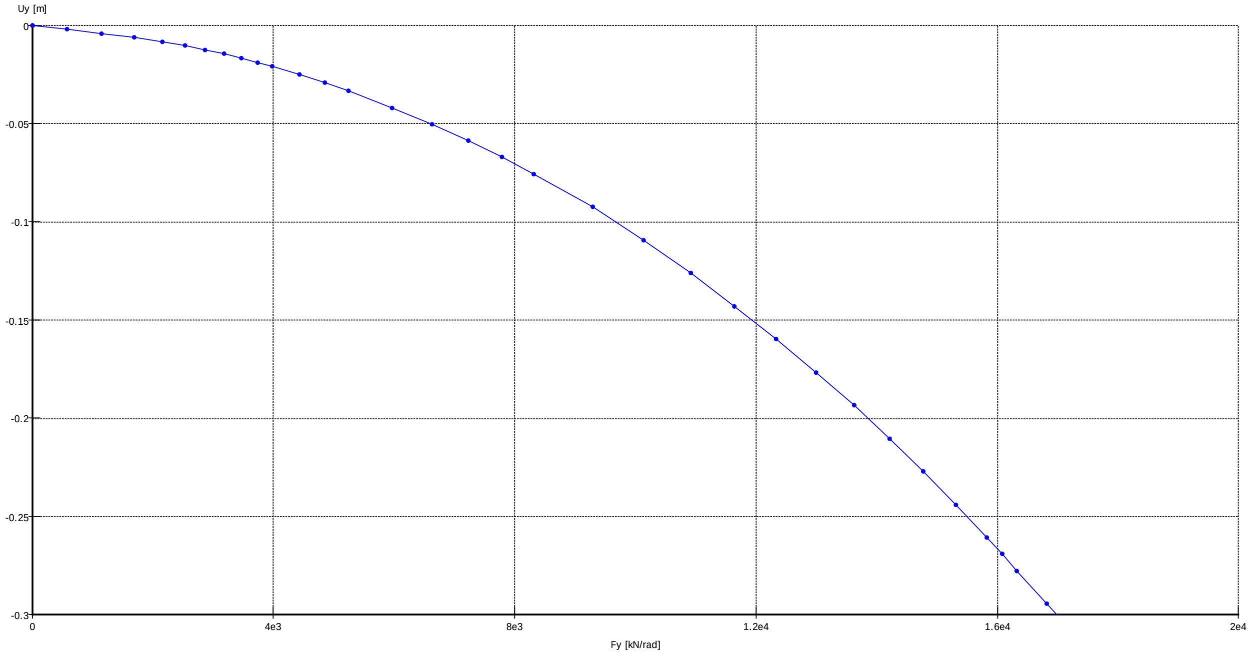
Uy [m]
0
-0.05
-0.1
-0.15
-0.2
-0.25
-0.3
0
4e3
8e3
1.2e4
1.6e4
2e4
Fy [kN/rad]

Fig. 9

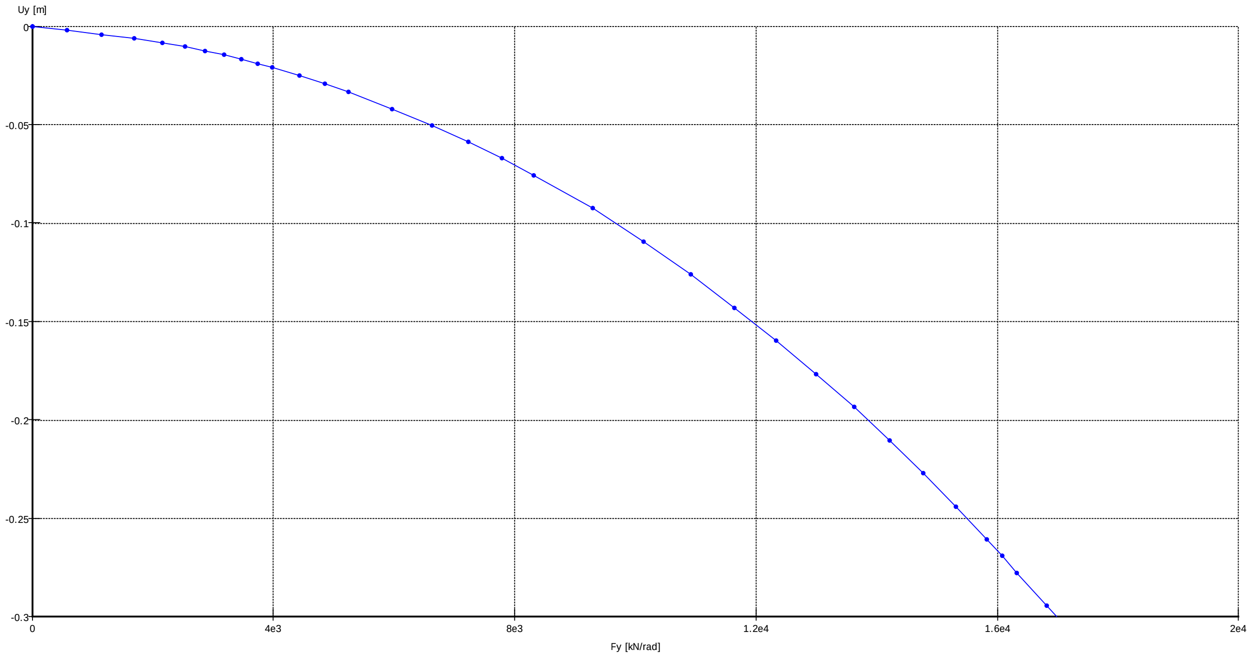
Uy [m]
0
-0.05
-0.1
-0.15
-0.2
-0.25
-0.3
0
4e3
8e3
1.2e4
1.6e4
2e4
Fy [kN/rad]

Fig. 10

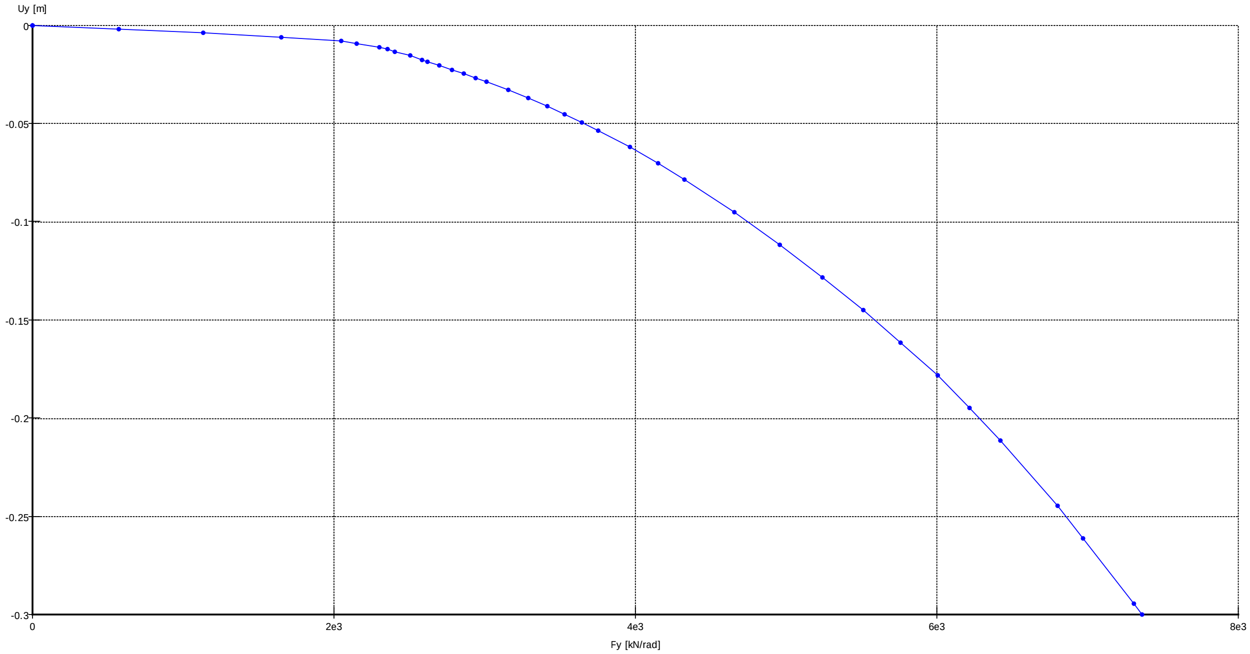
Uy [m]
0
-0.05
-0.1
-0.15
-0.2
-0.25
-0.3
0
2e3
4e3
6e3
8e3
Fy [kN/rad]

Fig. 11

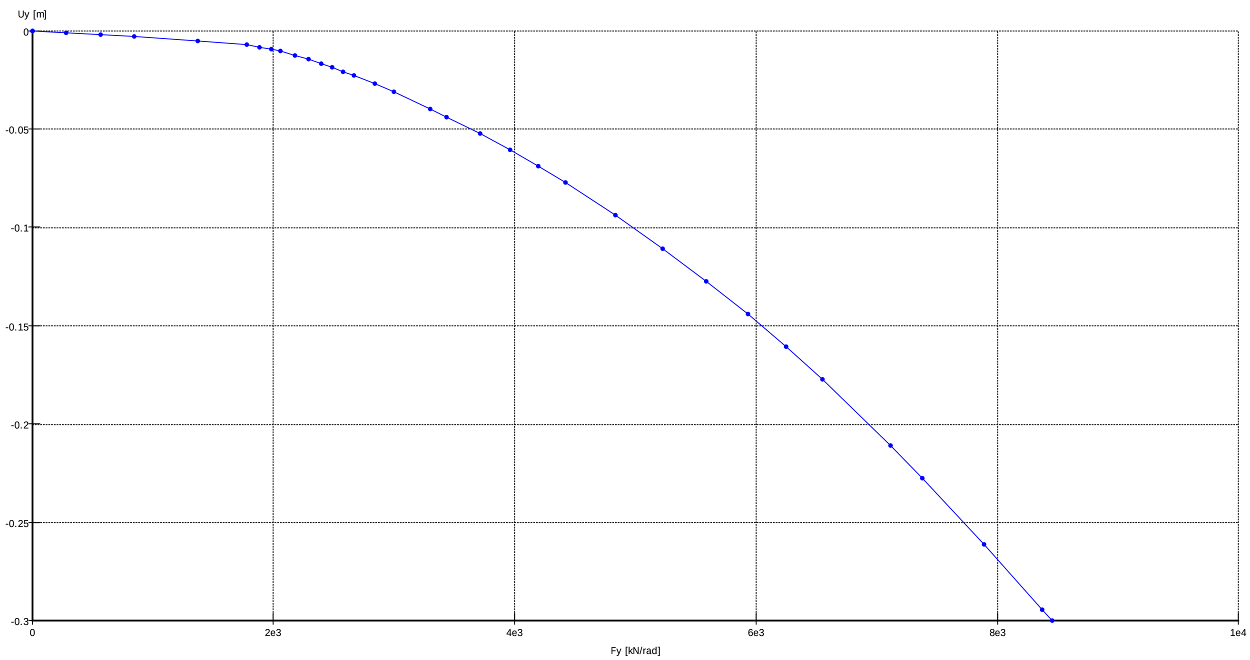
Uy [m]
0
-0.05
-0.1
-0.15
-0.2
-0.25
-0.3
0
2e3
4e3
6e3
8e3
1e4
Fy [kN/rad]

Fig. 12

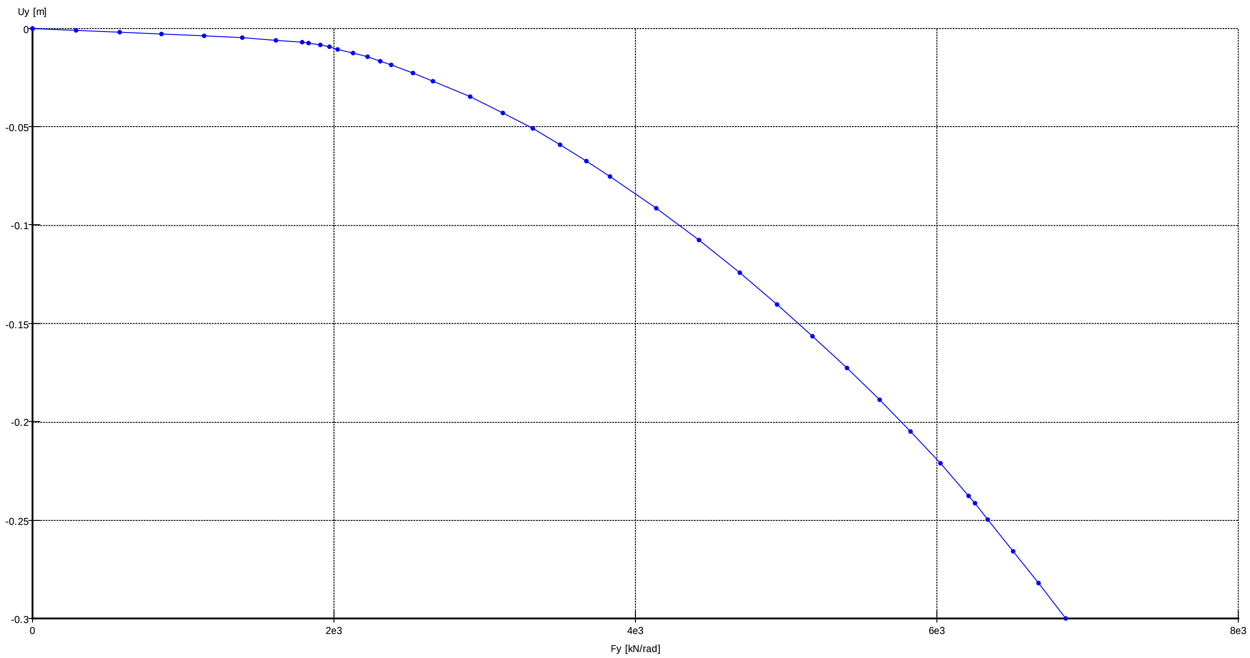
Uy [m]
0
-0.05
-0.1
-0.15
-0.2
-0.25
-0.3
0
2e3
4e3
6e3
8e3
Fy [kN/rad]

Fig. 13

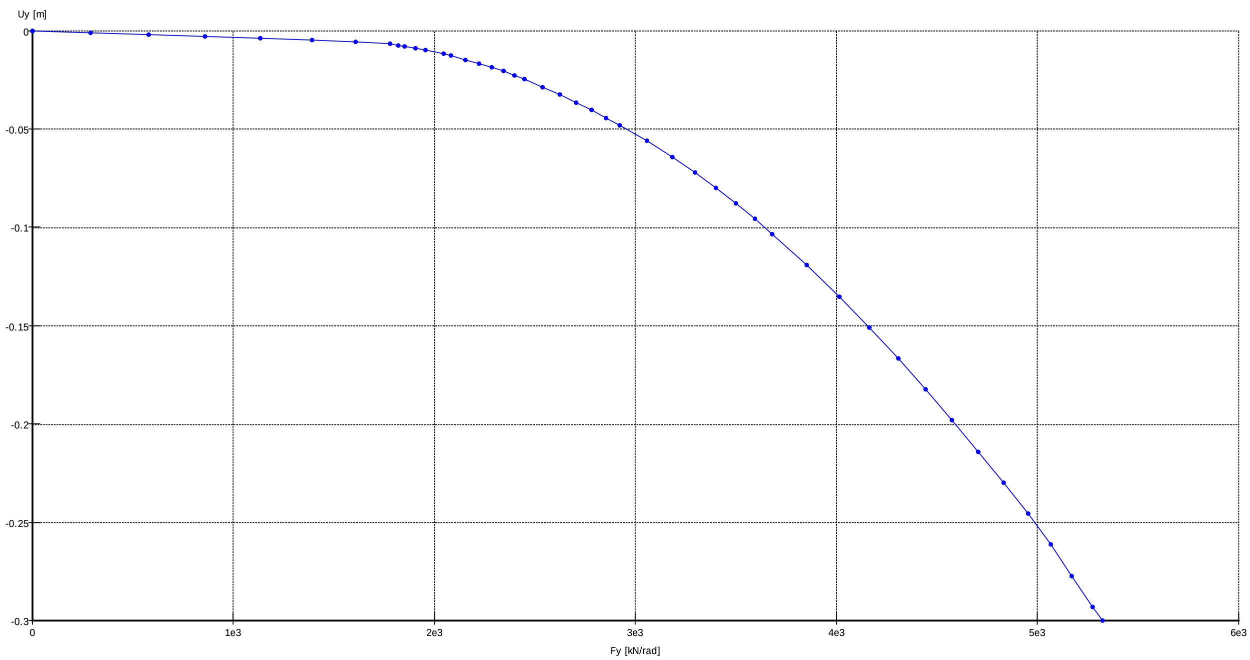
Uy [m]
0
-0.05
-0.1
-0.15
-0.2
-0.25
-0.3
0
1e3
2e3
3e3
4e3
5e3
6e3
Fy [kN/rad]

Fig. 14

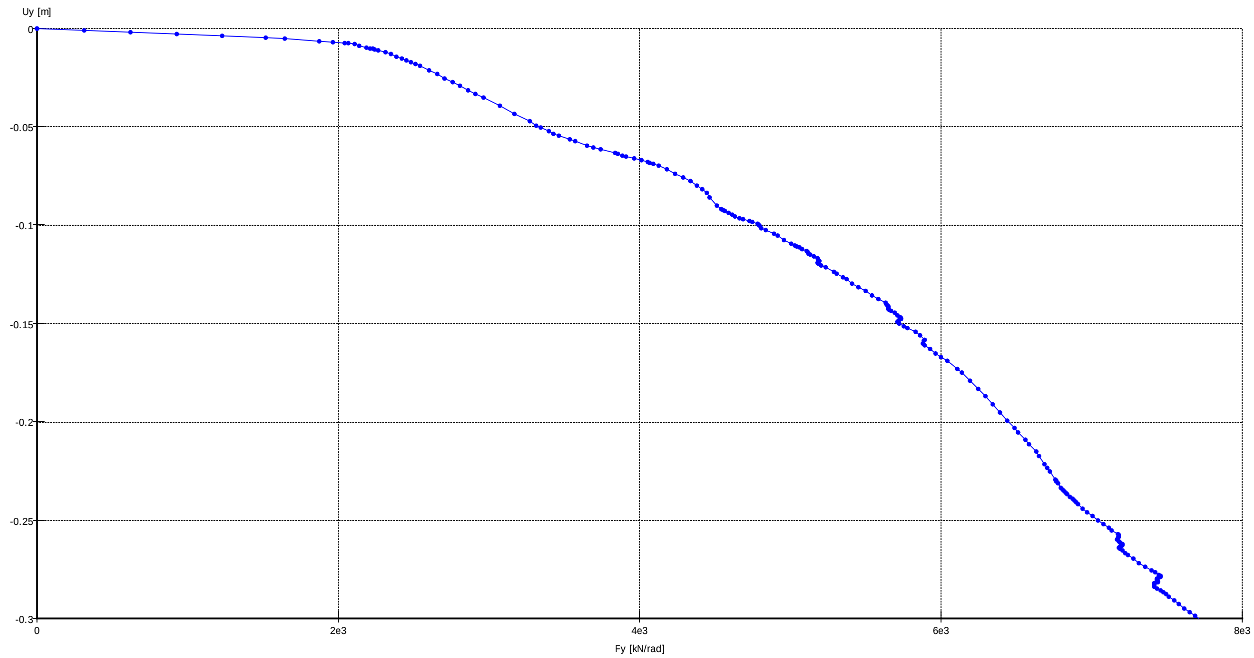
Uy [m]
0
-0.05
-0.1
-0.15
-0.2
-0.25
-0.3
0
2e3
4e3
6e3
8e3
Fy [kN/rad]

Fig. 15

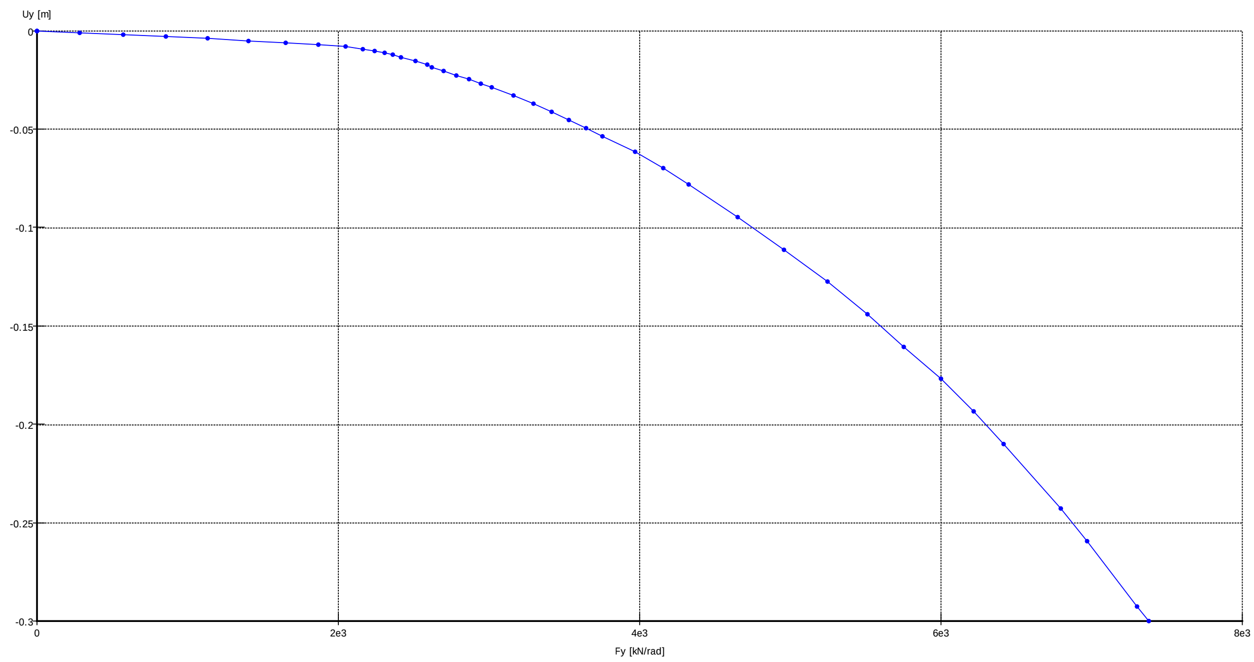
Uy [m]
0
-0.05
-0.1
-0.15
-0.2
-0.25
-0.3
0
2e3
4e3
6e3
8e3
Fy [kN/rad]

Fig. 16

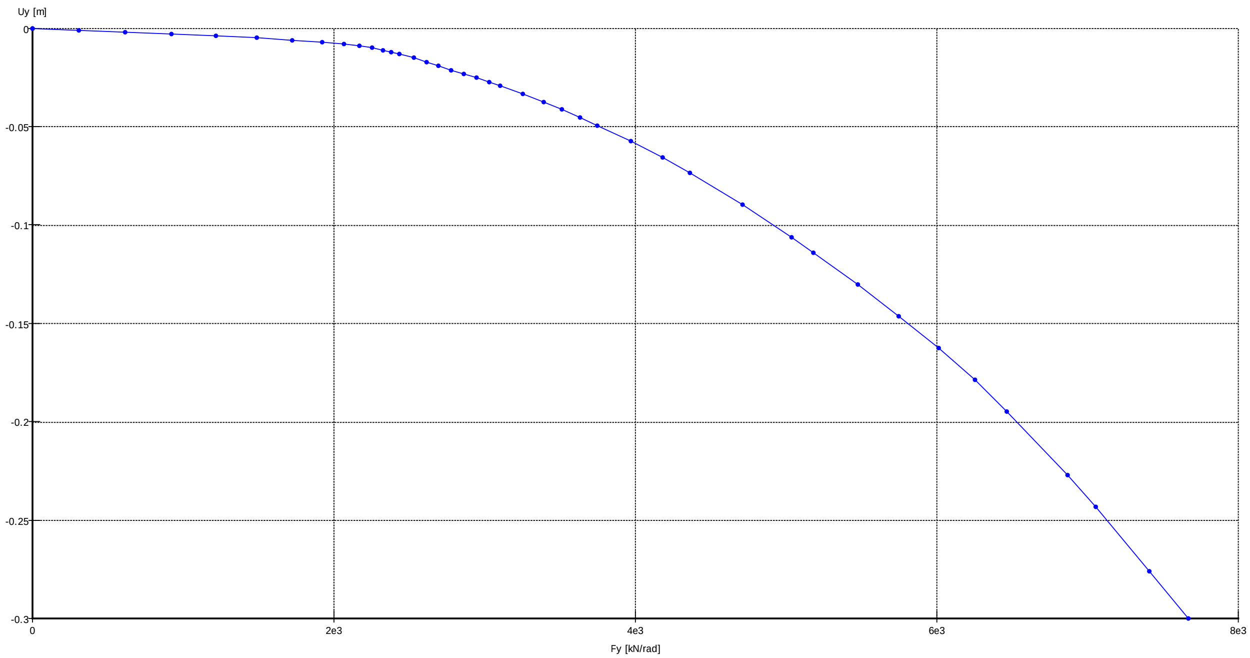
Uy [m]
0
-0.05
-0.1
-0.15
-0.2
-0.25
-0.3
0
2e3
4e3
6e3
8e3
Fy [kN/rad]

Fig. 17

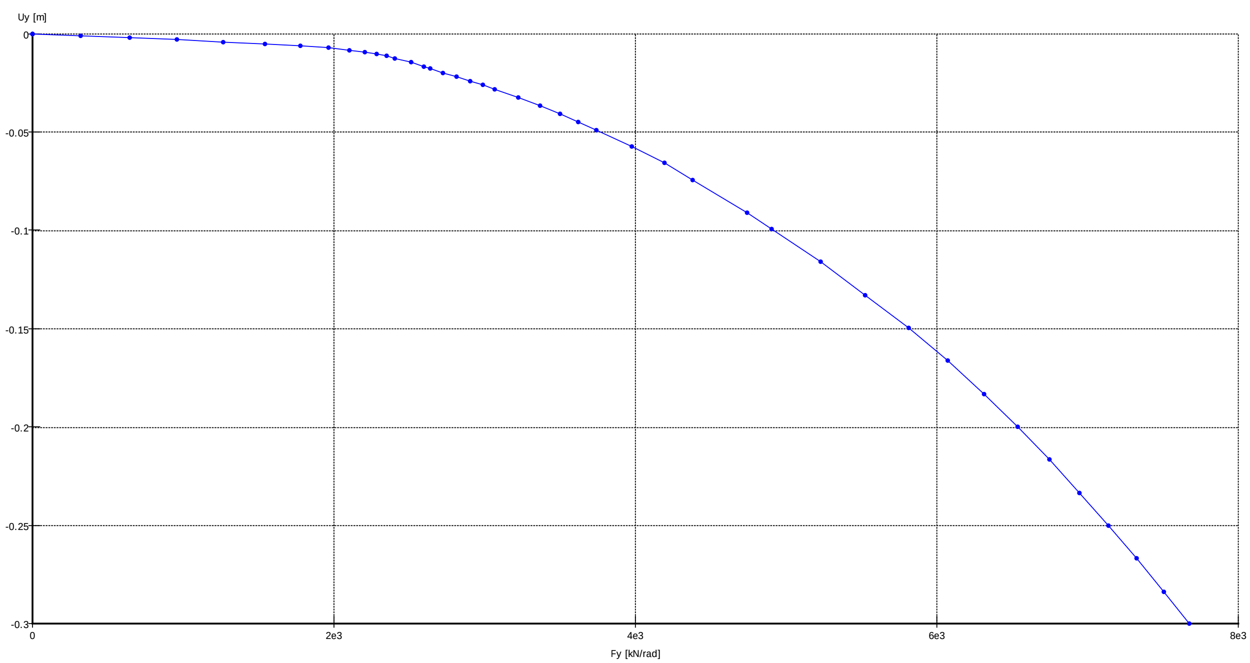
Uy [m]
0
-0.05
-0.1
-0.15
-0.2
-0.25
-0.3
0
2e3
4e3
6e3
8e3
Fy [kN/rad]

Fig. 18

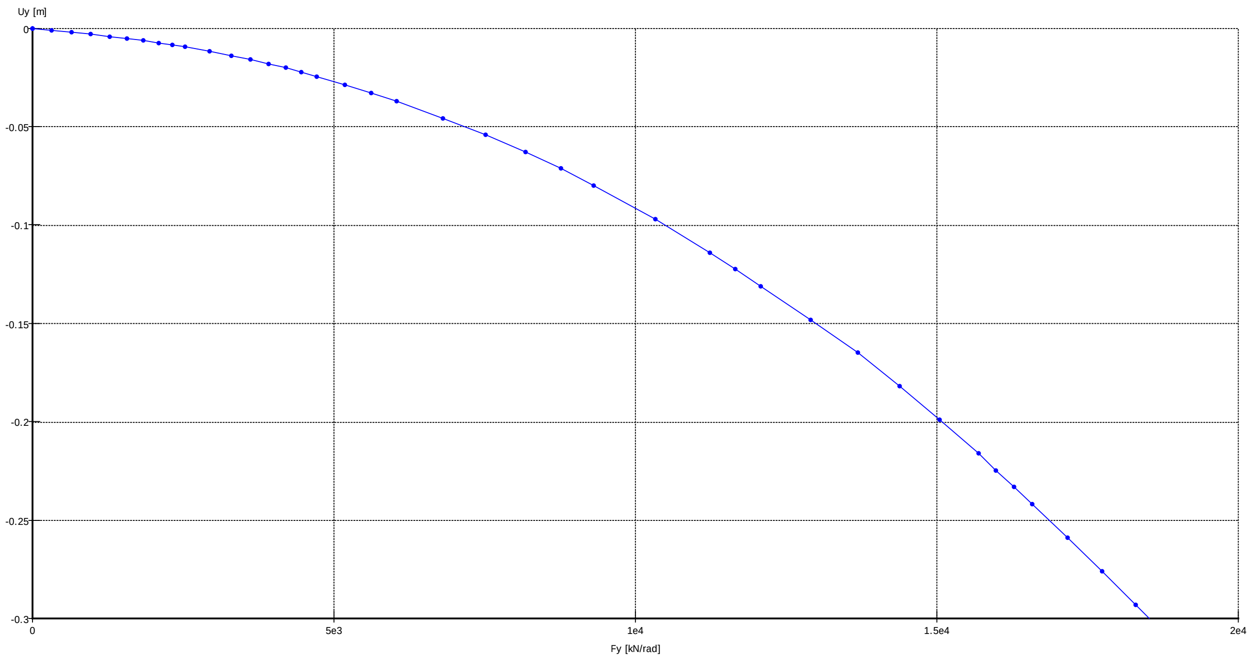

Fig. 19

Appendix [2] – List of Published Papers

1. Nabil, M. and Abu Tair, A. (2017). Comparison Between Theoretical and Practical Compression Capacities of Deep / Long Piles in Dubai. In: *3rd International Sustainable Buildings Symposium (ISBS 2017)*.
2. Nabil, M. and Abu Tair, A. (2017). Comparison Between Theoretical and Practical Compression Capacities of Deep / Long Piles in Dubai. In: *6th International Conference on Geological and Environmental Sciences*.
3. Nabil, M. and Abu Tair, A. (2017). Comparison Between Theoretical and Practical Compression Capacities of Deep / Long Piles in Dubai. *International Journal of Structural and Civil Engineering Research*, (E0002).
4. Nabil, M. and Abu Tair, A. (2017). Comparison Between Theoretical and Practical Compression Capacities of Deep / Long Piles in Dubai. *Springer*, Proceedings of 3rd International Sustainable Buildings Symposium. lSBS 2017(86924797).